1995

Sources of variability in nitrogen availability in Iowa cornfields

Carlos Honorio Perdomo
Iowa State University

Sources of variability in nitrogen availability in Iowa cornfields

by

Carlos Honorio Perdomo

A Dissertation Submitted to the

Graduate Faculty in Partial Fulfillment of the

Requirements for the Degree of

DOCTOR OF PHILOSOPHY

Department: Agronomy
Major: Soil Science (Soil Fertility)

Approved:

Signature was redacted for privacy.

In Charge of Major Work

Signature was redacted for privacy.

For the Major Department

Signature was redacted for privacy.

For the Graduate College

Members of the Committee:

Signature was redacted for privacy.

Signature was redacted for privacy.

Signature was redacted for privacy.

Signature was redacted for privacy.

Iowa State University
Ames, Iowa

1995

DEDICATION

To my parents

TABLE OF CONTENTS

GENERAL INTRODUCTION

Nitrogen fertilizer recommendations for corn in the Corn Belt are based primarily on yield goals. Such recommendations are based on the assumption that fertilizer N should be added in quantities expected to be taken up by plants and, therefore, that fertilizer requirements are proportional to the yields expected. Although this method is easy to use, it does not consider year-to-year variability in yields, amounts of N supplied by soils, and amounts of N lost from the soils. In practice, use of this method usually involves application of extra fertilizer N to ensure that most sites have adequate amounts. This results in overfertilization at many sites, and this overfertilization reduces profits for farmers and contributes to degradation of the environment.

Recent information collected in Iowa and other states in the northern half of the United States suggests that recommendations based on soil tests for NO_3^- are better than recommendations based on yield goals. The soil testing is done in late spring, a time when plants are starting to grow rapidly but have not yet taken up much N. By sampling at this time, the test enables site specific adjustments of fertilization rates after spring weather conditions have influenced the availability of N in the soil. Furthermore, this test gives feedback concerning the availability in late spring of fertilizer N applied earlier, so the test can be used by farmers who usually apply most of their N fertilizer before or at planting.

One problem that could limit the potential of this test is high variability in soil NO_3^- concentrations. In sites with high variability, large numbers of samples are needed to obtain reliable estimates of soil NO_3^- concentrations, and this would discourage use of the test.

Moreover, even when enough samples could be collected to establish the mean NO_3^- concentration for an area, this mean concentration may not be representative of the concentrations found within portions of the area sampled.

Results of recent studies clearly show that variability is high at some sites, and is low at other sites, but the cause of this variability has not yet been established. No information is available to determine whether this variability is natural (intrinsic variability) or if this variability is mainly related to man's activities (extrinsic variability). Studies of the amount and the structure of this variability at different sites should enable identification of the factors causing high variability and, therefore, avoid situations where the soil test could fail.

In this dissertation, I studied the amount and the structure of the variability in concentrations of soil NO_3^- in Iowa cornfields by using conventional statistics and geostatistical techniques. Objectives of this study included (i) evaluation of the possibility that windrows of soybean residue from a previous crop were a major source of variability in concentrations of soil NO_3^- and (ii) characterization of the amount and structure of variability of soil NO_3^- concentrations. An underlying assumption in these studies was that many common practices in row-crop agriculture should be expected to create cyclic variability in soil NO_3^- concentrations.

Dissertation Organization

The dissertation is presented as five papers intended for publication. The first paper will be submitted for publication in *Agronomy Journal*. The remaining papers will be

submitted for publication to the *Soil Science Society of America Journal*. The five papers are preceded by a General Introduction and succeeded by a General Summary.

NITROGEN AVAILABILITY IN CORNFIELDS AS AFFECTED BY SOYBEAN RESIDUE

A paper prepared for submission to *Agronomy Journal*

Carlos H. Perdomo and Alfred M. Blackmer

ABSTRACT

Studies were conducted in 1993 to learn more about (i) the net effect of soybean residue on availability of N to corn in the following year and (ii) the importance of windrows of soybean residue as a source of spatial variability on concentrations of NO_3^- and exchangeable NH_4^+ in soils. Measurements were made in six fields selected for uniformity of windrows of residue formed during combining in production agriculture. Soil samples collected within and between windrows at various times during the spring revealed that soybean residues had only slight effects on N availability and that the direction of the effect was to decrease N availability. These findings were consistent with assessments of N status by chlorophyll meter readings on plant leaves in late spring and by measurements of NO_3^- concentrations in cornstalks at the end of the season. Nonuniform applications of residue explained from insignificant to about half of the variability in concentrations of NO_3^- observed at the sites. The total amounts of variability were relatively small, however, at sites where the residue was responsible for a significant portion of the variability. Nonuniform application of N fertilizer seemed to be the most likely cause of spatial variability in soil NO_3^- concentrations at sites having the greatest variability.

INTRODUCTION

Soybean residues often are concentrated in windrows as combines harvest in a single pass many rows and deposit the residue on few rows. The effects of these windrows on the amounts and uniformity of available N for the next crop has recieved little attention. However, Douglas et al. (1992) reported that windrows of wheat (Triticum aestivum L.) residue left by combines should be expected to reduce availability of N to plants and create nonuniform conditions that increase the number of soil samples required to assess fertilizer needs.

Soybean residues tend to have higher concentrations of N than do wheat residues (Schepers and Mosier, 1991), and there is uncertainty as to whether the decomposition of soybean residues in soils result in net immobilization or net mineralization of N during the growth of the next crop. Power et al. (1986) conducted field studies with isotopically labeled soybean residue and reported that much of the N in the residue was recovered by the next crop. Such reports seem consistent with recommendations (Peterson and Voss, 1984) that less fertilizer N is needed when corn follows soybean than when it follows corn.

It is possible that the releases of labeled N reported by Power et al. (1986) could have occurred even if the net effect of decomposing residue was to decrease N availability. This possibility deserves attention because the decomposition of plant residues often results in substantial turnover of N in the soil NO_3^- pool (Blackmer and Green, 1995). Moreover, laboratory studies by Green and Blackmer (1995) indicate that the decomposition of soybean residue, like the decomposition of corn residue, results in net immobilization of N in soils.

The results of the laboratory studies also indicated that the usual difference in N fertilizer requirement could be explained by soybean crops leaving less residue than corn and, therefore, inducing less net immobilization of N. Studies of N availability within and between windrows of soybean residue provide opportunity to evaluate the relevance of the laboratory studies to field conditions.

The possibility that windrows of soybean residue are a major source of spatial variability in available N within fields deserves attention amid efforts (Magdoff et al., 1984, 1990; Blackmer et al., 1989; Fox et al., 1989; Binford et al., 1992; Meissinger et al, 1992) to develop soil tests for predicting the N fertilizer needs for corn. Studies in Iowa (Morris and Blackmer,1994; Perdomo and Blackmer, 1994) have shown that areas of seemingly uniform soil type within cornfields often have marked spatial variability in soil NO_3^- concentrations in late spring. These studies, however, were not designed so as to enable direct assements of the importance of nonuniform ditributions of residue as a source of this variability.

The objectives of this study were to learn more about (i) the net effects of soybean residue on availability of N to corn in the following year and (ii) the importance of windrows of soybean residue as a source of spatial variability in concentrations of NO_3^- and exchangeable NH_4^+ in soils.

MATERIALS AND METHODS

Six fields were selected for uniformity of residue windrows formed during the harvest of soybean in 1991. The fields were in production agriculture and had combine swaths 6 m wide (8 rows 76 cm apart) with residues from the entire swath concentrated on one-half to

one-quarter of this width. Some fields had been chisel plowed, but the windrows of residue could be clearly seen in the spring of 1992. An experimental site (12 swaths wide, 30 m long swaths) of seemingly uniform soil type was selected in each field (Table 1). The first 4 sites were established in early spring, and sites 5 and 6 were established shortly after planting. Site 3 was lost in the middle of the season for reasons unrelated to the study. All fields were managed by farmers according to their usual practices (including N fertilization) and no special treatments were applied for the study.

To measure the effects of soybean residue on concentrations of NO_3^- and exchangeable NH_4^+ in early April (before fertilization), 9 pairs of soil samples (16 cores with diam. of 3.2 cm to a depth of 30 cm) were collected from within and between windrows at each of the first 4 sites. To observe temporal patterns in concentration of NO_3^- and exchangeable NH_4^+, a pair of soil samples (composite of 24 cores each) was collected from within and between windrows at 1-week intervals from April 9 to July 1 at each of the first four sites. To more precisely measure the effects of soybean residue on concentrations of NO_3^- and exchangeable NH_4^+ in soils when corn plants were about 15 cm tall, 12 pairs of soil samples (24 cores each) were collected from within and between windrows at all six sites. The soil samples collected in early April also were used in laboratory incubation studies to determine the effects of the soybean residue on net mineralization of N under controlled conditions. Each field-moist sample was passed through a 2-mm sieve, treated with 45 mg KNO_3^--N kg^{-1} soil in enough water to adjust its water content to 60% of its maximum water-holding capacity, and incubated at 24 degrees C in a 19-L plastic bucket with lid. Maximum

Table 1. Selected properties of soils used in this study

Site	Series	Subgroup	County
1	Canisteo	Typic Haplaquoll	Boone
2	Clarion	Typic Hapludoll	Greene
3	Canisteo	Typic Haplaquoll	Boone
4	Webster		Greene
5	Canisteo	Typic Haplaquoll	Boone
6	Clarion	Typic Hapludoll	Boone

water holding capacity was estimated by saturating 25-g samples and letting them drain for 24 h. After 0.2, 1, 2, 3, 4, 6, 10, and 14 weeks the soil from each bucket was poured onto a sheet of plastic, mixed thoroughly, sampled for determination of NO_3^- and exchangeable NH_4^+, and then returned to the bucket. Soil samples to be analyzed for NO_3^- and exchangeable NH_4^+ were dried at 49 °C, crushed to pass a 2-mm sieve, and extracted with 1 M KCl. The extract was analyzed by using a flow-injected, automated technique (Kopp and Mc Kee, 1979)

Measurements of light absorbance by leaf chlorophyll, concentrations of NO_3^- in the lower cornstalk at the end of the season, and grain yields were made on plants within a 8-m band perpendicular to the swaths at each site. Twelve pairs of observations (one pair per swath) were made at each site. Light absorbance was measured by using a SPAD-502 chlorophyll meter (Minolta Camera Co., Ltd. Japan); each observation was the average of 20 readings taken on the youngest fully developed leaves of different plants when the plants were about 30-cm tall. Concentrations of NO_3^- in the lower cornstalk were determined as described by Binford et al. (1990); each observation involved collecting 30 segments of stalk cut between 15 and 35 cm above the ground about 2 weeks after black layers had formed on most kernels. Grain yields were determined by hand-harvesting; each observation involved picking 7 m of row.

Data from the laboratory studies were statistically analyzed as a complete randomized design, with residue distribution (i.e., residue and no residue) as a treatment effect. Data from the field were analyzed as a complete randomized block design, with swaths considered

as blocks and residue distribution as treatments. The true variances due to residue (σ^2_Residue), due to swaths (σ^2_Swaths), and due to error (σ^2_Error) were computed from the corresponding means squares (MS) in the Anova table according to:

$$\sigma^2\_Residue = (MS\_Residue - MS\_Error) /12 \quad [1]$$

$$\sigma^2\_Swaths = (MS\_Swaths - MS\_Error) /2 \quad [2]$$

$$\sigma^2\_Error = MS\_Error \quad [3]$$

The percentage of variability due to residue was calculated as :

$$Var.\_Residue(\%) = 100 [\sigma^2\_Residue / (\sigma^2\_Residue + \sigma^2\_Swaths + \sigma^2\_Error)] \quad [4].$$

Analyses of variance were done using ANOVA and GLM procedures in SAS (SAS Institute, Inc., 1989).

RESULTS AND DISCUSSION

Soil samples collected in early spring (before fertilization) showed significantly higher ($P \leq 0.05$) concentrations of NO_3^- between windrows than in windrows at 2 of the 4 sites sampled (Table 2). These differences, however, were small relative to the range of 21 to 26 mg N kg soil reported (Binford et al., 1992) to be optimal for corn in late spring. Differences in concentrations of exchangeable NH_4^+ also were small (Table 2), and no significant effects of residue were observed. These observations indicate that the soybean residue had only small effects on inorganic N concentrations in the soil at this time and that this small effect was in the direction of decreasing concentrations of inorganic N.

Table 2. Concentrations of N as NO_3^- or exchangeable NH_4^+ found in early spring before N fertilizers were applied.

Form of N	Site	Concentrations of N as NO_3^- or exchangeable NH_4^+		Statistical Significance[†]
		Residue	No Residue	
		----------mg N kg^{-1}----------		P>F
NO_3^-	1	5.6	8.2	0.0001
	2	4.2	4.7	0.1545
	3	5.2	7.3	0.0003
	4	4.4	3.8	0.0496
	Mean	4.8	6.0	0.2178
NH_4^+	1	7.7	8.8	0.0836
	2	11.3	8.2	0.0741
	3	11.7	11.3	0.6696
	4	10.4	10.8	0.3088
	Mean	10.3	9.8	0.5894

[†]An overall analysis of variance showed that the interactions of site and residue treatments had a P>F of 0.0001 for soil NO_3^- and 0.0356 for soil NH_4^+.

Incubation of the soil samples collected before planting showed a tendency to mineralize N during incubations in the laboratory (Figure. 1). The lack of a period of net immobilization similar to that observed by Green and Blackmer (1995) would be expected if some readily decomposable portion of the stover had decomposed (with or without leaching into the soil) before samples were collected. The results indicate that the soybean residue should be expected to have minimal direct effects on availability of N under field conditions. Indirect effects of the residue might be expected at some times in the field if the residue caused differences in temperature and moisture and, therefore, in rates of immobilization or mineralization as the soils warmed in the spring.

Soil samples collected from the field at approximately weekly intervals showed that concentrations of NO_3^- tended to increase with time until the plants were about 30 cm tall (June 6) and then to decrease with time (Figure 2). The early increases in concentration can be explained by fertilization, nitrification of fertilizer N, and(or) mineralization of N from soil organic matter. The subsequent decreases can be explained by N uptake by rapidly growing plants. The results show that the windrows of soybean residue had little or no effect on concentrations of exchangeable NH_4^+ (data not shown) or NO_3^- in soils during the spring at the four sites studied.

More intensive field sampling when the corn was about 30 cm tall showed that soil NO_3^- concentrations within and between windrows differed significantly ($P \leq 0.01$) only at 2 (Sites 1 and 3) of 6 sites (Figure 3). Mean concentrations of NO_3^--N across all sites were 25.1 mg N kg^{-1} without residue and 22.7 mg N kg^{-1} with residue. This difference was not

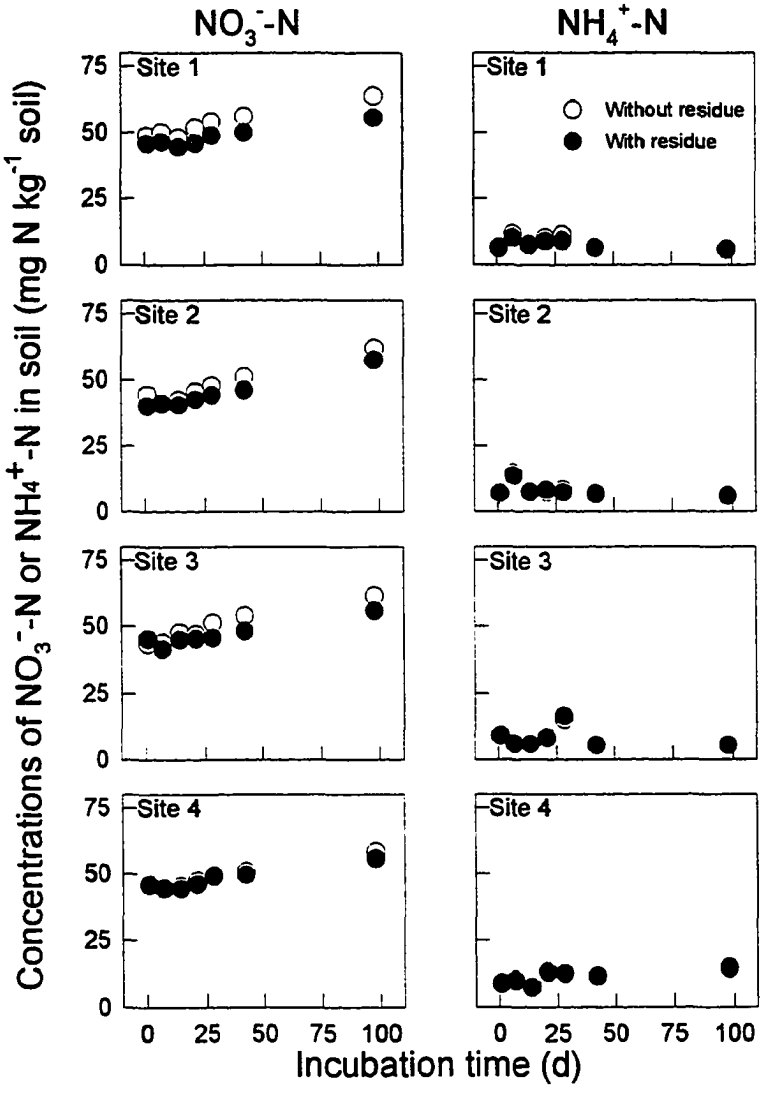

Figure 1. Changes in concentrations of mineral N in soil (NH_4^+ or NO_3^-) with time of incubation.

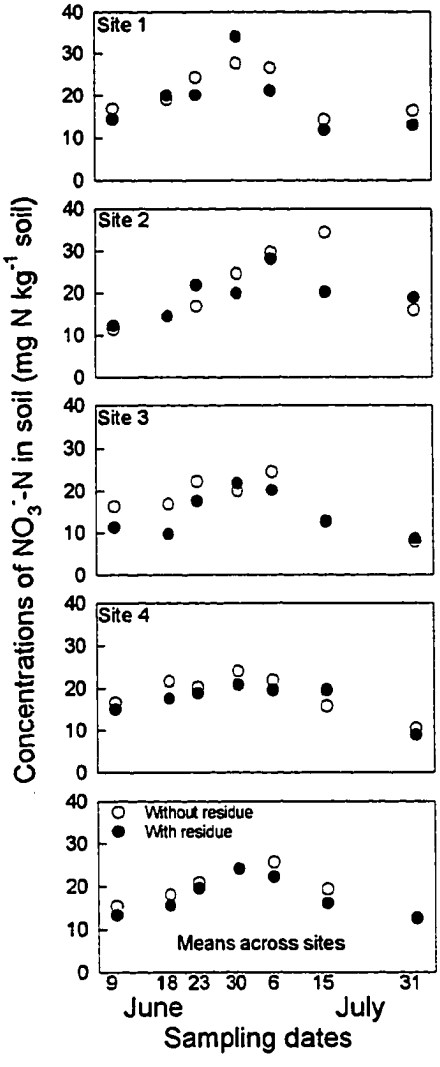

Figure 2. Changes in concentrations of soil NO_3^- with time of sampling in cornfields.

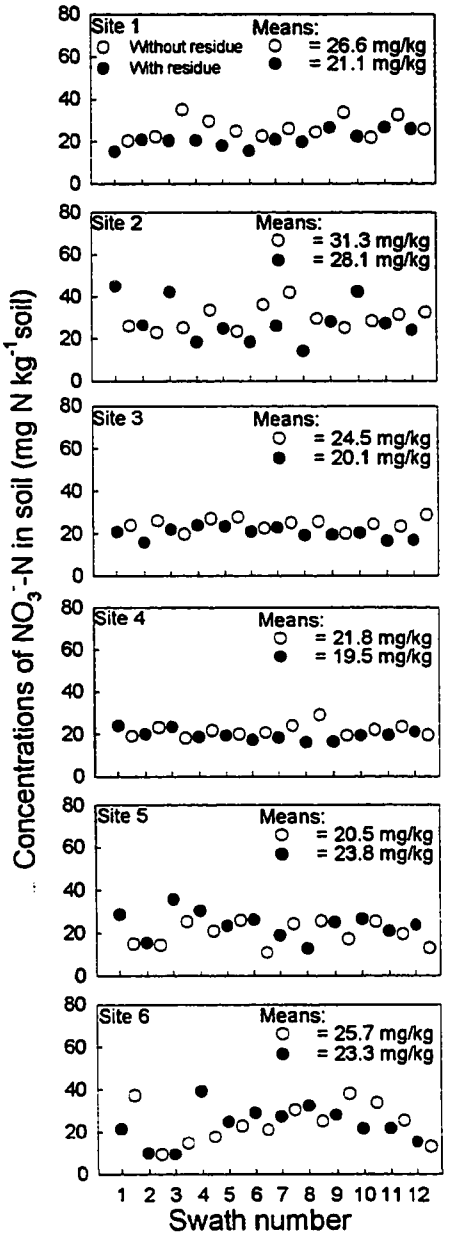

Figure 3. Concentrations of soil NO_3^- at positions in windrows (with residue)and bewteen windrows (without residue) at several sites (a swath comprises positions both in and between windrows).

statistically significant ($P \leq 0.204$). The results suggest that the windrows of residue were not the primary cause of variability in soil NO_3^- concentrations in many of the fields sampled. In those where it seemed to be a primary cause, the amounts of variability were relatively small.

Analyses of variance indicated that from negligible amounts to about half of the total variability in soil NO_3^- concentrations shown in Figure 3 could be explained by the windrows of residue (Table 3). Although adequate data was not collected to determine the amounts of variability explained by other factors, the coefficient of variation was 30.6% for fields fertilized only with anhydrous ammonia and 14.7% for fields treated only with UAN that was applied by spraying on the surface. It seems likely that the higher variability at sites treated with anhydrous ammonia was caused by nonuniform distributions of N fertilizer across the width of the applicator (usually 10 to 13 meters) because ammonia tends to change from the liquid to gas phase within hoses of the applicators and the amount of change would vary with factors as such as length of hoses. Moreover, nonuniform applications are not easily detected because the ammonia is injected into the soil and, therefore, differences in flow between injectors cannot be seen. In contrast, the UAN solutions remain as liquids and are sprayed through nozzles that can be easily checked for uniformity. Analyses presented in Part V of this dissertation presents evidence that nonuniform applications of N tend to be much greater problem where anhydrous ammonia has been applied than where UAN has been sprayed on the surface.

Table 3. Statistical parameters describing variability in soil nitrate concentration in late spring.

SITE[†]	SD[‡]	CV[§]	Variability explained by residue
	mg/kg	--%--	--%--
1 (AA+UAN)	5.1	21.6	42.5
2 (AA)	8.8	29.5	-1.0
3 (UAN)	3.5	15.6	54.1
4 (UAN)	2.9	13.9	17.7
5 (AA)	5.8	26.1	10.0
6 (AA)	8.9	36.2	-3.2

[†]AA=Farmer applied Anhydrous Ammonia at planting, UAN=farmer spread urea and ammonium nitrate solution at planting, AA+UAN=farmer applied both.
[‡]SD:Standard Deviation.
[§]CV:Coefficient of variation.

Corn growing between windrows at some sites tended to be slightly larger than corn growing in windrows early in the season. Corn in the windrow also tended to have a slightly lighter color of green at some sites, but measurements by using the chlorophyll meter when the plants were about 30 cm tall revealed that the differences were small (Table 4). Visual observations later in the season revealed that the plants between windrows tasseled and lost their green color a few days earlier than did the plants without residue. These observations suggest that part of the differences in height and color early in the season may have been caused by a slightly slower germination and growth in the windrows. The slower growth could be caused by allelopathy of soybean residues (Martin et al., 1990) or by differences on soil temperature or moisture contents. Plant counts at harvest revealed minor differences in population density (Table 5), a difference that could be caused partly by greater difficulty planting seeds in soils covered with residue.

Concentrations of NO_3^- in the cornstalks at the end of the season revealed that plants in windrows had less or similar amounts of available N than did plants growing between windrows (Table 6). The observed effects of residue on N availability seems relatively unimportant, however, because the optimal range for NO_3^- concentrations in cornstalks is between 700 and 2000 mg N kg^{-1}.

Grain yields tended to be higher between windrows than in windrows (Figure 4). These differences were significant ($P \leq 0.05$) at all sites. When averaged across sites, plants growing on soil with residue produced 815 kg ha^{-1} less, or a decrease of 6.7%, than plants growing on soil without residue. This difference was statistically significant ($P \leq 0.05$). If it

Table 4. Chlorophyll readings in corn leaves at late spring in residue and non-residue rows at several sites.

Site	Chlorophyll readings in corn leaves		Statistical Significance[†]
	Residue	No Residue	
			P>F
1	53	51	<0.001
2	43	43	0.886
3	48	47	0.196
4	45	44	0.091
5	56	54	0.001
6	60	58	0.001
Mean	51	49	0.020

[†]An overall analysis of variance showed that the interactions of site and residue treatments had a P>F of . 0.014.

Table 5. Number of plants per plot at harvest in residue and non-residue rows at several sites.

Site	Number of plants per plot at harvest		Statistical Significance
	Residue	No Residue	
			P>F
1	62	65	0.021
2	76	77	0.691
4	77	80	0.083
5	74	74	0.670
6	71	73	0.171
Mean	72	74	0.222

Table 6. Concentrations of NO_3^- in corn stalks in residue and non-residue rows at several sites.

Site	Concentration of NO_3^- in stalks		Statistical Significance[†]
	Residue	No residue	
	----------mg N kg^{-1}----------		P>F
1	565	1663	0.011
2	4421	4696	0.661
4	64	56	0.440
5	1295	1401	0.654
6	112	179	0.107
Mean	1291	1599	0.204

[†]An overall analysis of variance showed that the interactions of site and residue treatments had a P>F of 0.131.

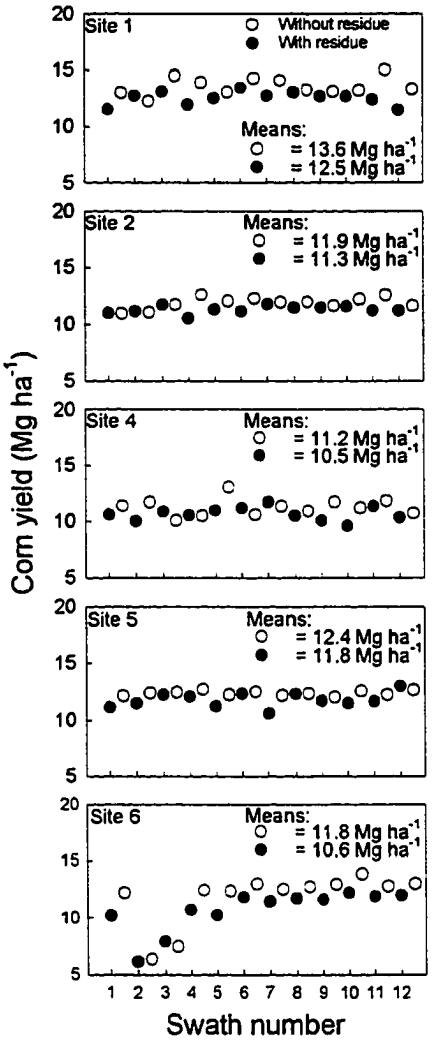

Figure 4. Corn yields in windrows (with residue)and bewteen windrows (without residue) at several sites (a swath comprises positions both in and between windrows).

were assumed that these differences were caused by N availability, then it would be concluded that soybean residue decreased the availability of N. Given other observations made in this paper, however, it seems more likely that soybean residue reduced corn yields for reasons not directly related to N availability. The low yields and soil nitrate values observed in swaths 2 and 3 at Site 6 (Figure 3 and Figure 4) seem to indicate an area missed during fertilizer application.

Overall, the results of this study show that windrows of soybean residue have relatively small effects on N availability in cornfields the following year. The windrows do introduce some variability in soil NO_3^- concentrations, but this variability is small compared to the total variability encountered in some fields. Nonuniform applications of fertilizer clearly deserves more attention as a major source of variability in soil NO_3^- concentrations within fields.

LITERATURE CITED

Binford, G.D., A.M. Blackmer, and N.M. El-Hout. 1990. Tissue test for excess nitrogen during corn production. Agron. J. 82(1):124-129.

Binford, G.D., A.M. Blackmer, and M.E. Cerrato. 1992. Relationships between corn yields and soil nitrate in late spring. Agron. J. 84:53-59.

Blackmer, A.M., and C.J. Green. 1995. Nitrogen turnover by sequential immobilization and mineralization during corn residue decomposition in soils. Soil Sci. Soc. Am. J. (in press).

Blackmer, A.M., D. Pottker, M.E. Cerrato, and J. Webb. 1989. Correlations between soil nitrate concentrations in late spring and corn yields in Iowa. J. Prod. Agric. 2:103-109.

Douglas, C.L.J., P.E. Rasmussen, and R.R. Allmaras. 1992. Nutrient distribution following wheat-residue dispersal by combines. Soil Sci. Soc. Am. J. 56(4):1171-1177.

Fox, R.H., G.W. Roth, K.V. Iverson, and W.P. Piekielek. 1989. Soil and tissue nitrate tests compared for predicting soil nitrogen availability to corn. Agron. J. 81:971-974.

Green C.J., A.M. Blackmer, and R. Horton. 1995. Nitrogen effects on conservation of carbon during corn residue decomposition in soil. Soil Sci. Soc. Am. J. (in press).

Kopp, J. E., and G. D. McKee. 1978. Methods for chemical analysis of water and wastes. Method 351.2, nitrogen, ammonia. EPA Report no. EPA-6000/4-79-020. EPA Environmental Monitoring and Support Laboratory, Cincinnati, OH.

Magdoff, F.R., D. Ross, and J. Amadon. 1984. A soil test for nitrogen availability to corn. Soil Sci. Soc. Am. J. 48:1301-1304.

Magdoff, F.R., W.E. Jokela, R.H. Fox, and G.F. Griffin. 1990. A soil test for nitrogen availability in the Northeastern United States. Commun. Soil Sci. Plant Anal. 21:1103-1115.

Martin, V.L., E.L. McCoy, and W.A. Dick. 1990. Allelopathy of crop residues influences corn seed germination and early growth. Agron. J. 82(3):555-560.

Meisinger, J.J., V.A. Bandel, J.S. Angle, B.E. O'Keefe, and C.M. Reynolds. 1992. Presidedress soil nitrate test evaluation in Maryland. Soil Sci. Soc. Am. J. 56:1527-1532.

Morris, T.F., and A. M. Blackmer. 1994. Errors associated with sampling cornfields for the late-spring soil test. p.310. *IN* Agronomy Abstracts, ASA. Madison, WI.

Perdomo, C.H., and A. M. Blackmer. 1994. Variability in nitrogen availability among microplots in cornfields. p.312. *IN* Agronomy Abstracts, ASA. Madison, WI.

Peterson, G.A., and R.D. Voss. 1984. Management of nitrogen in the west central states. p. 722-732. *In* R. D. Hauck (ed.) Nitrogen in crop production. ASA, CSSA, and SSSA, Madison, WI.

Power, J.F., and F.E. Broadbent. 1989. Proper accounting for N in cropping systems. p. 160-182. In R.F. Follett (ed.) Developments in agricultural and managed-forest ecology 21. Nitrogen management and groundwater protection. Elsevier, Amsterdam.

Power, J. F., J. W. Doran, and W. W. Wilhelm. 1986. Uptake of nitrogen from soil, fertilizer, and crop residue by no-till corn and soybean. Soil Sci. Soc. Am. J. 50:137-142.

Schepers, J. S., and A. R. Mosier. 1991. Accounting for nitrogen in nonequilibrium soil-crop systems p. 125-138. *In* R.F. Follett et al. (ed.) Managing nitrogen for groundwater quality and farm profitability, SSSA, Madison, WI.

Smith, J.H., and J.R. Peterson. 1982. Recycling of nitrogen through land application of agricultural, food processing, and municipal wastes. In F.J. Stevenson (ed.) Nitrogen in agricultural soils. Agron Monogr. 9. ASA and SSSA, Madison, WI.

SAS Institute. 1988. SAS/STAT user's guide. Version 6.03. SAS Inst., Inc., Cary, NC.

IDENTIFICATION OF CYCLIC SOURCES OF VARIABILITY IN SOILS

A paper prepared for submission to the *Soil Science Society of America Journal*

Carlos H. Perdomo and Alfred M. Blackmer

ABSTRACT

The objective of this work was to develop a method for characterization of cyclic components in variogram analysis and to compare this method to commonly used Fourier analysis methods. The study involved analysis of hypothetical datasets formed by imposing various levels of random noise on a cyclic function and analysis of a real dataset consisting of corn yield measurements made along a transect perpendicular to windrows of plant residue formed by harvesting the previous crop. Cyclic models were developed that identified cycles having appropriate periods in the hypothetical and real datasets. In the hypothetical dataset, a model consisting of a nugget and a cyclic component correctly identified the added periodicity even at the highest level of random noise. In the real dataset, a cyclic model consisting of a linear regionalized component and a cyclic component was superior to Fourier analysis for detecting the periodicity caused by windrows in a dataset with a strong regionalized component. This study led to the development of models that can partition spatial variability observed along transects into regionalized, cyclic, and random components.

INTRODUCTION

Many management practices common to rowcrop agriculture should be expected to produce cyclic trends in soil properties or crop yields measured along transects that are not parallel to the rows. Examples of practices that could produce such variability are applying

plant residues in windrows behind combines, banding fertilizers, and planting crops in rows. If these cyclic trends are not recognized, then the trends are considered random error and the sources of variability are not explained as well as they could be. Better methods of identifiying these cyclic patterns would enable design of more efficient studies.

Spectral analysis based on the Fourier series and transform is one of the most commonly used methods to detect cyclic trends. This technique is a statistical tool that permits transformations of sequences of data from the spatial or time domain (i.e., as a function of space or time) to the frequency domain (Carlson, 1975; Folorunso and Rolston, 1985). Results of this analysis are expressed as a graph showing the frequency composition of the data, or spectrum, from which it is possible to identify the specific frequencies at which the data seem to be cycling (Folorunso and Rolston, 1985).

An alternative to Fourier analyses is variogram analysis. Variogram analyses of cyclic data often show cyclic trends more clearly than the original data (Clark, 1979). However, although models commonly used to describe variograms distinguish between random and spatial sources of variability, they do not consider cyclic sources as an independent component of variability. The objectives of this work are (i.) to propose an extension of these models that enables characterization of cyclic variation and (ii.) to compare the ability of these modified models with that of the FFT analysis to identify cyclic trends in simulated and real datasets from fields.

VARIOGRAM ANALYSIS THEORY

Variogram analysis, or variography, can be used to describe the variance structure of a variable that is a function of space or time. Variography is based on the computation of the semivariogram, which describes the relationship between the semivariance and the distance between samples (the lag). Semivariance is defined as follows:

$$\gamma(h) = \frac{1}{\left[2m(h)\right]} \sum_{i=1}^{m(h)} \left[Z_{(x_i)} - Z_{(x_i+h)} \right]^2 \qquad [1]$$

where γ is the semivariance for m data pairs separated by the distance h, and Z is the value at positions x_i *and* $x_i + h$ (Webster, 1985). Following Isaaks and Srivastata, 1989, the term variogram is used here as a simpler term for semivariogram.

The central idea behind this analysis is that samples located closer together often tend to be more similar than samples located further apart. Variables that show such behavior are called regionalized variables (Matheron , 1965, Journel and Huijbregts, 1978). A variogram of a regionalized variable typically increases with the distance between samples until it reaches a plateau (Figure 1). The semivariance value at this plateau is called the sill and, like the ordinary sample variance, is an estimator of the "true" variance of the data (Clark, 1979).

The lag distance at which the variogram approachs this maximum is called the range of influence (often referred as the range) and it represents the range across which samples are spatially dependent, or correlated. After this range, samples become independent from each other. Variograms calculated from observational data may, or may not, show this sill depending on the amount of spatial dependence and on the maximum lag distance.

Theoretically, the variogram must be zero at lag zero because two samples measured at exactly the same position are really the same sample and must have the same value. Experimental variograms, however, often start at some value significantly above zero (Figure 1). This value is called the "nugget" and represents a residual source of variation that is present even at very small distances. It includes both random variation and variation with a range of influence much smaller than the distance between samples. Part of this random variation can be caused by measurement errors. The presence of a large nugget indicates that even samples located close together show differences that are random and unpredictable (Clark, 1979).

Many mathematical models have been proposed to describe relationships between semivariance and lag in experimental variograms. These models are useful because they can be used to estimate parameters like nugget, range, and sill from the variogram data. One of the most widely used models (Clark, 1979) is the spherical model:

$$\left.\begin{array}{l} y(h) = C_0 + C\left[\left(3h/2a\right) - \left(h^3/2a^3\right)\right] \text{ when } h \le a \\ \text{and} \\ y(h) = C_0 + C \text{ when } h \ge a \end{array}\right\} \qquad [2]$$

where C_0 is the nugget, $C_0 + C$ is the sill, h is the lag or lateral distance, and a is the range. A linear model (eq.[3]) is often used (Clark, 1979) for datasets having no sill or plateau:

$$y(h) = C_0 + bh \qquad [3]$$

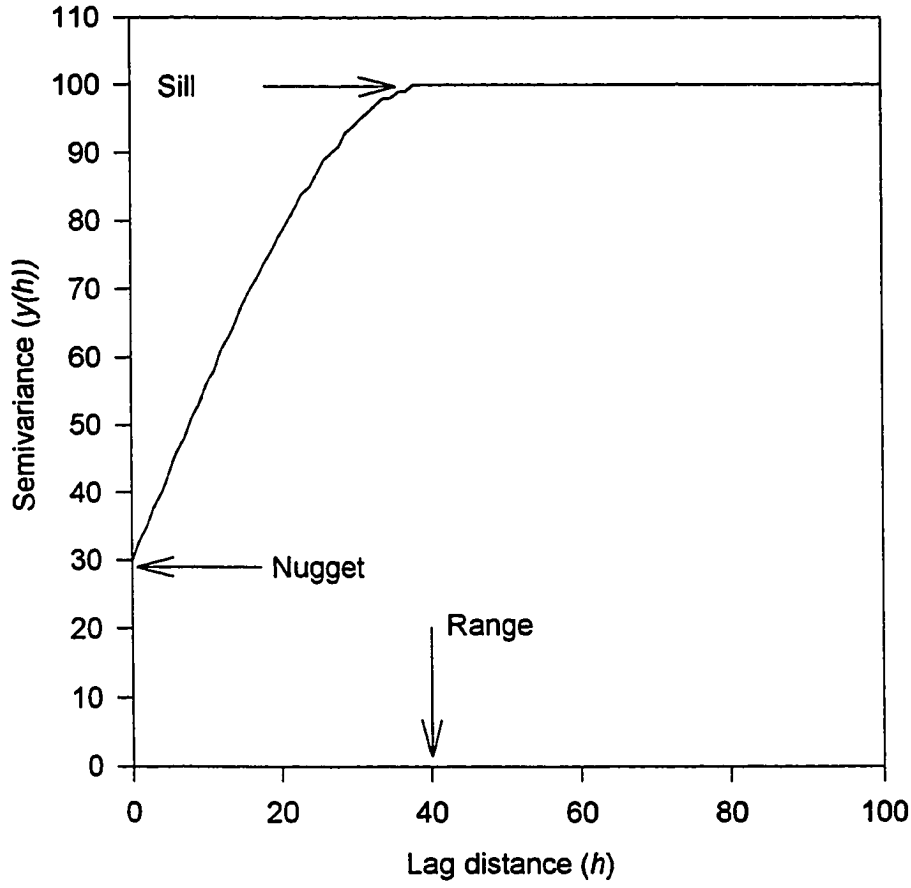

Figure 1. Typical variogram for a regionalized variable according to the Spherical model.

where b is the slope of the semivariance with respect to the lag. Variograms with no spatial component can be represented (Clark, 1979) by the nugget variance:

$$y(h) = C_0 \quad [4]$$

For a variogram that approaches a sill, the percentage of random (or nugget) variability can be defined by:

$$\text{Random\%} = \left[C_0 / (C_0 + C)\right] \times 100 \quad [5]$$

Clark (1979) noted that semivariogram models of experimental data are actually complex models composed of a nugget and a function representing the spatial component. In this paper we evaluate the possibility of adding an aditional cyclic component. A hypothetical semivariogram with only a cyclic component can be represented as:

$$y(h) = C_w \left[1 + Sin\ (\rho + \omega\ h)\right] \quad [6]$$

where C_w, ρ, and ω are parameters to be estimated from the variogram data. The term C_w represents the amplitude of the angle expressed in the same unit as the semivariance. The term ρ represents the phase of the angle expressed in radians and the term ω is the frequency, expressed in units of radians m^{-1} when the distance between samples is expressed in meters. According to eq. **[6]**, y would depend on h and could range from zero to 2 C_w, the mean variability due to the cyclic trend would be equal to C_w. Adding eq. **[6]** to eq. **[2]** gives the Spheric-Cyclic model:

$$\left.\begin{array}{l} y(h) = C_0 + C\left[(3h/2a) - \left(h^3/2a^3\right)\right] + C_w\left[1 + Sin(\rho + \omega h)\right] \ when\ h \le a \\ and \\ y(h) = C_0 + C + C_w\left[1 + Sin(\rho + \omega\ h)\right] \ when\ h \ge a \end{array}\right\} \quad [7]$$

Adding eq. **[6]** to eq. **[3]** gives eq. **[8]**, called here the Linear-Cyclic model:

$$C_0 + bh + C_w\left[1 + Sin(\rho + \omega\ \ h)\right] \quad [8]$$

In the same way, adding eq. **[6]** to eq. **[4]** gives the Nugget-Cyclic model:

$$C_0 + C_w\left[1 + Sin(\rho + \omega\ \ h)\right] \quad [9]$$

The resulting models can be used to mathematically describe and to quantify the importance of this cyclic source of variation among the other variation sources (i.e., nugget and regional sources of variation). The variogram can be partitioned into three terms: the Random (or Nugget) variance (C_0), the Regionalized variance,

$$\left.\begin{array}{l} y(h) = C\left(3\dfrac{h}{a} - \dfrac{h^3}{2a^3}\right) when\ h \le a \\ and \\ y(h) = C\ when\ h \ge a \end{array}\right\} \quad [10]$$

and the Cyclic variance (eq.**[6]**). For some of these models, it is possible to obtain an estimation of the "true" variance. In these situations, the variance estimator obtained from the model would closely match the ordinary sample variance (S^2). In the case of the Nugget-Cyclic model, the term (C_0+C_w) is an estimator of the "true" variance. In the case of the

Spheric-Cyclic model, the value of the model at the plateau (C_0+C_w+C) is also an estimator of the "true" variance. In the case of the Linear Cyclic model, however, an estimator of the "true" variance can not be derived from the model. When this estimator exists, the percentage of variation due to any of the three components (if they are present) can be calculated as the ratio between each particular component and the "true" variance estimator. For example, the percentage of Cyclic variation *(Cyc%)* can be calculated from:

$$Cyc\% = \frac{Cw}{C_T} \times 100 \qquad [11]$$

where C_T is an estimation of the "true" variance.

The period of the cyclic trend can be calculated directly from equation [7],

$$\Phi_M = \frac{2\pi}{\omega} \qquad [12]$$

where ω is a parameter in equation [6] and Φ_M is the period expressed in m cycle^{-1}. The inverse of this equation gives the frequency.

MATERIALS AND METHODS

Yield data were taken from an experiment to determine the effects of windrows of soybean residue on corn yields and nitrogen availability (Perdomo and Blackmer, 1995a). The windrows were made by combines spreading soybean residue from many soybean rows onto only a few rows. The data consisted of yields from 24 plots located along a transect going perpendicular to corn rows (Figure 2). The plots were located at essentially equal distances (3 meters) along the transect, and half were located on positions with soybean

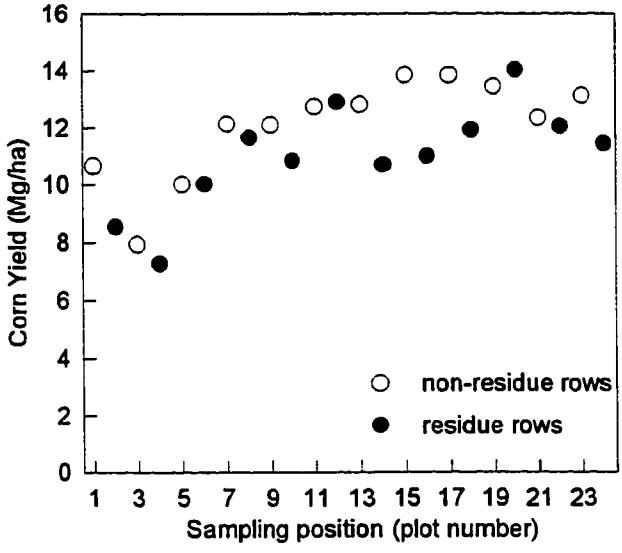

Figure 2. Grain yield of corn in residue-covered strips and bare strips of soil at 24 sampling positions.

residue and half on positions without residue. More detailed information about these experiments can be found in the referred publication (Perdomo and Blackmer, 1995a).

Six hypothetical datasets were created such that each simulated data collected from 64 plots along a transect. All datasets had a mean that was arbitrarily assigned a value of 14. Each of the six datasets had a different level of random noise added as shown in Figure 3. This was accomplished by generating a sequence of 64 random numbers between zero and one and then multiplying each by 0, 1, 2, 3, 4, or 5. These datasets are identified by the multiplier used.

Another set of six hypothetical datasets (Figure 4) was created by adding an identical cyclic signal to each of the datasets in Figure 3. This cyclic signal was generated by using the following equation:

$$Z_{(x_i)} = A_w \, Sin\left(\frac{2\pi P}{N h}\sum_{i=1}^{N} x_i\right) \qquad [13]$$

where Z is the value at sampling position x_i of a cyclic dataset composed of N samples (64 in these analyses) separated by a distance h of 1 m (sampling frequency). The term A_w represents the amplitude of the cyclic dataset and P represents the number of cycles or peaks in the data (6 in these analyses). It should be noted that the terms ($P N^{-1} h^{-1}$) represents the frequency expressed in cycles m^{-1} as later used in Fourier analysis. These terms multiplied by 2 π gives the frequency w in radians m^{-1} used in the cyclic models.

Isotropic semivariance of data was calculated using GS$^+$ geostatistical software (Gamma Design Software, 1993). Semivariance was calculated until 48 lags for the

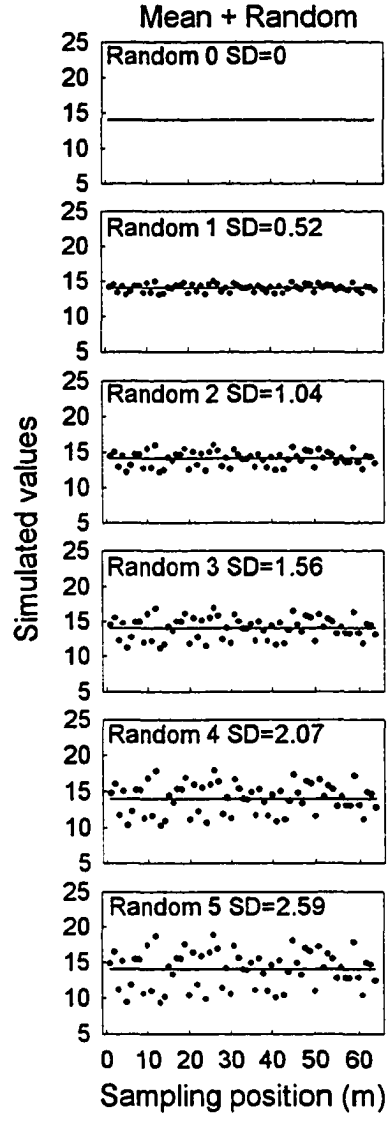

Figure 3. Simulated data produced by Mean + Random components.

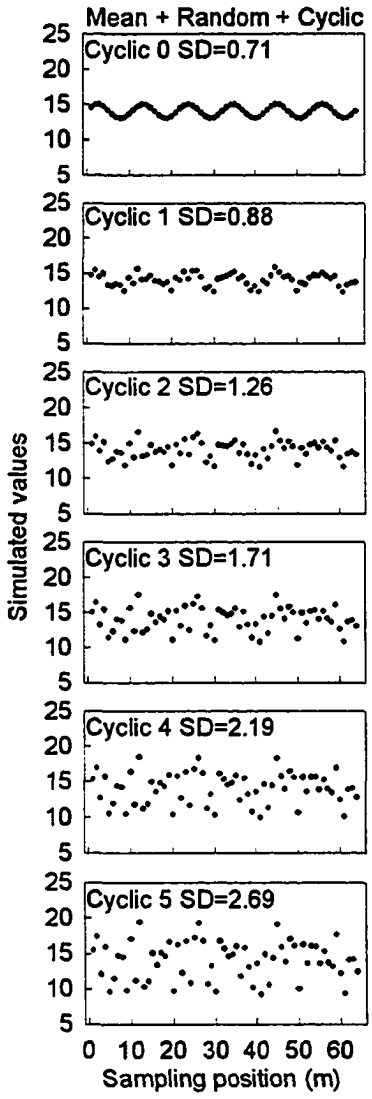

Figure 4. Simulated data produced by Mean + Random + Cyclic components.

simulated data and until 12 lags for the real data. This determined that the last lag class consisted of 16 and 12 data pairs for the simulated and real data respectively.

FFT analyses were performed using the algorithms available in the software package Mathematica (Wolfram, 1991). Equation **[14]** is the formula for obtaining the Fourier transforms for a discrete finite-length sequence of data, often called discrete Fourier transform or DFT (Oppenheim and Schafer, 1975):

$$H[k] = \sum_{n=0}^{N-1} Z[n] e^{-j(\frac{2\pi kn}{N})}, k = 0, 1, \ldots, N-1, \qquad \textbf{[14]}$$

where H represents the sequence of data in the discrete frequency k, Z represents the same sequence of data in the time or spatial discrete domain n, e is the base of natural logarithms, π is the number representing the ratio of circumference to diameter, and j is the imaginary number ($\sqrt{-1}$). Due to computational constraints, this formula is barely implemented as such in computational algorithms. Instead, more efficient algorithms are generally used. They are called fast Fourier transform (FFT hereafter) algorithms (Oppenheim and Schafer, 1975).

The discrete frequency k (which gives the total number of cycles in the dataset) was converted to frequency expressed in cycles m^{-1} according to:

$$f_F = k / (N \,.\, h) \qquad \textbf{[15]}$$

where f_F is the frequency expressed in cycles m^{-1} for the k position (counting from zero) within the spectrum, N is the number of data points, and h is the sampling frequency. In this

study we were interested in estimating the distance between cycles or period (Φ). The period of the cyclic signal from the FFT (Φ_F) was calculated from:

$$\Phi_F = \frac{1}{f_F} \qquad [16]$$

Cyclic models were fitted to semivariograms by using the NLIN Procedure of SAS (Ihnen and Goodnight, 1985). Because the simulated data included only a random and a cyclic component, the Pure Random-Cyclic Model was selected. For the real data, based on its highest R^2 , the Linear-Cyclic Model was selected.

RESULTS

Analysis on simulated data

Addition of random noise rapidly obstructed the visual detection of the cyclic signal in the simulated datasets (Figure 4). Each of these datasets, however, has a cyclic function with a known period. We reason that the method best able to characterize the known values amid the random noise would be the best method for identifying cyclic sources of variation in real datasets.

Figure 5 shows results of the FFT analyses on the 6 simulated cases. These analyses would reveal a clear peak at the frequency of 0.094 cycles m^{-1} (or 6 cycles in 64 m) if they correctly characterized the cyclic signal known to be present. Such a signal was found during the analysis of simulated datasets 0, 1, and 2. As levels of random noise increased, however, the random noise produced peaks that precluded characterization of the known cyclic signal.

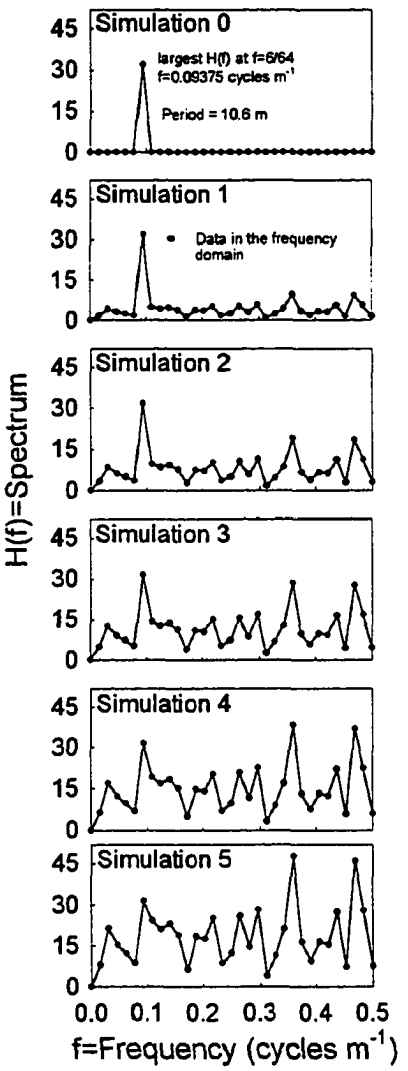

Figure 5 Fourier spectrum of raw data for simulations with increasing amount of random noise

The masking of the cyclic signal by the random noise in the spectrum is based on the property that the spectrum of the sum of two signals is equal to the sum of their spectrum (Carlson, 1975). An example of this property is shown in Figure 6, where the spectrum for Sim. 2 is clearly the sum of the spectrum for Random 2 and for Sim. 0. In these analyses the cyclic signal was always constant, so the spectrum for the cyclic component always remained constant. However, the spectrum for the random component continuously increased with the increase in the amount of random noise, producing an increased masking of the cyclic signal. As expected, the random component (Figure 5) showed no clear single peak.

The semivariograms for the six datasets from Figure 4 are shown by the points in Figure 7. In agreement with observations made by Clark (1979) the semivariograms sometimes revealed cyclic patterns better than did the datasets from which the semivariances were calculated. The cyclic model (i.e., the line in Figure 7) characterized the cyclic trend better than did the FFT analysis amid high levels of random noise. As expected, analysis of the random component alone did not reveal a cyclic trend (Figure 8). The coefficient of determination (R^2) of the model constantly decreased as the random error added to the cyclic signal increased (Figure 7), but this did not prevent the model from accurately estimating the distance between cycles. The ability of the model to identify cyclic components in these simulations gives basis for speculating that this methodology could work in a broad range of situations. The semivariance increased with each increasing level of random noise (Figure 7). As should be expected, increases in semivariance due to the random noise appeared as increases in the nugget components of the semivariograms. The nugget as identified by the

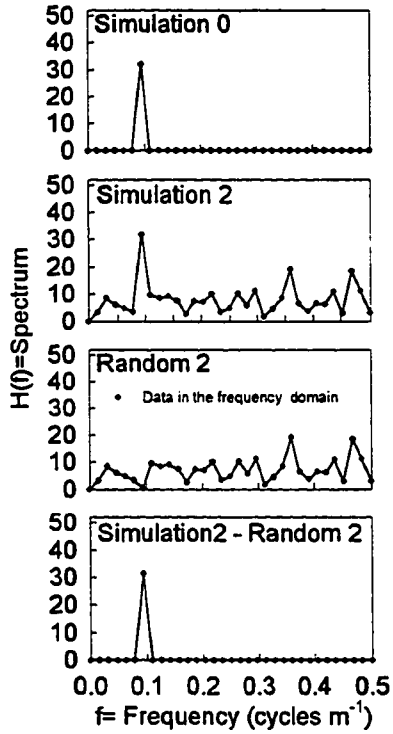

Figure 6. Fourier spectrum for Simulation 2 and its Random 2 and Cyclic 2 components as compared with the Fourier Spectrum for Simulation 0.

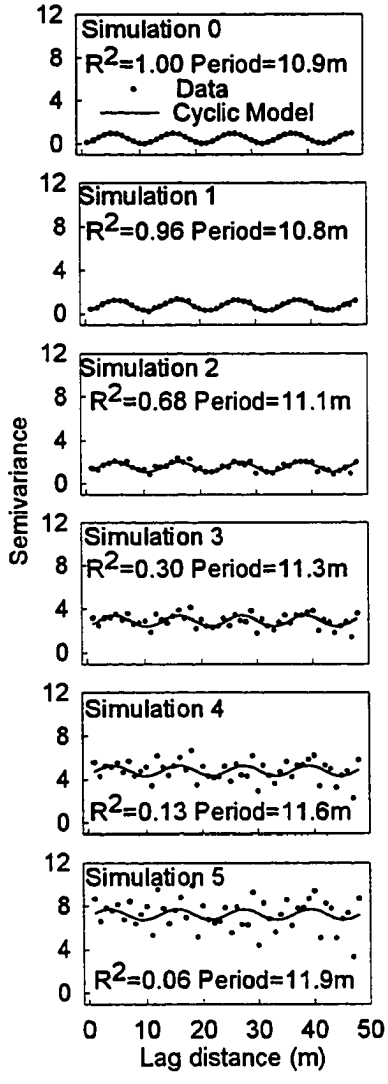

Figure 7. Semivariance values and cyclic model analyses for simulations with increasing amount of random noise.

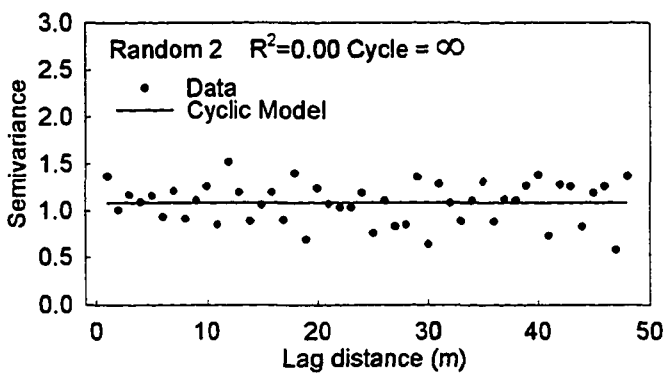

Figure 8. Semivariance values and cyclic model analysis for Random 2.

model, therefore, can be used as an estimator of the random component of the variation in the original dataset.

The reliability of this estimator can be evaluated by analyzing the simulated data because the random and cyclic component were added separately when the simulated datasets were created. Nearly perfect relationships between calculated and estimated amounts of random (Figure 9) and total (Figure 10) variability indicates that the cyclic model was a reliable estimator in this study. Additional evidence for the reliability of the model is indicated by the constancy of parameter C through all simulations. These observations suggest that the cyclic model, unlike the FFT analysis, can be used to partition variance.

Analysis on real data

As occurred with the simulated data having high levels of random noise added, no cyclic trend was evident from the plotting of the raw data (Figure 2). However, semivariogram analyses showed a clear cyclic shape. Moreover, the distance between cycles as calculated from the cyclic model was, as should be expected, the length of two plots (Figure 11). Contrary to what occurred in the simulated cases, where only regional and random components were present in the variogram, a strong linear regional trend was also present in the variogram of the corn yield data. When the data was analyzed using FFT, the analyses of neither the raw data nor the variogram data showed strong evidence of cyclic trends (Figure 12). However, when the linear trend was removed from the variogram data, FFT on the variogram then showed a very strong peak at exactly the same position predicted by the cyclic model. Obviously,the regional component of the variance was strong enough to

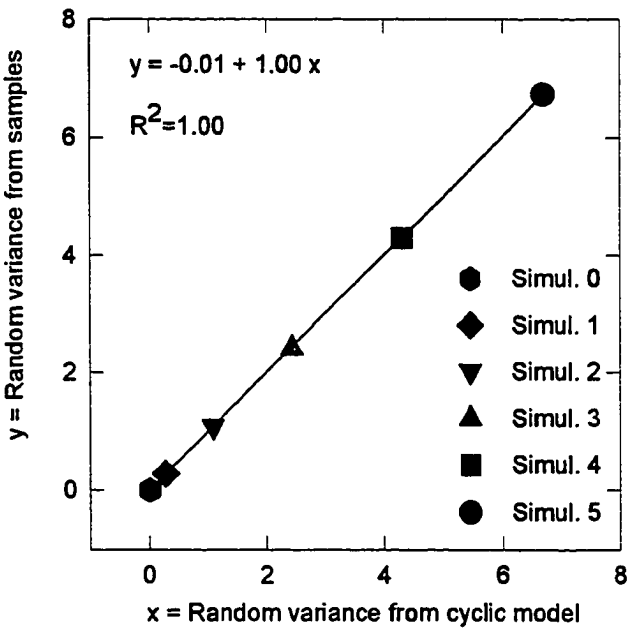

Figure 9 Relationship between the amounts of total variance estimated with the cyclic model and the amounts of total variance present in the simulated data.

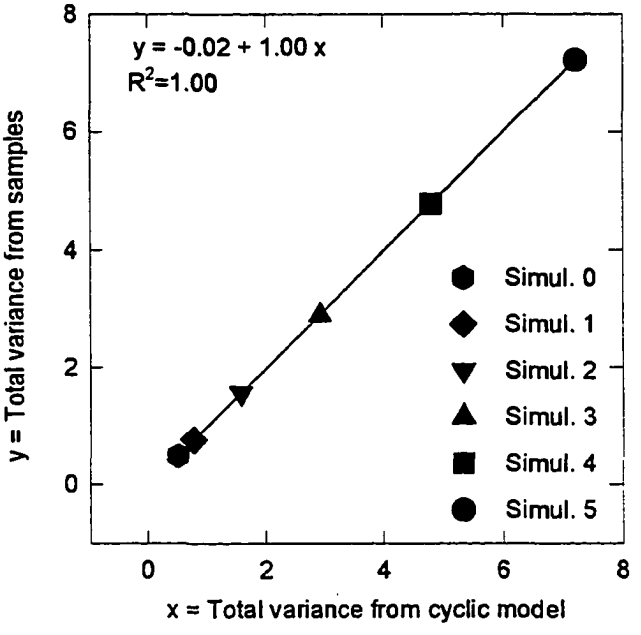

Figure 10. Relationship between the amounts of total variance estimated with the cyclic model and the amounts of total variance present in the simulated data.

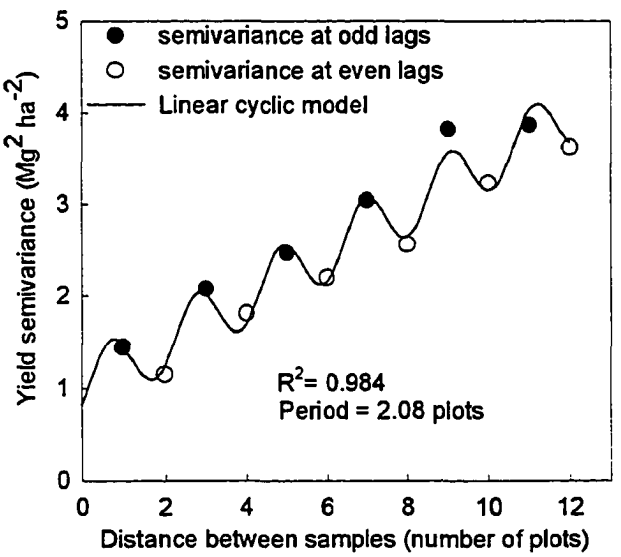

Figure 11. Semivariance values and cyclic model analyses on grain yield for corn growing on residue-covered strips and bare strips of soil.

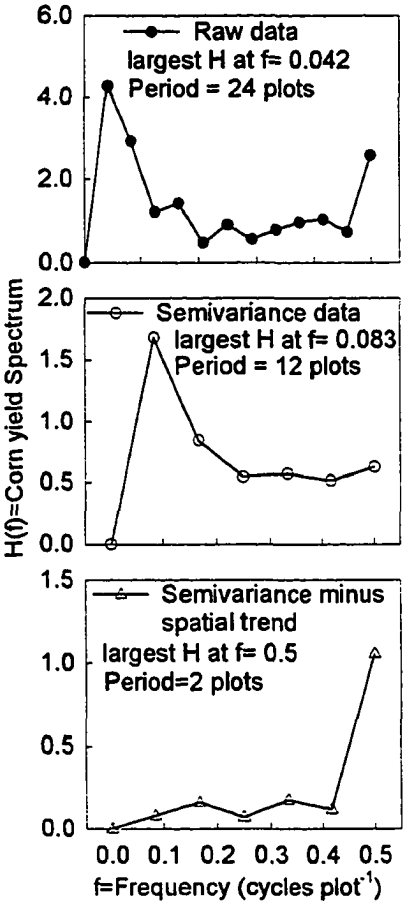

Figure 12 Fourier spectrum for grain yield of corn on raw data, on semivariance data, and on residual (regional variation removed) semivariance data.

interfere with the FFT analysis of the original variogram. This spatial component appeared as a peak at a very low frequency, an indication of a "cycle" with a extremely long period. Removing the spatial trend from the semivariance and then running FFT on the remainder can be considered analogous to using eq.[6] for calculating the distance between cycles. This analogy is also shown in Figure 12. After the spatial trend was removed from the semivariance data, the random and cyclic components of the cyclic model perfectly fit this new non-regionalized variogram.

Results of the analyses performed here seem to indicate that cyclic patterns can be successfully identified and separated from other sources of variability in distance series. This can be done even in the presence of important amounts of other sources of variation normally present in soils. Unlike analyses that consider only regional and random variability, those which include cyclic variability could help identify the origin or cause of this variability as well as methods of addressing this variability when sampling. If it is found that the cyclic variation is associated with management, improved practices could lead to a reduction of this variability source.

LITERATURE CITED

Carlson, A.B.1975. Communication systems. An introduction to signals and noise in electrical communication, 2d ed. McGraw-Hill Inc, New York, N.Y.

Clark, I. 1979. Practical Geostatistics. Applied Science Publishers, London.

Folorunso, O.A., and D.E.Rolston, 1985. Spatial and spectral relationships between field-measured denitrification gas fluxes and soil propierties. Soil Sci. Soc. Am. J. 49:1087-1093.

Gamma Design Software. 1993. Gs$^+$: Geostatistics for the environmental sciences 2.1 user's guide. Gamma Design Software, Plainwell, MI.

Ihnen, L.A., and J.H. Goodnight. 1985. The NLIN procedure. p. 575-606. *In* SAS user's guide: Statistics, 1985 ed. SAS Inst. Inc., Cary, N.C.

Isaaks, E.H., and R.M. Srivastava. 1989. Applied geostatistics. Oxford University Press, New York, N.Y.

Journel, A.G., and C.J. Huijbrets. 1978. Mining geostatistics. Academic Press,London.

Matheron, G 1965. Regionalized variables and their estimation. (in French.) Masson, Paris.

Oppenheim, A.V., and R.W. Schafer. 1975. Digital signal processing. 1975 ed. Prentice-Hall, Englewood Cliffs, N. J.

Perdomo, C.H., and A.M. Blackmer. 1995. Nitrogen availability in cornfields as affected by soybean residue. Agron. J. In preparation.

Webster, R. 1985. Quantitative spatial analysis of soil in the field. Adv. Soil Sci. 3:1-70.

Wolfram, S. 1991. Mathematica, a system for doing mathematics by computer, 2d ed. Addison-Wesley, Redwood City, CA.

DETECTING SUPERIMPOSED CYCLIC PATTERNS IN SOIL PROPERTIES

A paper prepared for submission to the *Soil Science Society of America Journal*

Carlos H. Perdomo and Alfred M. Blackmer

ABSTRACT

The objective of this work was to extend the methodology developed in a previous paper to partition variability when two or more cycles are superimposed in a dataset. The dataset used to test this approach was NO_3^- concentrations in 50 soil samples collected along a 76-m transect from a fertilized cornfield. Each sample was a composite of 16 3.2-cm-diam. cores collected at 9.37-cm intervals along the transect. A procedure was developed that involved fitting of a spherical model to a variogram, fitting a cyclic component to the residuals to make a spherical-one-cycle model, fitting another cyclic component to the residuals of the spherical-one-cycle model to make a spherical-two-cycle model, and repeating this process until the residuals show no statistically significant cyclic trends. Results showed that the amount of variability explained by the spherical component was small, and that an alternative model formed by a nugget and a three cyclic components was as least as good as the spherical-three-cycle model in describing the structure of the variogram. One of the cycles described by the models had a period resembling the width of fertilizer applicators commonly used in Iowa. Comparisons of the results from this model with FFT analysis showed that the cycles identified by the model agreed well with results from FFT. Overall, this result indicates that this technique can be used to identify superimposed cyclic trends in datasets collected along a transect.

INTRODUCTION

Variability in concentrations of plant-available nutrients in soils has long been recognized as a problem when sampling fields to assess nutrient availability and fertilizer needs. This problem has been addressed most often by assuming that most of the variability is caused by differences in soil characteristics that are described by modern methods of soil taxonomy as used in soil surveys. The problem also has been addressed by recognizing that a field often consists of two or more areas that were managed differently in the past. These considerations have led to recommendations that fields should be sampled by soil type or in a grid pattern. Such recommendations tacitly assume that differences due to soil type or recognizable differences in management history are much greater than definable patterns produced by cultural practices.

Recent studies (Perdomo and Blackmer, 1995a) have shown that windrows of residue formed during combining can influence concentrations of nutrients in soil and yields of grain in the corn crop that follows. A previous paper (Perdomo and Blackmer, 1995b) describes how the effects of the windrows can be described by adding a cyclic component to established geostatistical techniques that partition variability between regionalized and random components. This paper, however, does not address situations in which different factors cause different cyclic patterns that are superimposed. Superimposed cyclic patterns might be expected, for example, if concentrations of nutrients were simultaneously influenced by windrows of plant residue separated by a distance of 6 meters, rows of decaying plant root

systems separated by a distance of 0.76 meters, and rows of residual fertilizer in bands separated by a distance of 0.35 meters.

The objective of this report is to describe a method for partitioning variability when two or more superimposed cycles are present in datasets. Future papers will utilize this method to characterize the sources of spatial variability in soil NO_3^- concentrations found in cornfields in production agriculture.

THEORY

As indicated by Clark (1979), models generally used to represent the relationship between semivariance (y) and lag (h) in experimental variograms are, in fact, complex models composed of two or more components. One of these components is an estimator of the random variance and is called the Nugget (C_0).

$$y(h) = C_0 \qquad [1]$$

Another component describes the increase in semivariance with the increase in the lag and is called the spherical component,

$$\left.\begin{aligned} &y(h) = C\left[\left(3h/2a\right) - \left(h^3/2a^3\right)\right] \text{ when } h \le a \\ &\text{and} \\ &y(h) = C \text{ when } h \ge a \end{aligned}\right\} \qquad [2]$$

where the sill C indicates the value at which the spherical component levels off. The spherical model as normally used in geostatistics is a complex model composed of eq. [1] and [2]. When this model is used, the plateau $C_0 + C$ is an estimator of the population variance.

A previous paper (Perdomo and Blackmer, 1995b) describes use of a cyclic component for situations where wave or hole effects are detected:

$$y(h) = C_w \left[1 + Sin\ (\rho + \omega\ h)\right] \qquad [3]$$

There exists a real possibility that some datasets may have two or more cyclic patterns that are superimposed. Using eq. **[3]** as a basis, the cyclic term for multiple cycles can be expressed as:

$$y(h) = \sum_{i=1}^{n} C_{wi} \left[1 + Sin\ (\rho i + \omega i\ h)\right] \qquad [4]$$

where n in the summation term represents the number of cycles in the expression. This term can be called the n-cycle component.

The amplitude (C_w) in the single-cycle case gives an estimation of the variance due to the cycle (see Perdomo and Blackmer, 1995b). The summation of amplitudes

$$SC_w = \sum_{i}^{n} C_{wi} \qquad [5]$$

is an estimator of the variance due to multiple cycles. It is possible, therefore, to have a spherical-n-cycle model:

$$\left.\begin{aligned} &y(h) = C_0 + C\left[\left(3h/2a\right) - \left(h^3/2a^3\right)\right] + \sum_{i=1}^{n} C_{wi}\left[1 + Sin(\rho_i + \omega_i\ h)\right] \ \ when\ h \le a \\ &and \\ &y(h) = C_0 + C + \sum_{i=1}^{n} C_{wi}\left[1 + Sin\ (\rho_i + \omega_i\ h)\right] \ \ when\ h \ge a \end{aligned}\right\} \qquad [6]$$

The variance estimator (C_T) for the spherical-n-cycle would be:

$$C_T = C_0 + C + SC_w \quad [7]$$

where C_T represents the variance estimator from the model. The total variance can be partitioned into random, cyclic, and regionalized components according to

$$\text{Cyclic\%} = (SC_W / C_T) * 100 \quad [8]$$

$$\text{Regionalized\%} = (C / C_T) * 100 \quad [9]$$

$$\text{Random\%} = (C_0 / C_T) * 100 \quad [10]$$

The contribution from a particular cycle could be computed from

$$nth\text{\%-cycle} = (C_{w\text{-}nth} / C_T) * 100 \quad [11]$$

where *nth* represents the cycle number.

MATERIALS AND METHODS

The soil NO_3^- data used in this study were obtained in a more extensive study described in another paper (Perdomo and Blackmer, 1995c). The data were collected in early June from an area of seemingly uniform soil within a cornfield managed by a farmer using normal practices for the area. No treatments were applied for the study, but the farmer had applied anhydrous ammonia fertilizer in early spring. Fifty soil samples were taken to a depth of 30 cm along a 76.2-m transect perpendicular to the corn rows (76 cm apart). Each sample was a composite of sixteen 3.2-cm diameter cores collected at 9.37-cm intervals along the transect. Soil samples were dried in a forced-air oven at 49 °C and ground to pass a 2-mm sieve. Samples were later extracted with 2 *M* KCl, filtered, and analyzed for NO_3^- using a Lachat flow-injection procedure (Kopp and McKee, 1979).

Isotropic semivariance was calculated according to:

$$\gamma(h) = \frac{1}{[2m(h)]} \sum_{i=1}^{m(h)} \left[Z_{(x_i)} - Z_{(x_i+h)} \right]^2 \qquad [12]$$

where γ is the semivariance for m data pairs separated by a distance of h (known as a lag) and Z is the soil NO_3^- concentration at positions x_i *and* $x_i + h$ (Webster, 1985). Non-cyclic models described in a previous paper (Perdomo and Blackmer, 1995b) were fitted to the semivariance data using GS$^+$ geostatistical software (Gamma Design Software, 1993). Cyclic models described in the Theory section of this paper and in the Theory section of another paper (Perdomo and Blackmer, 1995b) were fitted to the semivariance data and to the residuals (semivariance minus model) by using the NLIN Procedure of SAS (Ihnen and Goodnight, 1985).

The fitting of complex models such as the spherical-nth-cyclic models was achieved through a succession of fitting steps. The procedure started with the fitting of a conventional geostatistical model using Gs$^+$ software. The next step was the computation of the residuals from this model. If visual observation suggested a cycle in the residuals, then the cyclic component described in the Theory section was fitted to this residual trend. If the fitting was statistically significant ($P \leq 0.05$), the cyclic component was combined with the spherical model into a single model. The term combining is used here (and hereafter) to represent the incorporation of a single cyclic trend into a more complex model. The combining process, however, was done independently of the fitting of the two separate models and required a new SAS program. The parameters obtained in the fitting of the single models were used as

initial values for the nonlinear iteration process that lead to the fitting of the combined model. More details about the fitting process are provided in the Results section.

When the final complex model was obtained, corrected residuals from the model were calculated by subtracting the value predicted by the complex model from the semivariance at each lag. Partitioning of the variance into random, regional, and cyclic components was performed as indicated in eq.**[8]** through **[11]** of the Theory section.

Fast Fourier transform (FFT) analyses were calculated on raw data and on semivariance data by using the algorithms available in the software package Mathematica (Wolfram, 1991). More information about FFT analysis were given in Perdomo and Blackmer (1995b). Frequency expressed in cycles m^{-1} was calculated according to:

$$f_{m\text{-}FFT} = k / (N \,.\, h) \qquad [13]$$

where k is the discrete frequency obtained from the Spectrum ranging from 0 to $N\text{-}1$, N is the number of samples (raw data) or lags (semivariance data), and h is the sampling frequency or lateral distance between samples (1.524 m in this work). To compare results from FFT with results from cyclic models, frequency from eq. **[13]** was transformed to frequency in radians m^{-1} (the units used to express the frequency in the cyclic models). This conversion was done according to:

$$f_{w\text{-}FFT} = f_{m\text{-}FFT} \,.\, 2\,\pi \qquad [14]$$

where π represents the ratio of circumference to diameter. The period (Φ), or wavelength, of the cycles (in meters) was calculated from the parameter w in the cyclic models according to

$$\Phi_{Model} = 2\,\pi\,/w \qquad [15]$$

and compared with the period calculated from FFT, either from expression **[13]**

$$\Phi_{FFT} = 1\,/\,f_{m\text{-}FFT} \qquad [16]$$

or from expression **[14]**

$$\Phi_{FFT} = 2\,\pi\,/\,f_{w\text{-}FFT} \qquad [17]$$

where results from eq. **[16]** and **[17]** are completely equivalent.

RESULTS

Concentrations of soil NO_3^- showed appreciable variability with no clearly recognizable pattern across the transect sampled (Figure 1). The observed degree of variability would be an important problem when sampling to assess N availability because optimum concentrations of soil NO_3^- are about 25 mg N kg^{-1} soil (Binford et al., 1992). Amid the observed levels of variability, sampling to determine the mean NO_3^- concentration within a 90% confidence interval of even 10 mg N kg^{-1} soil would be difficult.

Analysis of semivariance (Figure 2a) revealed that the shape of the variogram (i.e., the points) did not resemble the expected variogram shape for a regionalized variable. As shown by the spherical model selected by the Gs^+ (the line in Figure 2a) a typical regionalized variogram usually shows an increase in semivariance with increase in lag until a point at which the semivariance becomes more or less stable. Nevertheless, the geostatistical software used (Gs^+), selected the spherical model (i.e., the line), which is the typical model for describing a regionalized variable, as the best fitting model for this dataset. Visual observation of the fit of the model and consideration of the low R^2 value attained suggests

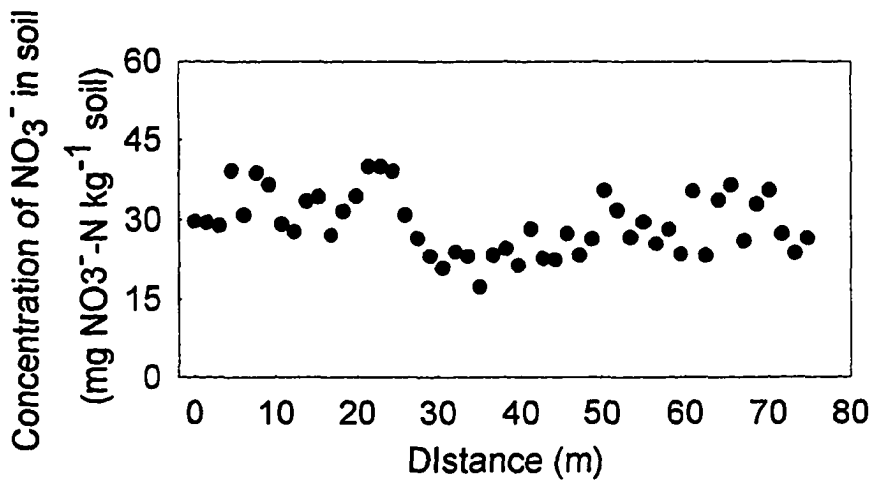

Figure 1. Concentration of NO_3^--N in soil at 50 sampling positions along a transect.

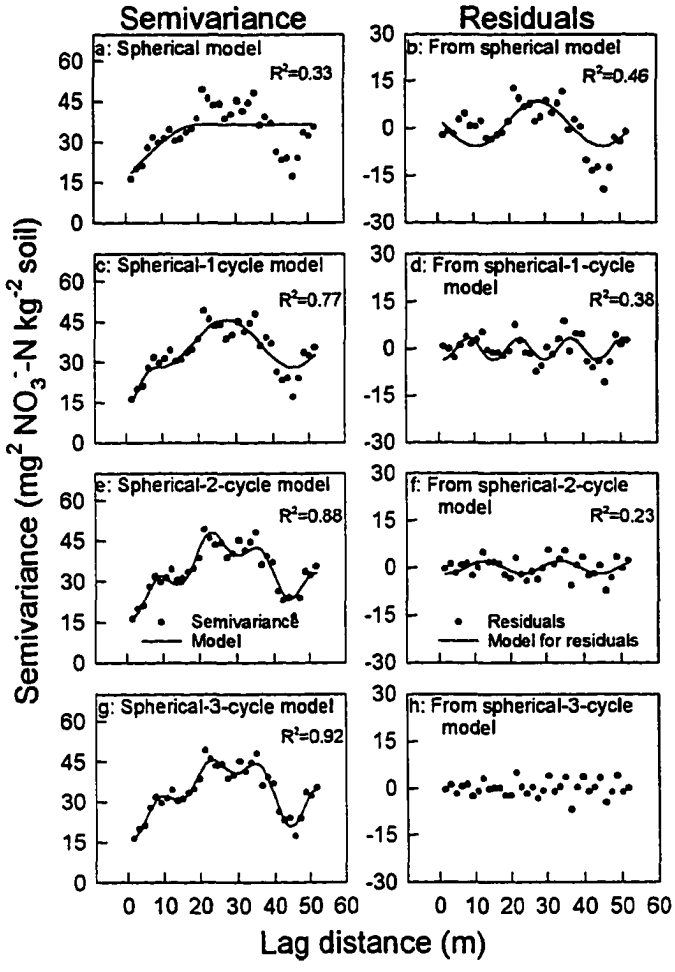

Figure 2. Fitting procedure of the experimental variogram for soil NO_3^- concentrations and residual analyses leading to the fitting of the Spherical-3-cycle model.

that the spherical model was not a good representation of the experimental variogram for this particular dataset. Furthermore, residual analysis (i.e., computing the difference between the data and the value predicted by the spherical model at each lag point) showed a cyclic pattern in the residuals (Figure 2b). Indeed, a cyclic component fit reasonably well to this residuals (Figure 2b). Combining the spherical model shown in Figure 2a with the cyclic model shown in Figure 2b resulted in the spherical-1-cycle model shown in Figure 2c. Visual analysis and computation of the R^2 value clearly showed that the combined model did a better job of explaining the variogram shape than did the spherical model alone. Further residual analysis showed, however, that a significant cyclic trend still remained in the semivariance. This cyclic trend could be clearly represented by another cyclic component (Figure 2d).

Combining the spherical-1-cycle model shown in Figure 2c with the cyclic model shown in Figure 2d resulted in the spherical-2-cycle model shown in Figure 2e. Again, the combined model clearly represented the variogram shape better than did the spherical-1-cycle model. Analysis showed, however, that a new cyclic trend was observed in the residuals (Figure 2f). It would be reasonable to question if there were a real cycling pattern in the residuals shown in Figure 2f, but simulation analyses presented in a previous paper (Perdomo and Blackmer, 1995b) showed that only small amounts of noise can obscure visual detection of cyclic patterns. For the purpose of this analysis, therefore, the existence of the third cyclic pattern is accepted because the fit of the model was statistically significant.

Combining the spherical-2-cycle model shown in Figure 2e with the cyclic model shown in Figure 2f resulted in the spherical-3-cycle model shown in Figure 2g. When

evaluated by comparisons of R^2 values, the spherical-3-cycle model did a slightly better job of explaining the variogram shape than did the spherical-2-cycle model. Residual analysis showed no further cyclic patterns in the semivariance. Indeed the residuals shown in Figure 2h show no obvious patterns in the distribution around zero.

Analyses of the corrected residuals (Figure 3) revealed that the regionalized component seem relatively unimportant after cyclic patterns were removed. This finding suggests that a new model composed of a nugget and three cyclic trends (nugget-3-cycle model) might provide a reasonable description of the semivariance. Corrected residuals for the different components of such a model are illustrated in Figure 4, and the fit of the model to the variogram is shown in Figure 5. Although the spherical model was not used to develop Figure 4 or 5, the frequencies of the cycles identified were similar to those obtained when the spherical model was used (Table 1). Because the nugget-3-cycle model had a slightly higher R^2 than did the spherical-3-cycle model (Table 1), it seems reasonable to conclude that there was no regionalized component in the dataset analyzed.

Partitioning of the variance by the spherical model and the cyclic models (Table 2) showed that part of the variability described as random or regional by the spherical model was explained as cyclic by both cyclic models. This result clearly indicates that analysis of spatial variability in NO_3^- concentrations by methods that do not consider cyclic patterns would not have been effective for describing the observed variability. Indeed, part of the variability explained by considering cyclic patterns could reasonably be produced by normal management practices.

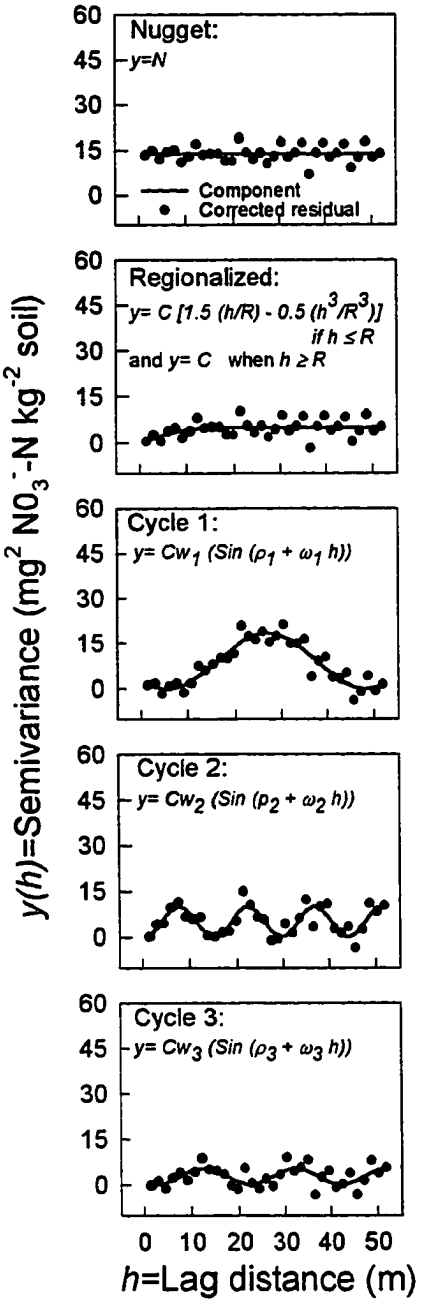

Figure 3. Corrected residuals for the components of the Spherical-3-cycle model.

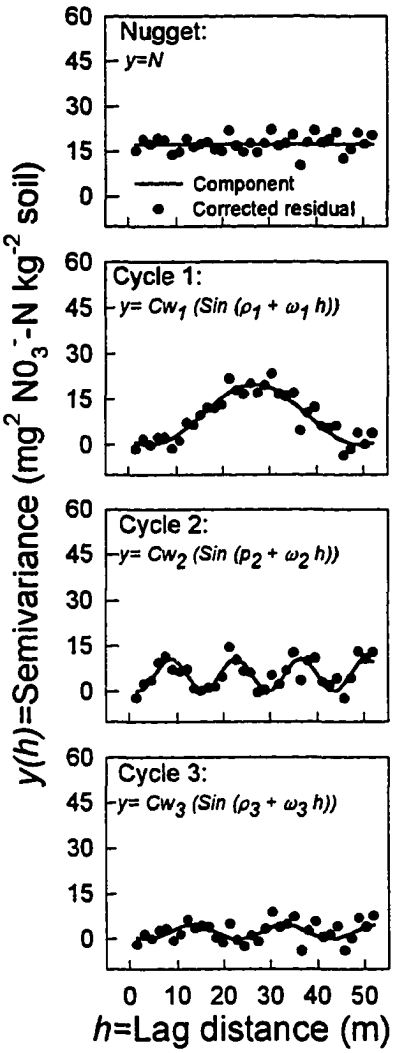

Figure 4. Corrected residuals for the components of the Nugget-3-cycle model.

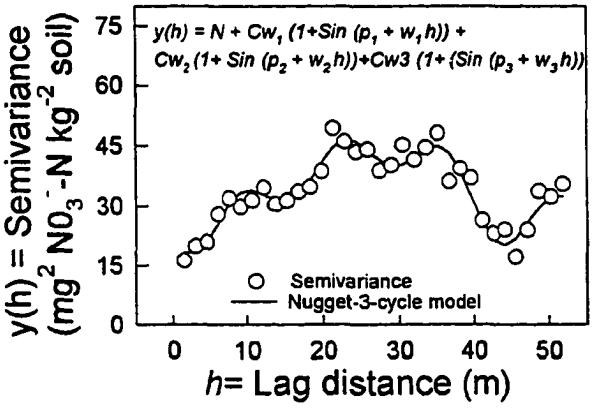

Figure 5. Fitting of the Nugget-3-cycle model to the variogram for soil NO_3^- concentrations

Table 1. Parameters of several geostatistical models for soil NO_3^-.

	$\rho 1$	$\rho 2$	$\rho 3$	$\omega 1$	$\omega 2$	$\omega 3$	C_0	C_{W1}	C_{W2}	C_{W3}	C	RANGE	R^2
	--------- radians ---------			------- radians m^{-1} -------			---------- mg^2 NO_3^--N kg^{-2}soil ----------					---m---	
Spherical	NA	NA	NA	NA	NA	NA	16.353	NA	NA	NA	20.218	20.598	0.327
Spherical-3-cycle	3.911	4.550	3.896	0.146	0.430	0.316	13.684	9.246	5.084	2.703	4.985	14.462	0.917
Nugget-3-cycle	4.112	3.910	3.642	0.140	0.452	0.319	17.362	9.909	5.410	2.345	NA†	NA	0.950

†NA=Not applicable

Table 2. Amount of variability estimated by several models and partition of this variability in different sources by the models.

Model†	Estimated total variance	Partition of variability						
		Random	Regional	Cycle 1	Cycle 2	Cycle 3	Total Cyclic	Total
	$mg^2\ NO_3^-\text{-}N\ kg^{-2}soil$	%						
Sp.	36.6	44.7	55.3	NA‡	NA	NA	NA	100.0
Sp-3-C	35.7	38.3	14.0	25.9	14.2	7.6	47.7	100.0
N-3-C	35.0	49.6	NA	28.3	15.4	6.7	50.4	100.0
S^2	32.5	NA	NA	NA	NA	NA	NA	NA

†Sp=spherical model, Sp-3-C=spherical-3-cycle model, N-3-C=nugget-3-cycle model, S^2=ordinary sample variance.
‡NA=Not applicable

Fast Fourier transform (FFT) analysis of the raw data (Figure 6a) revealed peaks at frequencies corresponding to the most important peaks identified by the nugget-3-cycle model. This finding provides support for the conclusion that the cyclic patterns were real. Also, the FFT spectrum of the raw data showed peaks at essentially the same wavelengths as did the FFT spectrum of the semivariance (Figure 6b). This finding corroborates observations (Perdomo and Blackmer, 1995b) that variograms tend to maintain the cyclic structure of raw data.

The periods, or wavelengths, of the cycles were estimated from the frequency obtained by using the two cyclic models as well as by using the FFT analyses (Table 3). For the FFT analyses, only the period calculated from the two main peaks in the spectrum were considered. Similar results were obtained from the two models and from the FFT.

Information about the periods or wavelengths of the cycles is useful because it can be used to identify the probable causes of the observed variability in soil NO_3^- concentrations. For example, the period of cycle 2 corresponds to the width of the fertilizer applicator used in the field studied, so it seems likely that a portion of the observed variability in soil NO_3^- concentration was caused by non-uniform pattern of application across the width of the applicator (for example, higher rates of application in the middle than at the ends).

It should be noted that the exact methods used to collect soil samples could have great impact in the nature of the variability observed. The method used in this study (compositing several cores collected as close as possible in a line), for example, minimized any regionalized variability having a range less than 1 meter or any cyclic patterns having

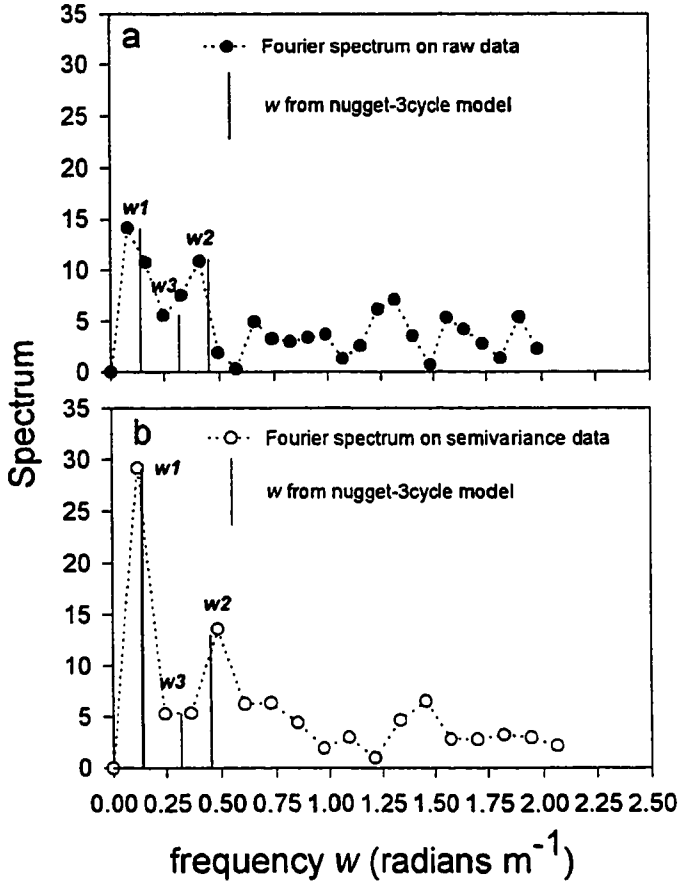

Figure 6. Fourier spectrum of raw and semivariance data for soil NO_3^-.

Table 3. Period of each cycle in the variogram as given by several models.

Model	Period		
	Cycle 1	Cycle 2	Cycle 3
	m		
Spherical-3-cycle	43	15	20
Nugget-3-cycle	45	14	20
FFT (on variogram)	52	13	NC[†]

periods less than 1 meter and, therefore, helped identify cyclic patterns having longer periods. In contrast, analysis of individual cores that were collected as close as possible along a line (as done in Perdomo et al., 1995) would reveal any cyclic patterns having shorter periods, and cyclic patterns having relatively long periods would appear as a regionalized component of variability. Unless a complex nested pattern of sampling is done, any system of sampling should be expected to falsely identify cyclic patterns having some periods as random or regionalized variability.

The possibility of important cyclic patterns having periods of several meters or more deserves special attention. Such patterns obviously could be produced by modern fertilizer applicators that are improperly adjusted, and they should be expected to result in large amounts of unexplained variability whether one samples by soil type or in a grid pattern. Failure to recognize the existence of the cyclic patterns would lead one to conclude that it is impossible to develop more efficient sampling methods. Moreover, failure to detect these patterns would prevent one from recognizing possible benefits of using better methods of applying fertilizers.

LITERATURE CITED

Binford, G.D., A.M. Blackmer, and M.E. Cerrato. 1992. Relationships between corn yields and soil nitrate in late spring. Agron. J. 84:53-59.

Clark, I. 1979. Practical Geostatistics. Applied Science Publishers, London.

Gamma Design Software. 1993. Gs$^+$. Geostatistics for the environmental sciences 2.1 user's guide. Gamma Design Software, Plainwell, MI.

Ihnen, L.A., and J.H. Goodnight. 1985. The NLIN procedure. p. 575-606. *In* SAS user's guide: Statistics, 1985 ed. SAS Inst. Inc., Cary, N.C.

Kopp, J. E., and G. D. McKee. 1978. Methods for chemical analysis of water and wastes. Method 351.2, nitrogen, ammonia. EPA Report no. EPA-6000/4-79-020. EPA Environmental Monitoring and Support Laboratory, Cincinnati, OH.

Perdomo, C.H., and A.M. Blackmer. 1995a. Nitrogen availability in cornfields as affected by soybean residue. Agron. J. In preparation.

Perdomo, C.H., and A.M. Blackmer. 1995b. Identification of cyclic sources of variability in soils. Soil Sci. Soc. Am. J. In preparation.

Perdomo, C.H., and A.M. Blackmer. 1995c. Large-scale cycles in the spatial structure of soil nitrate concentrations of cornfields. Soil Sci. Soc. Am. J. In preparation.

Perdomo, C.H., A.M. Blackmer, and. C.J. Green. 1995. Small-scale cycles in the spatial structure of soil nitrate concentrations of cornfields. Soil Sci. Soc. Am. J. In preparation.

Webster, R. 1985. Quantitative spatial analysis of soil in the field. Adv. Soil Sci. 3:1-70.

Wolfram, S. 1991. Mathematica, a system for doing mathematics by computer, 2d ed. Addison-Wesley, Redwood City, CA.

SMALL-SCALE CYCLES IN THE SPATIAL STRUCTURE OF SOIL NITRATE CONCENTRATIONS OF CORNFIELDS

A paper prepared for submission to the *Soil Science Society of America Journal*

Carlos H. Perdomo, Alfred M. Blackmer, and Cary J. Green

ABSTRACT

This paper studied the amount and structure of small-scale variability in soil NO_3^- concentrations and soil water content at 10 different cornfields in 1994. At each site, 120 samples were collected from the surface 30-cm layer of soil along a 9.1-m transect. Results showed that variability in concentrations of soil NO_3^- tended to be higher in sites that received N fertilization and that young plants in rows were an important source of variability in concentrations of soil NO_3^- and soil water content. Geostatistical models previously developed were used to characterize this variability, that at many sites appeared in variograms analysis as a cycle with a period determined by the distance between rows.

INTRODUCTION

Soil testing to determine concentrations of NO_3^- in late spring has been identified as a promising method for improving N management during the production of corn in the northern half of the United States (Magdoff et al., 1984, 1990; Blackmer et al., 1989; Fox et al., 1989; Binford et al., 1992; Meissinger et al, 1992). Such testing provides assessments of available N in the soil after losses induced by spring rainfall and after losses or gains of available N due to immobilization or mineralization as soil temperatures increase in the spring. These assessments enable site-specific adjustments in fertilization rates at the time of

sidedressing. In situations where it is necessary to apply N fertilizer before or at the time of planting, these assessments provide feedback that can be used to improve N management in future years.

Soil sampling in late spring (i.e., when corn plants are 15 to 30 cm tall) requires consideration of the location at which cores should be collected relative to plants or rows of plants. This consideration is necessary because it should be suspected that the presence of small plants could introduce variability in concentrations of NO_3^- in the soil. If the small plants do induce patterns in soil NO_3^- concentrations, then sampling bias would be introduced unless an appropriate sampling pattern were used. In absences of a given sampling pattern, inadvertent differences in pattern among individuals collecting samples could introduce unexplainable variability into the concentrations of NO_3^- observed. The importance of this possible problem in soil NO_3^- testing has received little attention.

Assessments of the importance of the effects of young plants on variability in soil NO_3^- concentrations require information about the amount and the spatial structure of NO_3^- concentrations in soils. Part of this information can be obtained by using geostatistical techniques (Dahiya et al., 1985, Van Meirvenne and Hoffman, 1989, Goovaerts and Chiang , 1993, Cahn et al., 1994, Cambardella et al., 1994). It was noted by Perdomo and Blackmer (1995 a), however, that these techniques do not consider cyclic spatial trends, which should be expected in fields where crops are managed in rows. It also was noted that cyclic patterns were not easily seen in raw data because small amounts of random noise tended to prevent visual detection of cyclic patterns when they occurred. Analyses presented in a previous

paper (Perdomo and Blackmer, 1995b) showed that simultaneous occurrence of two or more superimposed cyclic patterns also tended to prevent visual detection of cyclic patterns when they occurred. For these reasons, attempts to characterize the amounts of variability and the spatial structure of soil NO_3^- concentrations in cornfields must give careful consideration to the possible importance of cyclic trends.

The objective of this report is to describe the spatial structure of soil NO_3^- concentrations found when several cornfields were sampled in late spring of 1994 by using methods that should be expected to detect cyclic patters having periods of about 0.5 to 5 meters. Another paper (Perdomo and Blackmer, 1995 c) describes the spatial structure of soil NO_3^- concentrations found when several cornfields were sampled in late spring of 1993 by using methods that should be expected to detect cyclic patters having periods of about 5 to 30 meters.

MATERIALS AND METHODS.

The data used in this study were collected from cornfields in production agriculture in late spring of 1994. All sites were managed by farmers using normal practices for the area, and this often involved application of fertilizer N before planting. In some cases, separate samples were collected from fertilized and nonfertilized sites within a single field. Each site consisted of an area of seemingly uniform soil type. Information about sites is presented in Table 1.

Each site was sampled by collecting a 120 individual soil cores (diam. of 3.2 cm each) to a depth of 30 cm along a 9.1-m transect. The soil from each core was mixed thoroughly

Table 1.Soil description at each field and fertilization applied to each experimental site.

			Fertilization at each site	
Field number	Location	Series	Site 1	Site 2
1	Creston	Sharpsburg	NF[†]	FL[‡]
2	Creston	Macksburg	NF	FL
3	Scranton	Webster	M[§]	M
4	Rainbeck	Klinger	NF	FL
5	Rainbeck	Dinsdale	NF	FL

[†]NF=Non fertilized
[‡]FL=Urea Ammonium Nitrate solution applied
[§]M=Manure applied

and a subsample was taken for determination of water content. The remainder of the core was extracted with 2 *M* KCl, filtered, and analyzed for NO_3^- using a Lachat flow-injection procedure (Kopp and McKee, 1978). Soil subsamples collected for water content determination were dried in a forced-air oven at 105 °C for 24 hours and the soil water content was determined gravimetrically. Soil NO_3^- concentrations were adjusted to a dry weight basis.

Variograms for soil NO_3^- and soil water content were computed as described in another paper (Perdomo and Blackmer, 1995a). The maximum lag distance used was equivalent to 83 cores, which means that the semivariance at the last lag was estimated with 37 samples. Conventional geostatistical models (non-cyclic models) described in other papers (Perdomo and Blackmer, 1995a , 1995b) were fitted to the semivariance data by using GS^+ geostatistical software (Gamma Design Software, 1993). Cyclic models described in two other papers (Perdomo and Blackmer, 1995a , 1995b) were fitted to the semivariance data by using the NLIN Procedure of SAS (Ihnen and Goodnight, 1985).). The estimations of total variance from cyclic and non-cyclic models were computed using formulas previously described in other papers (Perdomo and Blackmer, 1995a , 1995b). Two exceptions, however, were made. The variance estimators for sites with regionalized components showing a linear trend were arbitrarily calculated as the maximum value predicted by the model because geostatistical models with linear trends cannot be used as variance estimators (Clark, 1979). At sites 2-FL and 3-M1, the variance estimators from the cyclic models were arbitrarily calculated as $C_0 + 1.5\ C_w$ instead of $C_0 + C_w$. The reason for the change was

because the cyclic model at those sites described only half of a cycle, and in this situation C_w is not longer an estimator of the cyclic variability. Corrected residuals for cyclic models were computed according to procedures already described in another paper (Perdomo and Blackmer, 1995b). Variograms showing calculated semivariance and models as well as figures showing corrected residuals and components of cyclic models were expressed as percentages of the maximum observed semivariance for this dataset. This form of expression is referred to as "relative semivariance" in this dissertation, and it was used only to facilitate graphing and visualization of the structure of variograms from sites having great differences in amounts of total variance.

Fast Fourier transform (FFT) analyses were calculated on raw and on semivariance data using the algorithms available in the software package Mathematica (Wolfang, 1991). To compare results from FFT with results from cyclic models, frequency from FFT ($f_{w\text{-}FFT}$) was expressed in radians m^{-1} according to

$$fw\text{-}FFT = 2\,p\,k\,/\,(N\,.\,h) \qquad [1]$$

where k is the discrete frequency obtained from the Spectrum ranging from 0 to N-1, N is the number of samples (raw data), or lags (semivariance data), h is the sampling frequency or lateral distance between samples (0.0762 m in this work) and π is the number representing the ratio of circumference to diameter. As occurred with variogram data, for graphing convenience spectrum values were expressed as a percentage of the maximum value for each dataset. Regression and correlation analysis were done using the REG (Ihnen et al., 1985) and CORR (Delong, 1985) Procedures of SAS.

RESULTS

Mean concentrations of soil NO_3^- within sites ranged from 9.6 to 34.5 mg NO_3^- kg^{-1} soil, and the standard deviations for these concentrations ranged from 3.5 to 26.2 mg NO_3^- N kg^{-1} soil (Figure 1). The standard deviations for NO_3^- concentrations tended to increase with mean NO_3^- concentrations, so variability in fertilized soils tended to be greater than the variability in nonfertilized soils. The highest variability was observed at a manured site, and this variability undoubtedly reflects non-uniform application of manure by the farmer. According to the late-spring soil test, the optimum NO_3^- concentration for corn at this time is 21 to 26 mg N (Binford et al., 1992). Concentrations of soil NO_3^- observed in this study were within the range usually found in Iowa cornfields in late spring (Blackmer et al., 1992). The reasons for the differences in concentrations and variability in soil NO_3^- concentrations among sites are of course several, and there is no intention to cover this topic here. Agricultural activities, however, seems to be an important source of variability.

Variograms for NO_3^- concentrations are indicated by the points in Figure 2. The dashed lines in this figure illustrate the geostatistical model selected for each dataset by the Gs^+ software. This software is commonly used for geostatistical analysis, and is frequently mentioned in recent publications in soil related studies (Gambardella et al. 1994, Chan et al., 1994). Relevant information about these models is presented in Table 2. The solid lines in Figure 2 illustrate the best fitting cyclic models selected at each site by using procedures described by Perdomo and Blackmer (1995b). Relevant information about these models is presented in Table 3. Figures 3 and 4 illustrates the various components of the best fitting

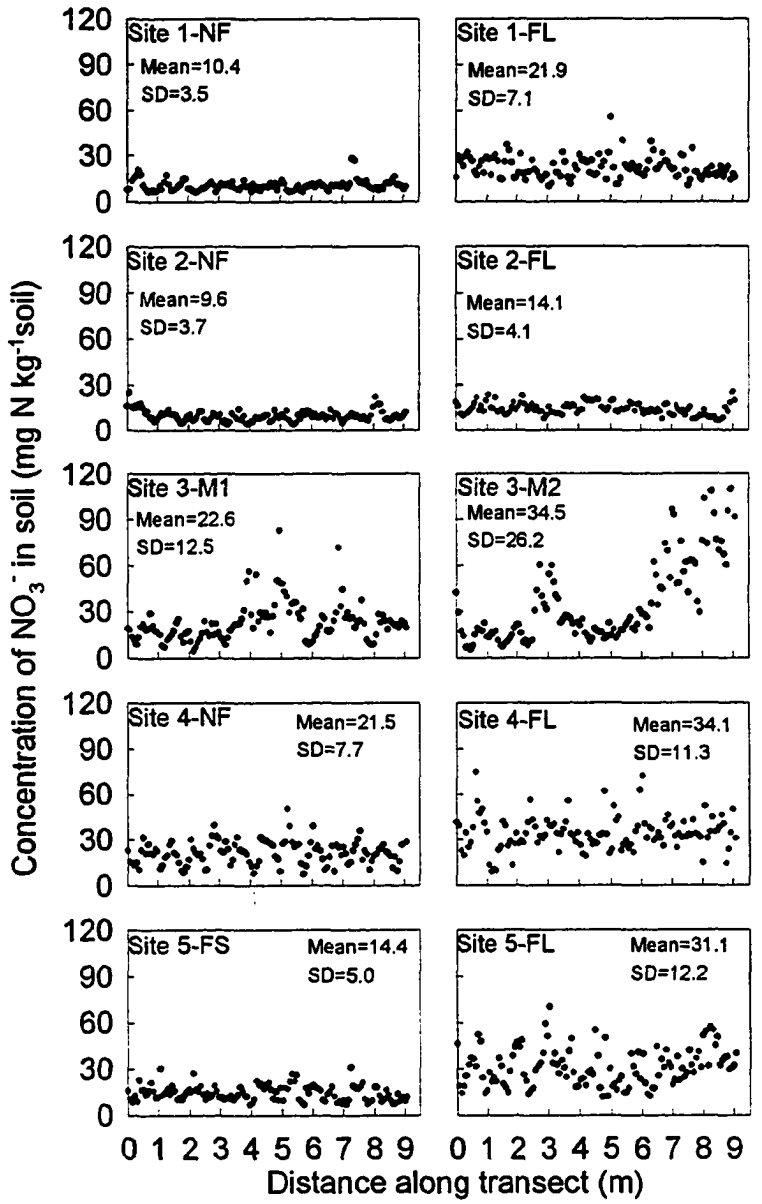

Figure 1. Soil NO_3^- concentrations along a 9.1 m transect at several sites.

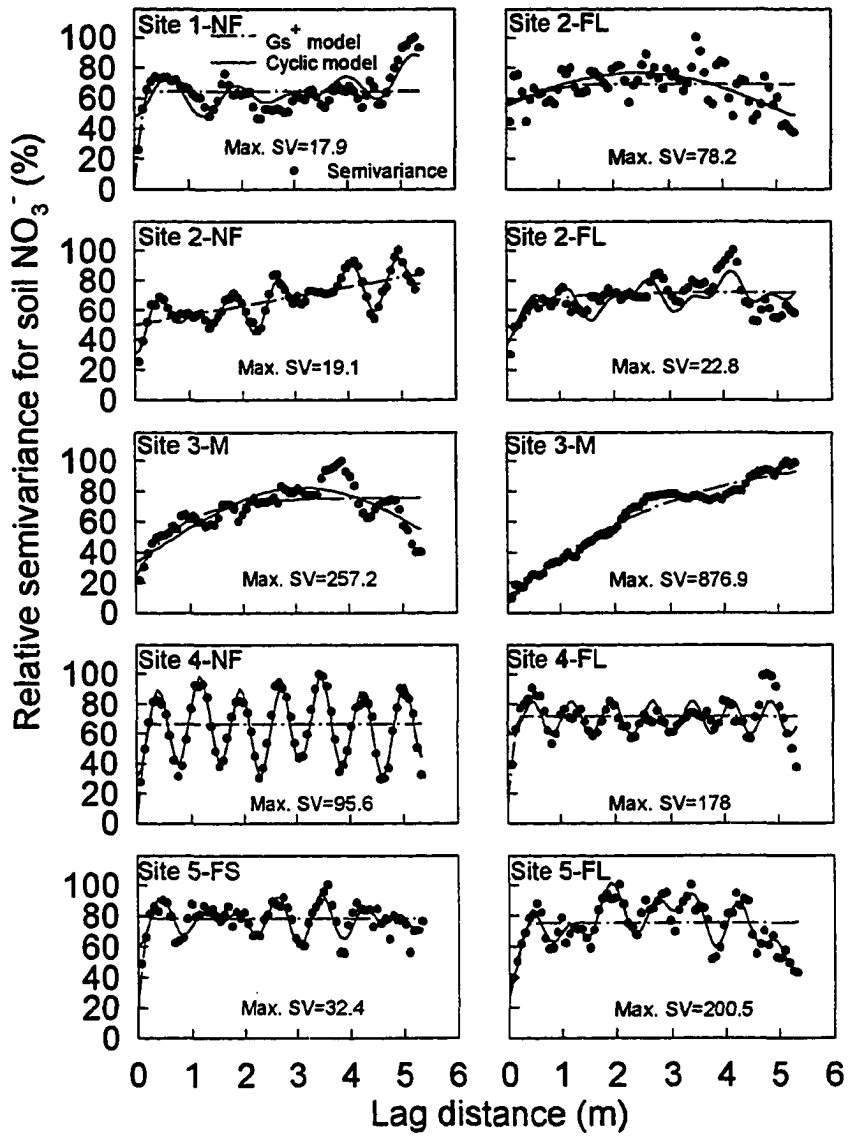

Figure 2. Calculated variograms for soil NO_3^- concentration and cyclic and non-cylic models fitted to the variograms at several sites. Maximum semivariance at each site (Max. SV) is expressed in units of mg^2 NO_3^- N kg^{-2} soil.

Table 2. Coefficient of determination (R^2), and estimations of total variance, percentage of nugget variance, and range of influence obtained from the fitting of Gs^+ models to soil NO_3^- variograms at several site-orientations.

Site	F†	Model	R^2	Total variance	Nugget variance	Range
				----mg^2 NO_3^--N kg^{-2} soil----	– % –	- m -
1	N	Spherical	0.16	11.5	0.1	0.25
1	UAN	Spherical	0.05	54.0	83.3	1.70
2	N	Linear	0.49	16.1	59.3	≥5.33
2	UAN	Exponential	0.30	16.4	50.5	0.47
3	M1	Exponential	0.53	194.8	32.3	0.78
3	M2	Exponential	0.97	950.6	6.2	2.84
4	N	Spherical	0.06	63.6	6.4	0.27
4	UAN	Spherical	0.13	127.5	16.3	0.23
5	S	Spherical	0.14	25.3	34.5	0.25
5	UAN	Spherical	0.14	151.4	36.5	0.43

† F=Fertilization: UAN=Urea Ammonium Nitrogen, N=No fertilized, M=Manure, S=Solid Urea

Table 3. Coefficient of determination (R^2), and estimations of total variance, percentages of nugget, cyclic, and regionalized variances, and range of influence obtained from the fitting of cyclic models to soil NO_3^- variograms at several sites.

Site	F†	Regionalized Component	R^2	Total variance	Nugget variance	Cyclic variance				Regionalized variance	Range
						Cycle 1	Cycle 2	Cycle 3	Total		
				---- mg^2 NO_3^--N kg^{-2} soil ----		---------- % ----------					- m -
1	N	Spherical	0.37	11.5	0.0	0.0	13.0	0.0	13.0	87.0	0.28
1	UAN	None	0.42	50.2	42.2	57.8	0.0	0.0	57.8	0.0	0.00
2	N	Linear	0.95	16.3	32.3	3.3	10.6	10.8	24.7	43.0	≥5.33
2	UAN	Linear	0.45	17.2	64.2	0.0	11.5	7.3	18.8	17.0	≥5.33
3	M1	None	0.72	160.3	97.2	2.8	0.0	0.0	2.8	0.0	0.00
3	M2	Linear	1.00	925.8	8.6	8.3	3.7	0.0	12.1	79.3	≥5.33
4	N	None	0.95	62.3	48.1	0.0	8.6	43.3	51.9	0.0	0.00
4	UAN	None	0.49	126.2	83.9	0.0	0.0	16.1	16.1	0.0	0.00
5	S	None	0.64	25.2	78.1	0.0	9.6	12.2	21.9	0.0	0.00
5	UAN	None	0.84	124.9	31.8	36.4	15.2	16.6	68.2	0.0	0.00

† F=Fertilization: UAN=Urea Ammonium Nitrogen, N=No fertilized, M=Manure, S=Solid Urea

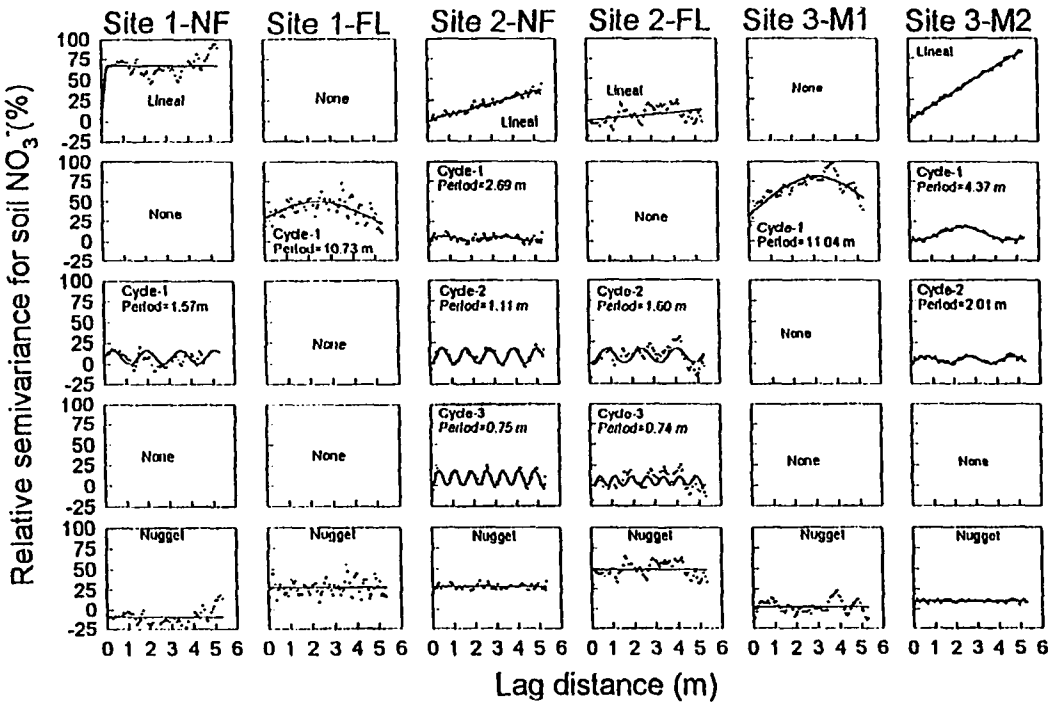

Figure 3. Components for cylic models and corrected residuals for soil NO_3^- semivariance data for sites 1 to 3.

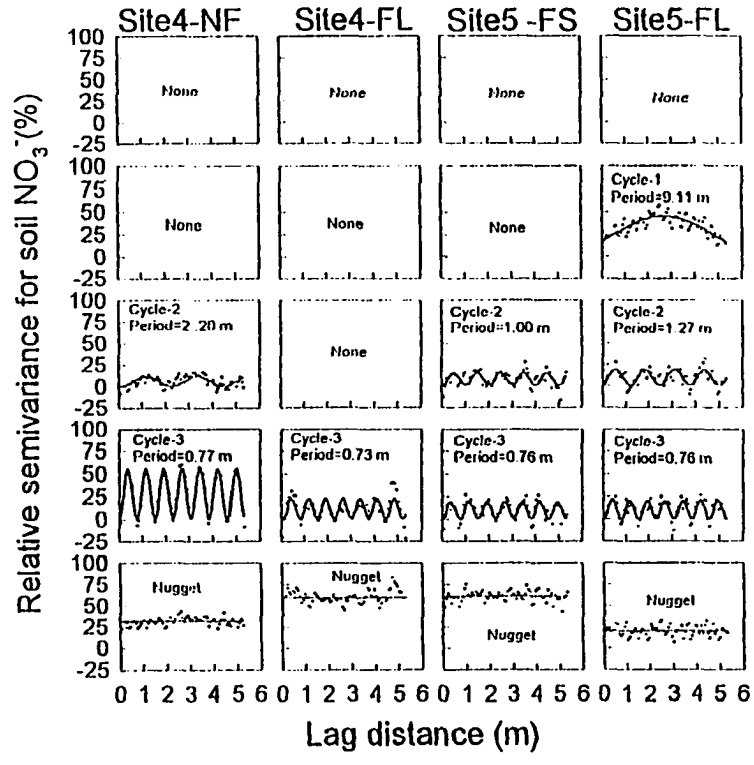

Figure 4. Components for cylic models and corrected residuals for soil NO_3^- semivariance data for sites 4 to 5.

cyclic models and the corresponding corrected residuals. The R^2 values for the best fitting cyclic models (Table 3) were higher than the corresponding R^2 values of the models fitted by the Gs$^+$ software (Table 2). Use of cyclic models can be defended because cyclic trends were clearly evident in some of the calculated variograms and because these trends were not described by the model selected by the Gs$^+$ software. In sites where clear cyclic variograms were observed, the R^2 values for the Gs$^+$ models were often very low whereas the corresponding R^2 values for the cyclic models were high.

The best fitting cyclic models did not contain a regionalized component at seven of the 10 sites (Table 3). The Gs$^+$ models always contain a regionalized component (Table 2), but the range of this component often seemed to be determined by the position of the first cycle in the variogram. The range tended to be close to zero if the maximum in the first cycle was near lag zero. The range also tended to increase as the first maximum moved a greater distance from lag zero. These observations raise questions concerning the validity of estimates of ranges as indicated by the Gs$^+$ models when cycles were present. Because these models partition variance between regionalized and random (nugget) components, errors in evaluation of the random components must accompany errors in the regionalized component.

Additional support for the existence of cycles in concentration of soil NO_3^- in this study is provided by considerations of soil water content in the same samples. Mean soil water concentrations within sites ranged from 18.8 to 28.9 % and standard deviations for these concentrations ranged from 0.8 to 1.4 % (Figure 5). Results of variogram analysis (Figure 6) showed that cyclic patterns existed in soil water content. As observed with soil

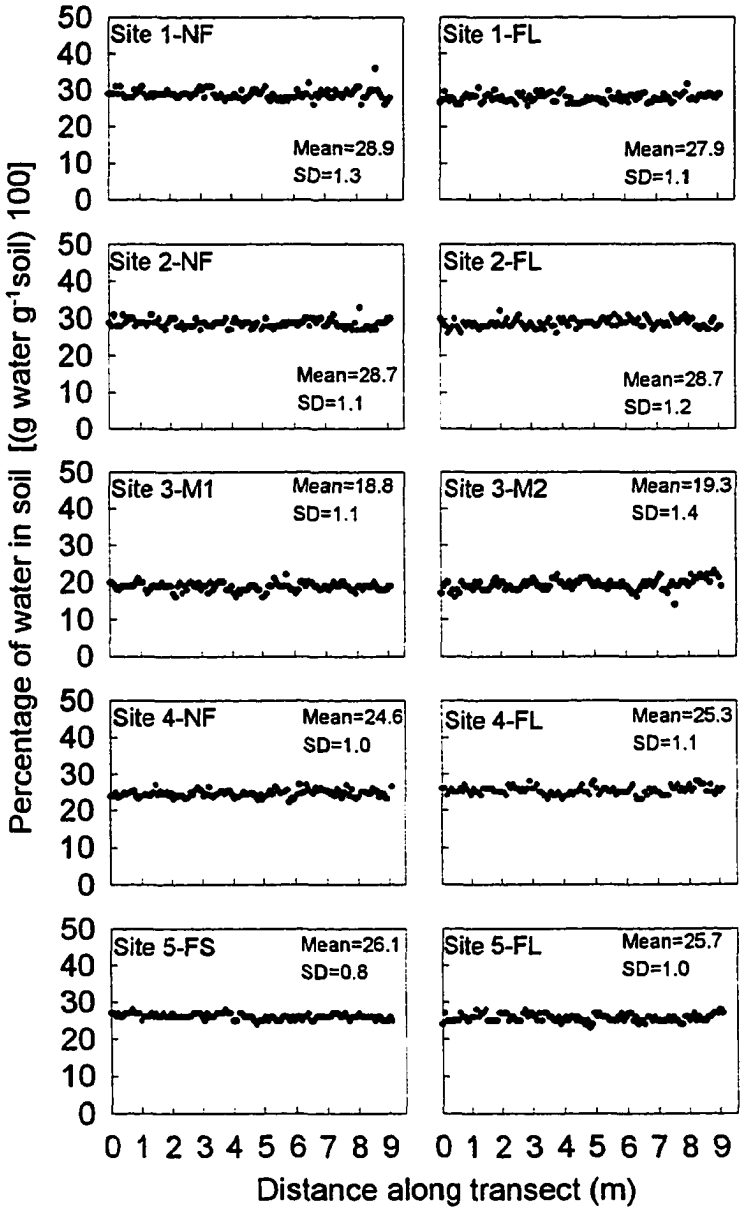

Figure 5. Soil water content along a 9.1 m transect at several sites.

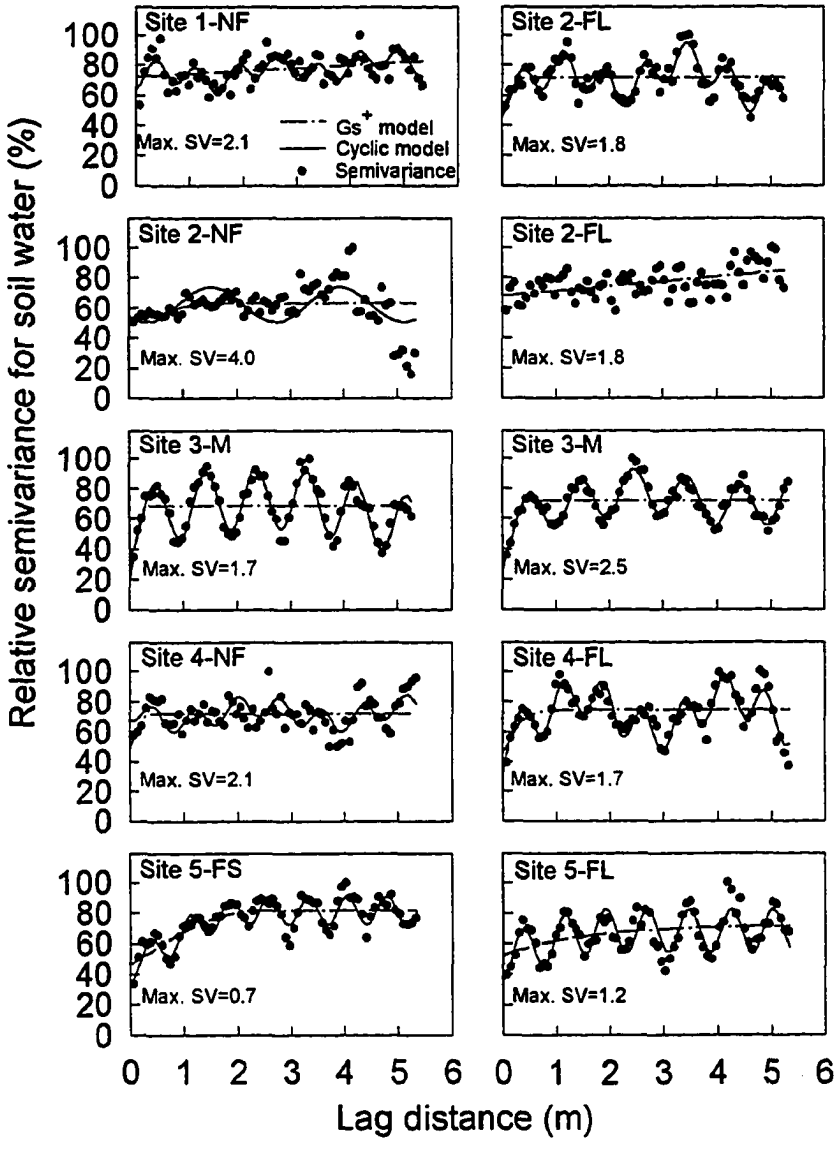

Figure 6. Calculated variograms for soil water content and cyclic and non-cylic models fitted to the variograms at several sites. Maximum semivariance at each site (Max. SV) is expressed in units of g^2 H_2O g^{-2} soil 10^4.

data, the Gs^+ models often failed to adequately describe the variogram shape(Figure 6) and very low R^2 values resulted from the fitting of non-cyclic models to data from sites where variograms showed a clear periodicity (Table 4). Cyclic models, however, clearly accounted for the presence of these cycles (Figure 6) and resulted in much higher R^2 values (Table 5). Figures 7 and 8 illustrate the various components of the best fitting cyclic models and the corresponding corrected residuals.

As with the soil NO_3^- data , the best fitting cyclic models for soil moisture content did not contain a regionalized component at many (five of the 10) sites (Table 5). The Gs^+ models always contained a regionalized component (Table 4), but the range of this component often seemed to be determined by the position of the first cycle in the variogram. Also, the range tended to be close to zero if the maximum in the first cycle was near lag zero and tended to increase as the first maximum moved greater distance from lag zero. These observations support the conclusion that the standard geostatistical models resulted in a questionable partitioning of variance between the regionalized and random components when periodicity is present.

Evidence that the cyclic models gave reasonable estimates of total variance within datasets is provided in Figure 9, which shows that the estimates given by the cyclic models were correlated with ordinary sample variance, which is another estimate of the true variance. Non-cyclic models with a plateau have been shown to be good estimators of variance (Clark, 1979), and data in Figure 9 show that non-cyclic models were correlated with the ordinary sample variance in this study. Although estimates of variance by the cyclic model disagreed

Table 4. Coefficient of determination (R^2), and estimations of total variance, percentage of nugget variance, and range of influence obtained from the fitting of Gs[+] models to soil water variograms at several sites.

Site	F[†]	Model	R^2	Total variance	Nugget variance	Range
				---- $g^2 H_20\ g^{-2}$ soil $1x10^4$ ----	-- % --	- m -
1	N	Linear	0.10	1.697	87.3	5.33
1	UAN	Spherical	0.04	1.298	70.4	0.46
2	N	Spherical	0.04	2.543	79.6	1.59
2	UAN	Linear	0.24	1.487	80.2	5.33
3	M1	Spherical	0.08	1.147	28.0	0.33
3	M2	Spherical	0.21	1.780	36.0	0.50
4	N	Spherical	0.05	1.479	68.0	0.38
4	UAN	Exponential	0.12	1.254	43.7	0.21
5	S	Spherical	0.54	0.597	56.8	2.35
5	UAN	Exponential	0.13	0.832	73.1	1.49

[†] F=Fertilization: UAN=Urea Ammonium Nitrogen, N=No fertilized, M=Manure, S=Solid Urea

Table 5. Coefficient of determination (R^2), and estimations of total variance, percentages of nugget, cyclic, and regionalized variances, and range of influence obtained from the fitting of cyclic models to soil water variograms at several sites.

Site	F†	Regionalized Component	R^2	Total variance	Nugget variance	Cyclic variance				Regionalized variance	Range
						Cycle 1	Cycle 2	Cycle 3	Total		
				---- $g^2 H_2 0\ g^{-2}$ soil $1x10^4$-		---------- % ----------					- m -
1	N	Linear	0.48	---1.7	71.3	0.0	8.8	5.7	14.4	14.3	≥5.33
1	UAN	None	0.82	1.3	63.8	6.2	13.8	16.3	36.2	0.0	0.00
2	N	None	0.34	2.5	81.2	0.0	18.8	0.0	18.8	0.0	0.00
2	UAN	Linear	0.24	1.5	80.2	0.0	0.0	0.0	0.0	19.8	≥5.33
3	M	None	0.88	0.9	27.7	35.0	0.0	37.3	72.3	0.0	0.00
3	M2	Spherical	0.91	1.8	36.7	7.2	0.0	20.3	27.5	35.8	0.94
4	N	None	0.37	1.5	82.5	0.0	10.3	7.2	17.5	0.0	0.00
4	UAN	None	0.82	1.2	64.3	0.0	18.5	17.2	35.7	0.0	0.00
5	S	Spherical	0.76	0.6	41.3	0.0	0.0	11.8	11.8	46.9	2.28
5	UAN	Linear	0.68	0.9	59.8	0.0	0.0	19.1	19.1	21.1	≥5.33

† F=Fertilization: UAN=Urea Ammonium Nitrogen, N=No fertilized, M=Manure, S=Solid Urea

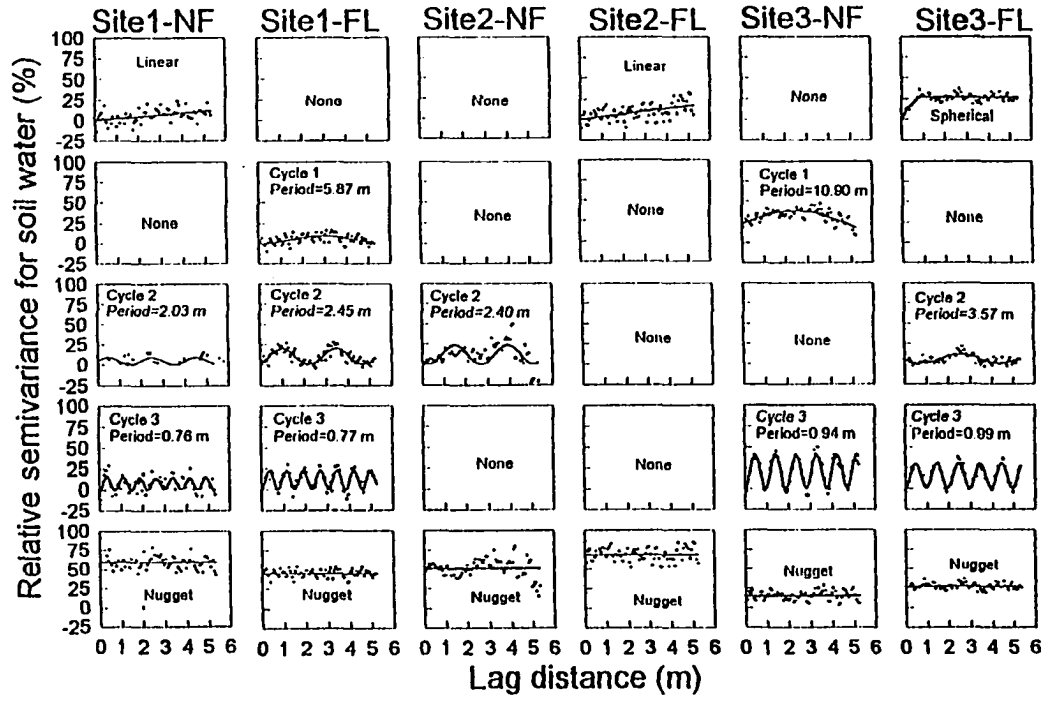

Figure 7. Components for cylic models and corrected residuals for soil water semivariance data for sites 1 to 3.

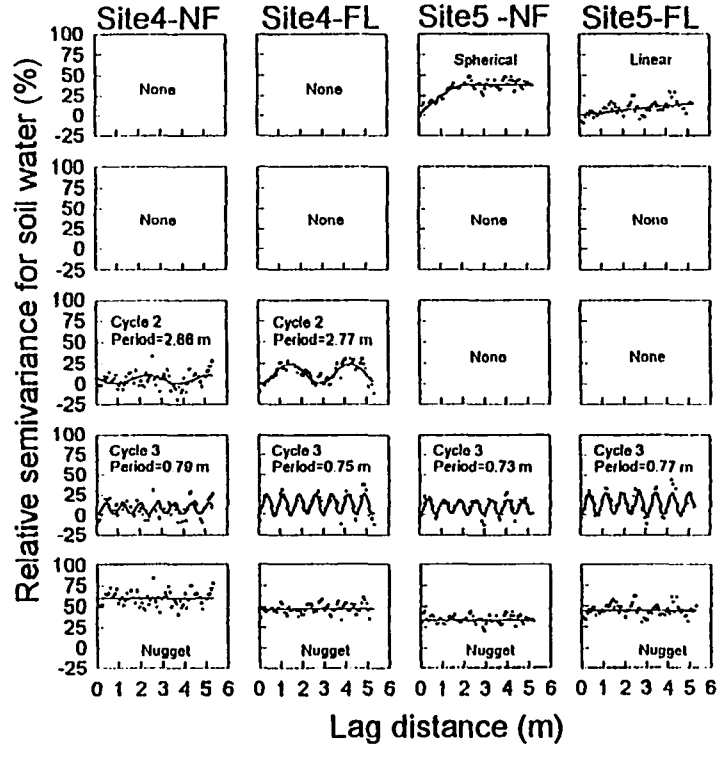

Figure 8. Components for cylic models and corrected residuals for soil water semivariance data for sites 4 to 5.

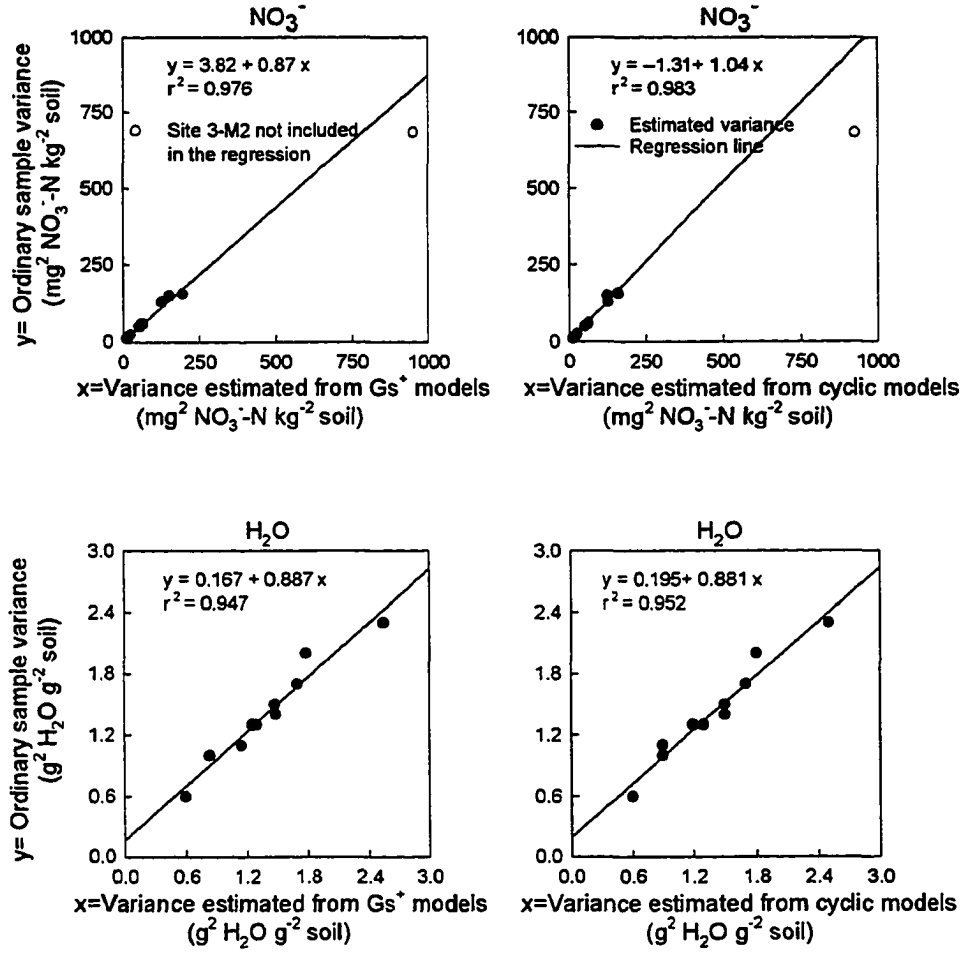

Figure 9. Observed relationships between the ordinary sample variance and the estimations of total variance from cyclic and non-cyclic models for soil NO_3^- concentrations and soil water content at several sites.

with ordinary sample variance at one site having extreme variability, estimates of variance by the Gs^+ models also disagree with ordinary sample variance in this situation. The results suggest that the cyclic models gave estimates of variance that were as reliable as did the Gs^+ models. It should be noted that small disagreements between either the cyclic or non-cyclic models and the ordinary sample variance must be expected because models with linear trends are not reliable estimators of the true variance (Clark, 1979).

Because cyclic and non-cyclic models identified essentially the same total amount of variance, the major differences between the models is how they partition the variance among components (Tables 2, 3 and 4, 5). Possible cyclic-trend induced errors in estimates of the range and nugget by the Gs^- model could be important at many sites because the cyclic models indicated that cyclic patterns accounted for from 2.8 to 68.2% of the variability in soil NO_3^- concentrations and from 0 to 72.3% of the variability in soil water content. The cyclic components explained more variability than did the regionalized component in 7 of the 10 datasets for soil NO_3^- (Table 3) and in 5 of 10 datasets for water (Table 5). All of this variability was classified as either random (nugget) or regionalized by the non-cyclic models, and this classification was incorrect in situations where periodicity existed. These results indicate a major shortcoming of commonly used geostatistical models.

The best fitting cyclic models identified as many as three cycles in variograms of soil NO_3^- concentrations (Figures 3 and 4) and soil water content (Figures 7 and 8). The periods of the cyclic components ranged from 0.73 to 10.73 m for soil NO_3^- and from 0.73 to 10.90 m for soil water. Evidence that the cycles were real is provided by the finding that a

consistent cycle with a period resembling the distance between plant rows (0.76 m at most sites and 0.92 m at sites M1 and M2) was found at 8 of the 10 cases for water and in 6 of the 10 cases for NO_3^-. An obvious explanation for these cycles is uptake of water and NO_3^- by young plants in rows. It should be noted that cyclic patterns having relatively long periods are impossible to distinguish from regionalized trends in this study.

It should be noted that the soil NO_3^- concentrations and soil water content were not normally distributed at most sites (Figures 10 and 11). Kurtosis was significant at 8 of 10 sites for NO_3^- and all sites for water. Skewness was significant at all sites. Other authors have observed similar results (Cahn et al., 1994; Cambardella et al., 1994). In most cases in our study, log transformations did not noticeably change the shape of the variogram or eliminate the skewness or kurtosis (data not shown). Significant kurtosis indicated that samples tended to be grouped around the mean and far away from the mean, with less samples falling in between these two extremes (Snedecor and Cochran, 1980). Significant kurtosis is often found in soil datasets and have not precluded other authors to perform variogram analysis (Cahn et al., 1994; Cambardella et al., 1994).

Chan et al. (1994) reported that the shape of a variogram is often biased by values greater than four standard deviations from the mean. In our study we observed no NO_3^- concentration exceeding three standard deviations from the mean. Some samples of water, however, were eliminated because they were obvious outliers, products of errors during sampling processing. The elimination of only one datapoint at site M1 changed the variogram from an unidentified shape to a clear cyclic pattern.

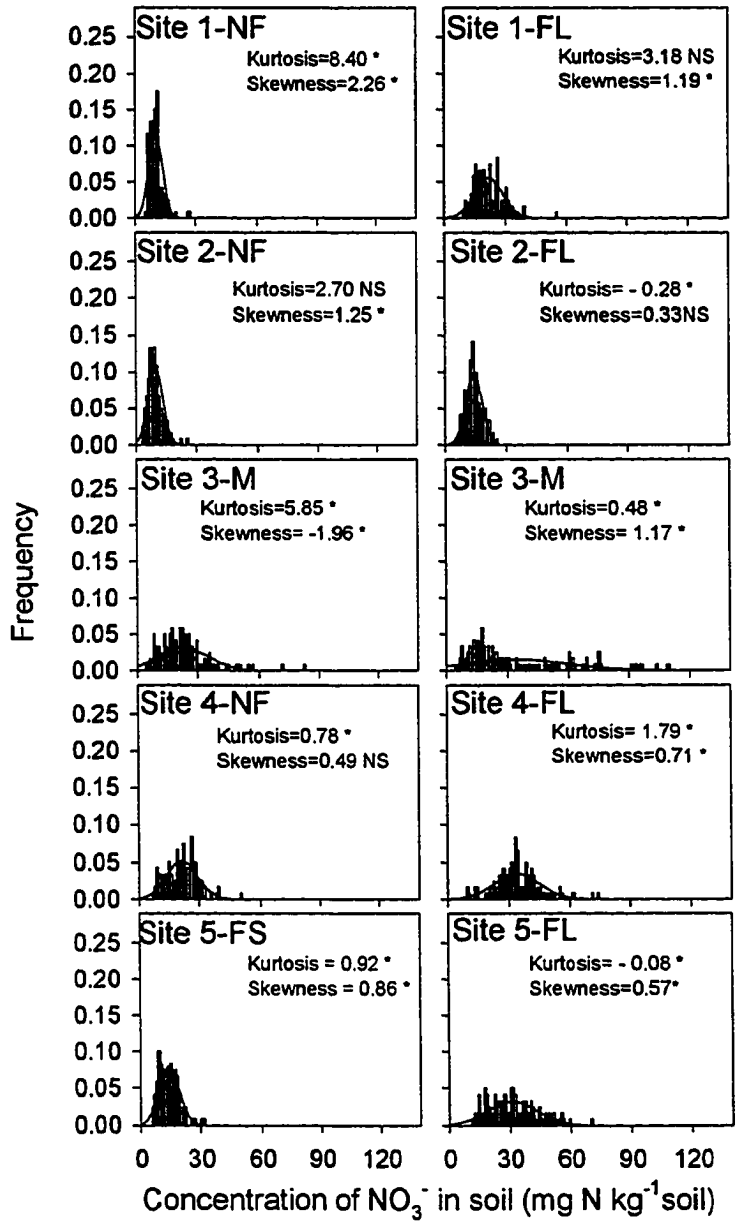

Figure 10. Observed frequency distribution and theoretical normal distribution for soil NO_3^- concentrations at several sites.

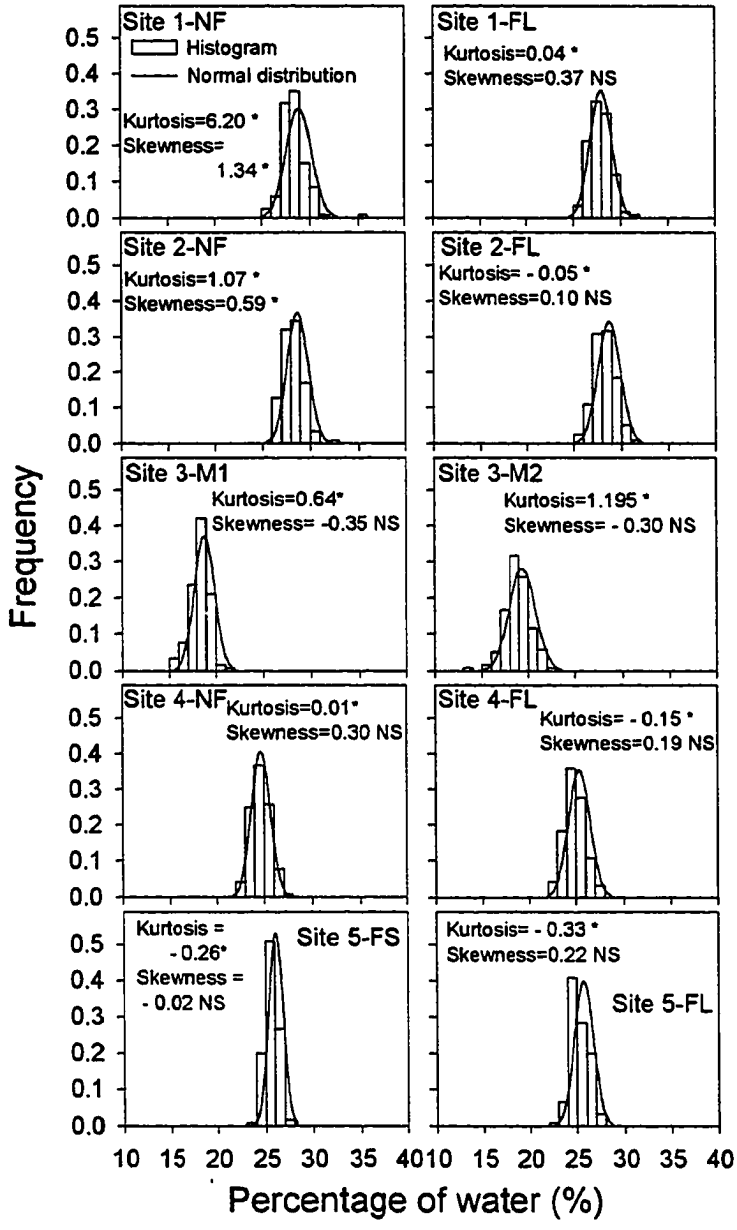

Figure 11. Observed frequency distribution and theoretical normal distribution for soil water content at several sites.

FFT analyses for soil NO_3^- concentrations performed on the raw (Figure 12) and on the semivariance data (Figure 13) often showed peaks at frequencies resembling the ones identified by the cyclic models. FFT analyses performed on the semivariance data often showed clearer peaks than FFT analyses performed on the raw data, a result which agrees with previous observations (Perdomo and Blackmer, 1995b) showing that FFT analysis had greater resolution when performed on semivariance data than on raw data. Similar results were obtained for FFT analyses on soil water content (Figures 14 and 15). These results confirm that the cyclic models were correct when they indicated the existence of periodicity in the data for both soil NO_3^- concentrations and soil water content.

Overall, the results of this study indicate that periodicity in soil NO_3^- concentrations can occur in many agricultural soils. One of the sources of the periodicity detected in this paper were probably produced by rows of young corn plants absorbing more water and NO_3^- from the soil closer to the rows. The ability to characterize these periodicity is important because the resulting information should enable design of more efficient sampling patterns to assess average concentrations of NO_3^- within areas of soil. Sampling problems associated with periodicity caused by rows of young plants, for example, could be minimized by collecting cores in pairs, one in the row and one midway between rows.

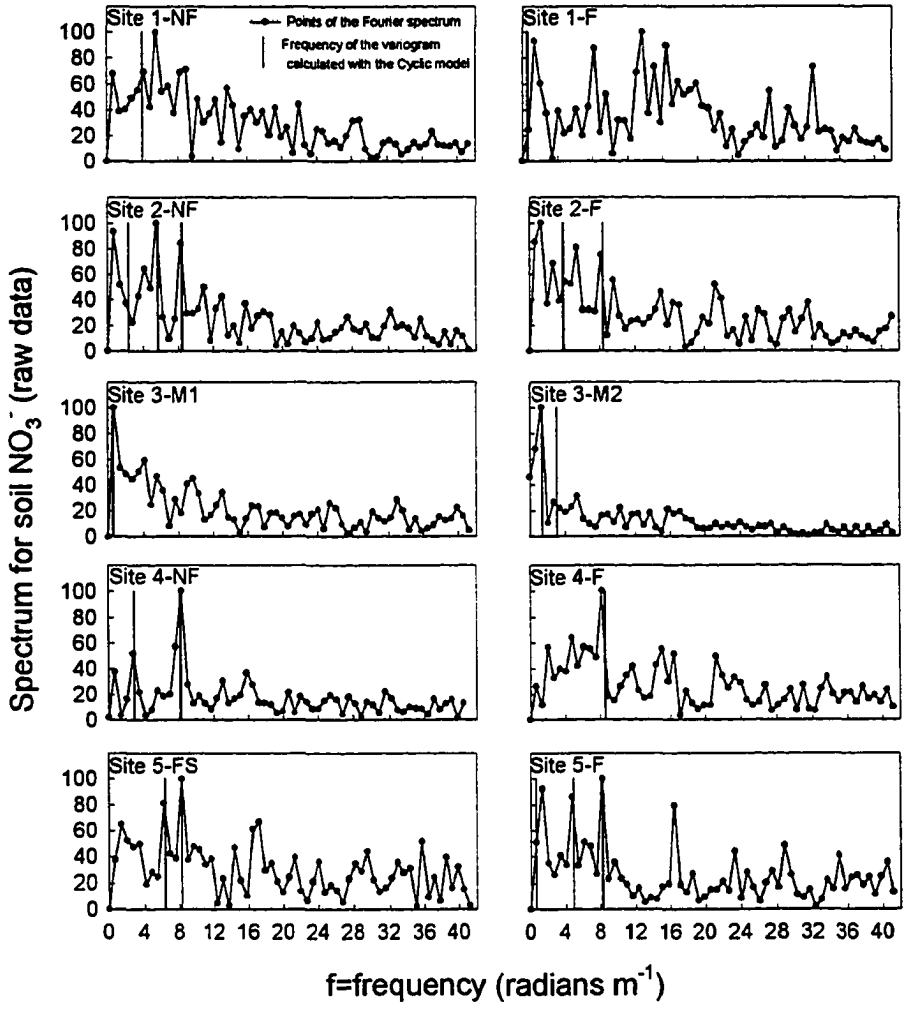

Figure 12. FFT analysis on raw data for soil NO_3^- concentrations at several sites.

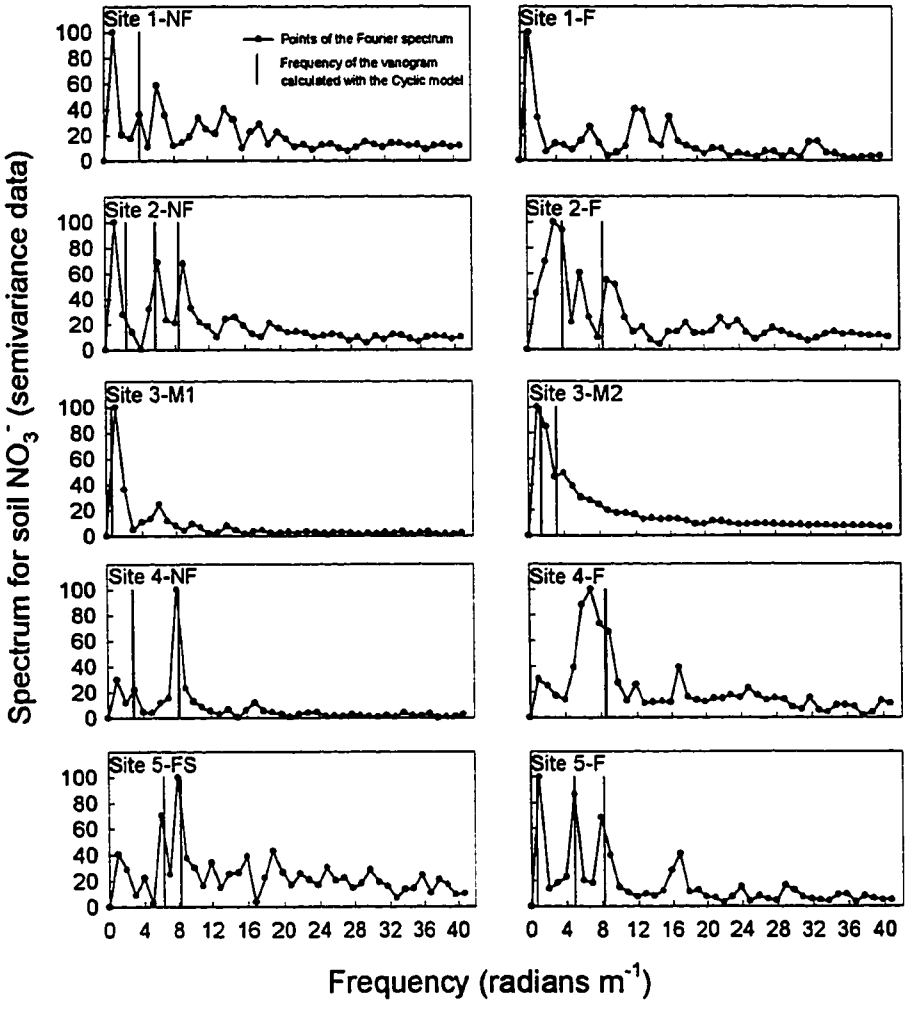

Figure 13. FFT analysis on semivariance data for soil NO_3^- at several sites.

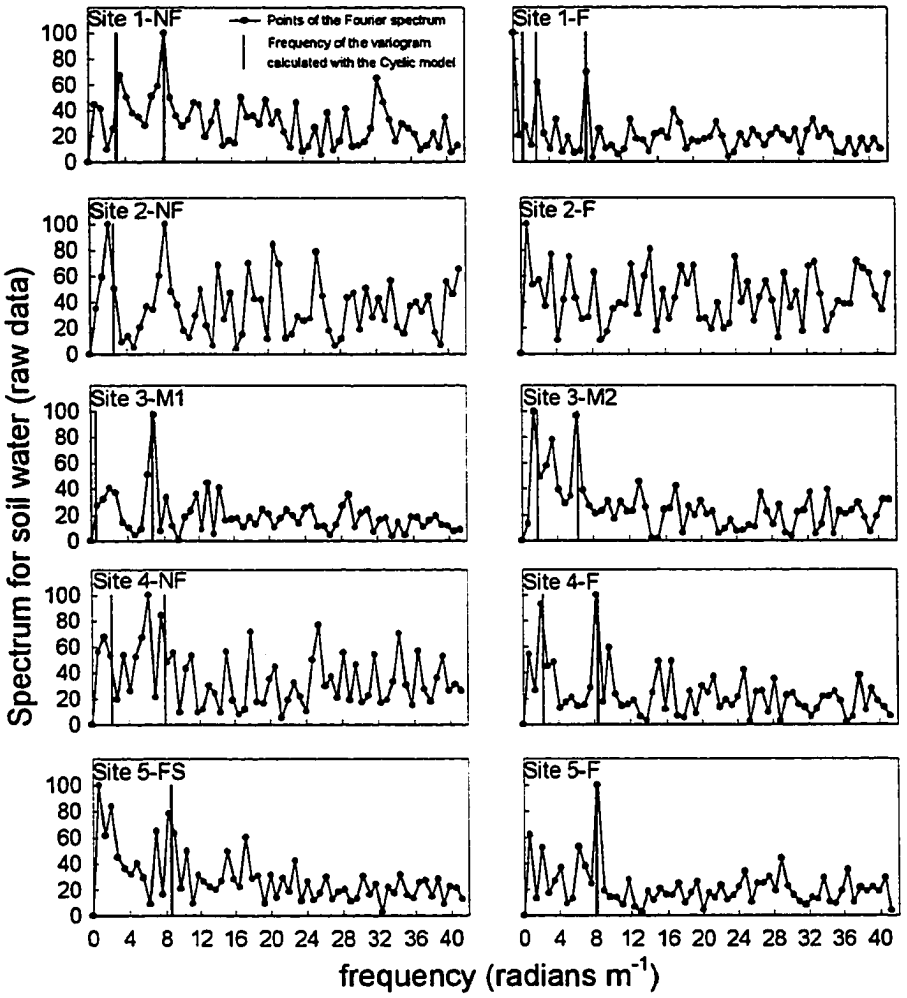

Figure 14. FFT analysis on raw data for soil water content at several sites.

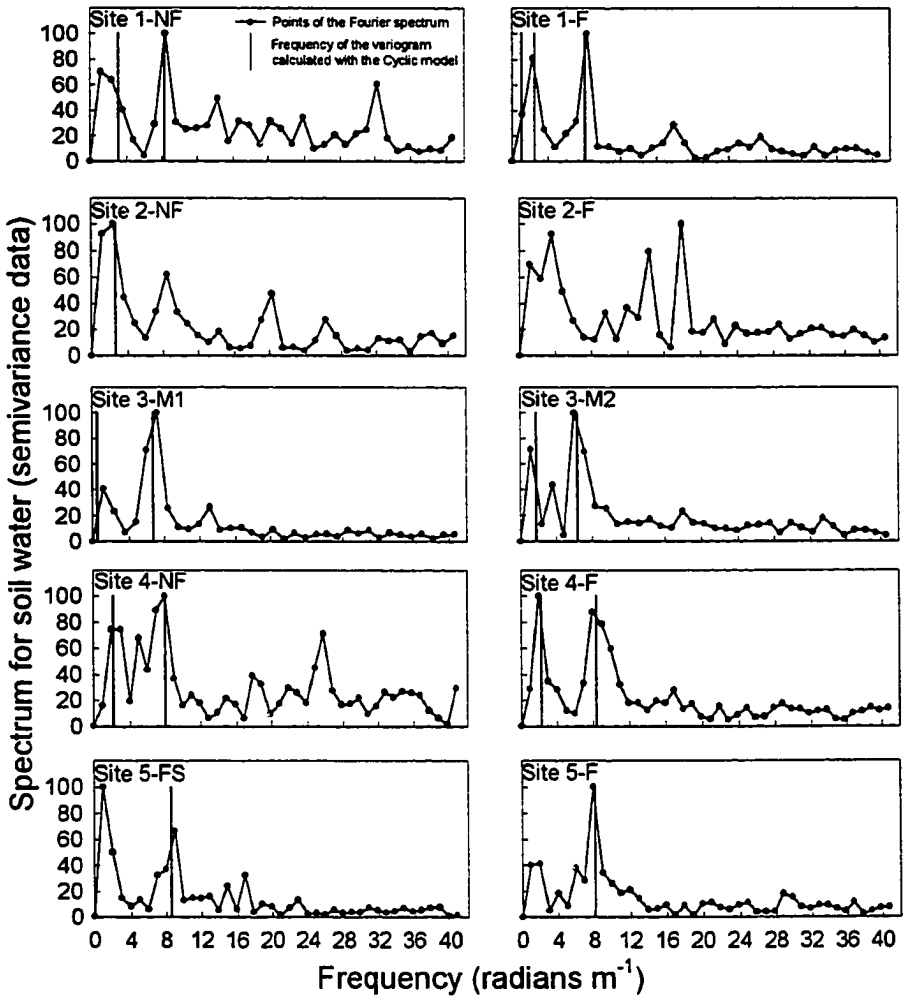

Figure 15. FFT analysis on semivariance data for soil water content at several sites.

LITERATURE CITED

Binford, G.D., A.M. Blackmer, and M.E. Cerrato. 1992. Relationships between corn yields and soil nitrate in late spring. Agron. J. 84:53-59.

Blackmer, A.M., D. Pottker, M.E. Cerrato, and J. Webb. 1989. Correlations between soil nitrate concentrations in late spring and corn yields in Iowa. J. Prod. Agric. 2:103-109.

Blackmer, A.M., T.F. Morris, G.D. Binford. 1992. Predicting N fertilizer needs for corn in humid regions: Advances in Iowa. P. 58-72. *In* B.R. Bock and K.R. Kelley (eds.) Predicting N fertilizer needs for corn in humid regions. Bull. Y-226. National Fertilizer and Environmental Research Center, Tenesee Valley Authority, Muscle Schoals, AL.

Cahn, M. D., J. W. Hummel and B. H. Brouer. 1994. Spatial analysis of soil fertility for site-specific crop management. Soil Sci. Soc. Am. J. 58:1240-1248.

Cambardella, C. A., T. B. Moorman, J. M. Novak, T. B. Parkin, D. L. Karlen, Turco R.F. and A. E. Konopka. 1994. Field scale variability of soil properties in central Iowa soils. Soil Sci. Soc. Am. J. 588:1501-1511.

Clark, I. 1979. Practical Geostatistics. Applied Science Publishers, London.

Dahiya, I.S., K.C. Anluf, K.C. Kersebaum, and J. Richter. 1985. Spatial variability of some nutrient constituents of an Alfisol from loess. II. Geostatistical analysis. Z. Plfanzenernaehr. Bodenkd. 148:268-277.

Delong D.M. 1985. The CORR procedure. p. 861-874. *In* SAS user's guide: Basics, 1985 ed. SAS Inst. Inc., Cary, N.C.

Fox, R.H., G.W. Roth, K.V. Iverson, and W.P. Piekielek. 1989. Soil and tissue nitrate tests compared for predicting soil nitrogen availability to corn. Agron. J. 81:971-974.

Gamma Design Software. 1993. Gs^+ : Geostatistics for the environmental sciences 2.1 user's guide. Gamma Design Software, Plainwell, MI.

Goovaerts, P. Chiang ,. C.N. 1993. Temporal persistence of spatial patterns for mineralizable nitrogen and selected soil properties. Soil Sci. Soc. Am. J 57:372-381.

Ihnen, L.A., and J.P. Sall. 1985. The REG procedure. p. 655-709. *In* SAS user's guide: Statistics, 1985 ed. SAS Inst. Inc., Cary, N.C.

Ihnen, L.A., and J.H. Goodnight. 1985. The NLIN procedure. p. 575-606. *In* SAS user's guide: Statistics, 1985 ed. SAS Inst. Inc., Cary, N.C.

Kopp, J. E., and G. D. McKee. 1978. Methods for chemical analysis of water and wastes. Method 351.2, nitrogen, ammonia. EPA Report no. EPA-6000/4-79-020. EPA Environmental Monitoring and Support Laboratory, Cincinnati, OH.

Magdoff, F.R., D. Ross, and J. Amadon. 1984. A soil test for nitrogen availability to corn. Soil Sci. Soc. Am. J. 48:1301-1304.

Magdoff, F.R., W.E. Jokela, R.H. Fox, and G.F. Griffin. 1990. A soil test for nitrogen availability in the Northeastern United States. Commun. Soil Sci. Plant Anal. 21:1103-1115.

Meisinger, J.J., V.A. Bandel, J.S. Angle, B.E. O'Keefe, and C.M. Reynolds. 1992. Presidedress soil nitrate test evaluation in Maryland. Soil Sci. Soc. Am. J. 56:1527-1532.

Perdomo, C.H., and A.M. Blackmer. 1995a. Identification of cyclic sources of variability in soils. Soil Sci. Soc. Am. J. In preparation.

Perdomo, C.H., and A.M. Blackmer. 1995b. Detecting superimposed cyclic patterns in soil properties. Soil Sci. Soc. Am. J. In preparation.

Perdomo, C.H., and A.M. Blackmer. 1995c. Large-scale cycles in the spatial structure of soil nitrate concentrations of cornfields. Soil Sci. Soc. Am. J. In preparation.

Snedecor, G.W., and W.G. Cochran. 1980. Statistical methods. 7th ed. Iowa State Univ. Press, Ames.

Van Meirvenne, M., and G. Hofman. 1989. Spatial variability of soil nitrate nitrogen after potatoes and its change during winter. Plant Soil 120:103-110.

Wolfram, S. 1991. Mathematica, a system for doing mathematics by computer, 2d ed. Addison-Wesley, Redwood City, CA.

LARGE-SCALE CYCLES IN THE SPATIAL STRUCTURE OF SOIL NITRATE CONCENTRATIONS OF CORNFIELDS.

A paper prepared for submission to the *Soil Science Society of America Journal*

Carlos H. Perdomo and Alfred M. Blackmer

ABSTRACT

This paper studied the amount and structure of large-scale variability in concentrations of soil NO_3^- at 8 different cornfields in 1993. At each site, 50 samples were collected from the surface 30-cm layer of soil along 75-m transects along and across corn rows. To minimize small-scale variability, each soil sample was a composite sample of 16 cores collected along a 1.5-m line perpendicular to the corn rows. Results showed that the amounts of variability in soil NO_3^- concentrations varied among sites and that cyclic patterns were detected in variogram analyses at most sites. Some of these cyclic patterns seem to be caused by fertilizer applicators or other farming operations.

Overall, results of studies reported in this dissertation show that cyclic patterns are an important component of the spatial structure of soil NO_3^- concentrations in cornfields. Consideration of these cyclic patterns should enable more complete characterization of the spatial structure of soil NO_3^- concentrations in fields and, therefore, enable design of more efficient sampling strategies to assess NO_3^- concentrations within these fields. In addition, the ability to detect previously unrecognized cyclic patterns in soil NO_3^- concentrations gives the ability to demonstrate the benefits of using practices that minimize formation of troublesome cyclic patterns in fields.

INTRODUCTION

Recent studies (Perdomo et al., 1995) show that soil NO_3^- concentrations in cornfields in late spring often vary in cyclic patterns having periods of about 0.5 to 5 meters. Some of these cycles seem to be caused by the effects of rows of young corn plants and some of these appear to be caused by other management practices. Whatever their cause, these cyclic trends must be considered when characterizing the spatial structure of soil NO_3^- concentrations and when trying to identify optimal sampling patterns to determine soil NO_3^- concentrations within any given area of soil. There is practical need for optimizing such sampling patterns because soil testing to determine concentrations of NO_3^- in late spring has been identified as a promising method for improving N management during the production of corn in the northern half of the United States (Magdoff et al., 1984, 1990; Blackmer et al., 1989; Fox et al., 1989; Binford et al., 1992; Meissinger et al, 1992).

Studies by Perdomo and Blackmer (1995a) showed that yields of corn varied in cyclic patterns caused by windrows of plant residue formed during harvest of the previous soybean crop. Although it is likely that the windrows of residue also had effects on concentrations of NO_3^- in soils, the sampling patterns used to assess soil NO_3^- concentrations precluded detection of cyclic patterns if they were present. The sampling strategy used in an study on NO_3^- variability at a relatively small scale (Perdomo et al.,1995) precluded detection of such cyclic patterns because the cyclic patterns of this period could not be distinguished from the "range", as this term is usually used in geostatistical analyses (Clark, 1979). Other studies to evaluate the spatial structure of soil NO_3^- concentrations have not considered the possible

importance of cyclic trends (Dahiya et al., 1985, Van Meirvenne and Hoffman, 1989, Goovaerts and Chiang , 1993, Cahn et al., 1994, Cambardella et al., 1994).

The objective of this report is to describe the spatial structure of soil NO_3^- concentrations found when several cornfields were sampled in late spring of 1993 by using methods that should be expected to detect cyclic patters having periods of about 5 to 30 meters. It was anticipated that sampling problems caused by small-scale cyclic patterns could make it difficult to detect large-scale cyclic patterns, so the soil sampling pattern used to assess concentrations NO_3^- in this study was specifically selected to minimize sampling problems caused by cyclic patterns having periods of about 1.5 m or less.

MATERIALS AND METHODS

Eight cornfields located in Greene County (Iowa) were randomly selected immediately after corn was planted in 1993. The fields were managed by farmers using their usual practices, and no special treatments were applied for this study. Information about forms, times, rates, and direction of N application by the farmers is presented in Table 1. An experimental area (75 by 75 m) of seemingly uniform soil type was selected within each field.

Fifty plots (1.5 by 1.5 m) were marked in the experimental area along each of two lines, one perpendicular to the corn rows and one parallel to the corn rows. The corn rows were 0.75 m apart. Soil samples were taken in late spring (i.e., when corn plants were 15 to 30 cm tall) by collecting a composite sample of 16 cores (3.2-cm diam.) from the first 30-cm layer of soil from each plot. The cores were taken at 9.5-cm intervals along lines perpendicular to the corn rows: for the 50 plots in lines perpendicular to the rows, all cores

Table 1. Form, rate, and direction of N application as reported by farmers for all sites.

Site	Fertilizer application		
	Rate		
	Fall	Planting	Direction[†]
	---------- Kg N / ha ----------		
1		100 (AA[‡])	Diagonal
2	180 (AA)	30 (UAN[§])	Parallel
3		80 (UAN)	Parallel
4	50 (Dry)	100 (UAN)	Parallel
5		100 (UAN)	Parallel
6		120 (AA)	Diagonal
7		130 (AA)	Diagonal
8		130 (AA)	Diagonal

[†]Direction in relation to corn rows.
[‡]Anhydrous ammonia.
[§]Urea Ammonium Nitrate solution.

for the 50 soil samples were collected along a single line; for the 50 plots in a line parallel to the rows, the cores were collected along 50 parallel lines that crossed the same two rows of corn. Soil samples were dried in a forced-air oven at 49 ^{o}C and ground to pass a 2-mm sieve. Samples were later extracted with 2 *M* KCl, filtered, and analyzed for NO_3^- using a Lachat flow-injection procedure (Kopp and McKee, 1978).

All following parameters were calculated for each site-orientation. Ordinary sample variance was calculated from the raw data. The frequency distribution of soil NO_3^-concentration for each site was calculated using an histogram width of 5 mg NO_3^--N kg^{-1} soil. The normal distribution curve computed from the mean and standard deviation for each site-orientation was superimposed to the corresponding frequency distribution graph.

Experimental isotropic variograms were calculated for 36 lags, resulting in a minimum number of data pairs of 14 samples. Geostatistical models (linear, linear-sill, spherical, exponential, and gaussian) were estimated using the Gs^+ geostatistical software (Gamma Design Software, 1993). The best fitting model as suggested by the software was selected to represent the variogram.

Cyclic models (Perdomo and Blackmer, 1995b , 1995c) were also fitted to the semivariance data using the NLIN procedure of SAS (Ihnen and Goodnight, 1985). Because often more than one cycle was detected in the variogram, cycles were ordered in relation to their frequency. The cycle with the largest period or lowest frequency was identified as Cycle-1, the following as Cycle-2, etc. Variograms and models were finally expressed as a percentage of the maximum semivariance at each lag orientation. This form of expression

was chosen because it permits to compare the structure of variability among sites with different amount of variance. Regresion analysis were performed using the REG procedure of SAS (Ihnen and Sall, 1985).

Fast Fourier transform (FFT) analyses were calculated on raw and on semivariance data using the algorithms available in the software package Mathematica (Wolfram, 1991). To compare cyclic frequencies obtained with the cyclic models with frequency results obtained with FFT, the FFT Spectra was converted from cycles m^{-1} to radians m^{-1} according to formulas reported in another paper (Perdomo and Blackmer, 1995c). More information about FFT analysis is also available in two other papers (Perdomo and Blackmer, 1995b , 1995c).

In spite of the non-normality shown for most sites, the variograms presented here were calculated based on the raw untransformed data. Non-transformed data was chosen because log transformations did not significantly affect the shape of the variogram. Chan et al., 1994, reported that the shape of the variogram is often biased by values greater than four standard deviations from the mean. According to this author, these values should be considered outliers and they should be removed because they can significantly change the shape of the variogram. In these studies, however, and probably because each sample was the average of 18 cores, not outliers even at a range of 3 standard deviations from the mean were detected in the raw data.

RESULTS

Soil NO_3^- concentrations showed considerable variation within and between sites (Figure 1). The mean concentrations for most sites (Table 2) tended to be close to the optimal range of 21 to 26 mg NO_3^- as reported by Binford et al. (1992), but two sites receiving UAN were below this optimum value. The reason for this lower NO_3^- concentration was not determined, but it seems likely that losses of the surface-applied N by NH_3 volatilization or by NO_3^- leaching may have been important. Unusually high (about twice normal) amounts of rainfall occurred between N application and soil sampling in Greene County in 1993.

Variograms calculated from the NO_3^- concentrations in Figure 1 are indicated by the points in Figure 2. The dashed lines in Figure 2 illustrate the geostatistical model selected for each dataset by the Gs^+ software. The solid lines in Figure 2 illustrate the best fitting cyclic models fitted by using procedures described in other paper (Perdomo and Blackmer, 1995c). In 13 of the 16 datasets, the Gs^+ software selected the spherical model, which shows a nugget-sill shape. In the remaining 3 datasets, the software package selected a linear model, which means that no sill was observed. Irrespective of the model selected for each dataset, however, the observed datapoints often deviated substantially from the model.
The deviations from the Gs^+ models often seemed to show a cyclic pattern. The cyclic patterns were more evident in the variograms than in the raw data, an observation consistent with analyses reported by Perdomo and Blackmer (1995b). Traces of cyclic patterns could

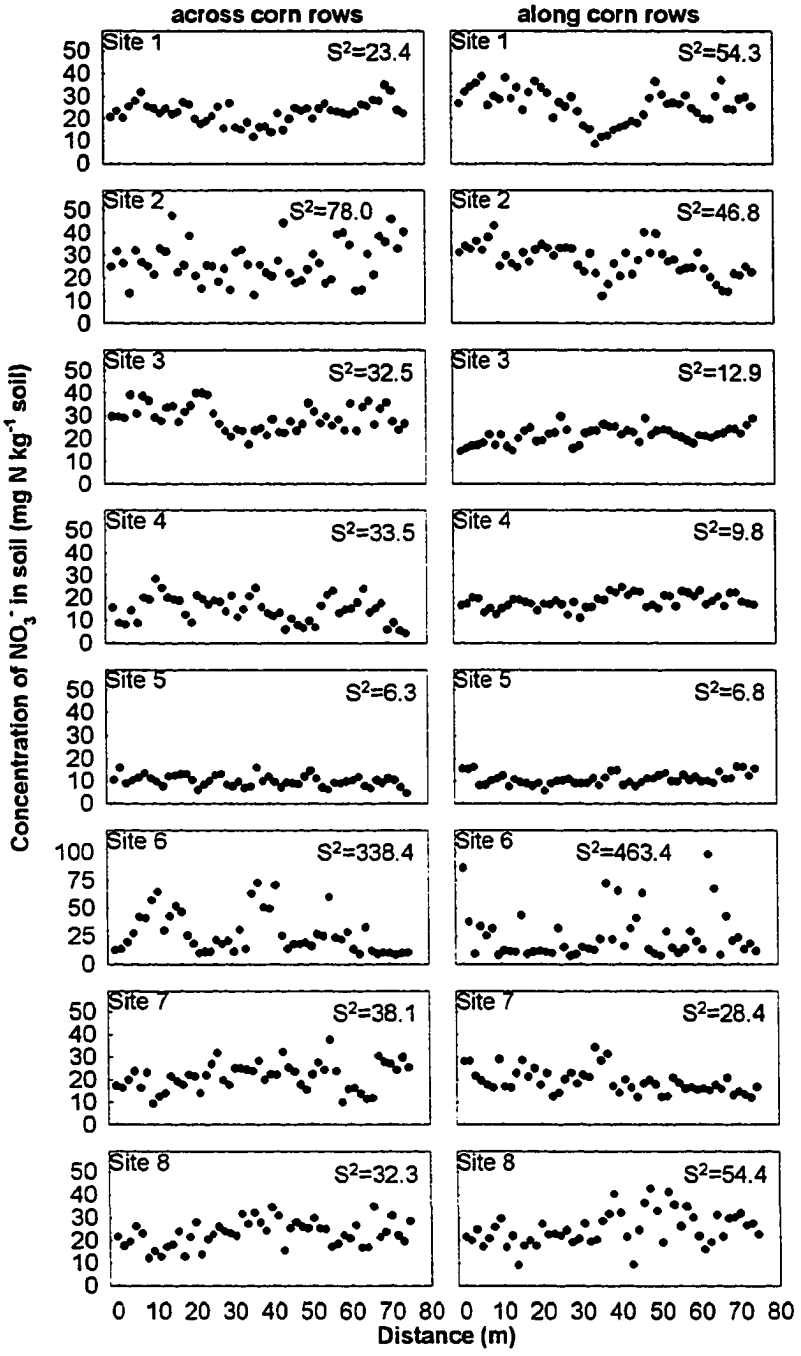

Figure 1. Soil NO_3^- concentrations along a 77 m transect at several sites.

Table 2. Some descriptive statistical parameters for soil NO_3^- concentrations in late spring at several sites.

Site	Mean	Range	SD
	mg NO_3^--N kg^{-1} soil		
1	24.4	30.2	6.4
2	27.3	35.5	7.9
3	25.3	25.6	6.1
4	16.7	24.0	4.9
5	10.4	11.9	2.6
6	26.3	90.7	19.9
7	20.3	28.3	5.8
8	24.0	33.9	6.6

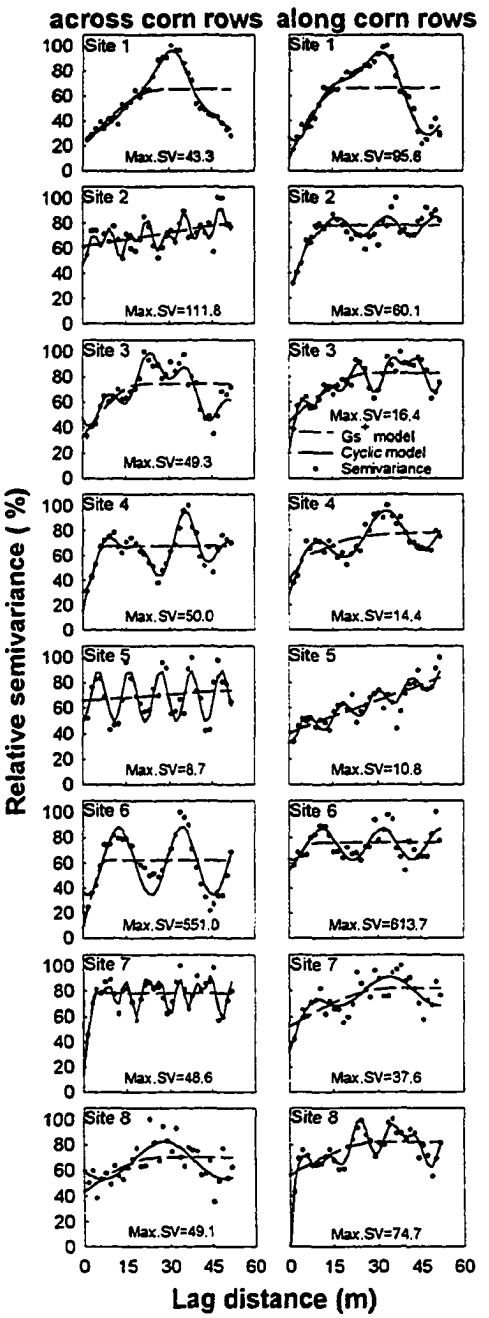

Figure 2. Calculated variograms for soil NO_3^- concentration and cyclic and non-cylic models fitted to the variograms at several sites. Maximum semivariance at each site (Max. SV) is expressed in units of mg^2 NO_3^--N kg^{-2} soil.

be seen, however, in the raw data at some sites. FFT analyses confirmed that cyclic patterns were present in the raw data (Figure 3) and in the variograms (Figure 4).

Visual analyses indicated that the best-fitting cyclic models tended to describe the cyclic patterns in the variograms. These visual analyses are confirmed by R^2 values, which were substantially greater for the best-fitting cyclic models (Table 3) than for the corresponding Gs$^+$ models (Table 4). The various components and the corrected residuals of the best-fitting cyclic models are shown in Figures 5 and 6. The best-fitting cyclic models identified a regionalized component in 8 of the 16 datasets, 3 of which were linear and 5 of which were spherical. Some dataset contained 1 cycle whereas others contained 2 or 3 cycles.

Regression analysis showed that estimations of variance by the cyclic and non-cyclic models agreed well with the ordinary sample variance (Figure 7). The variance estimators for sites with regionalized components showing a linear trend were arbitrarily calculated as the maximum value predicted by the model because geostatistical models with linear trends cannot be used as variance estimators (Clark, 1979). The small deviations from the 1/1 line observed in Figure 7 reveal that only small errors were introduced by this arbitrarily selected method of estimating variance.

The ranges identified by the Gs$^+$ package varied from 8 to 34 m (Table 4), which is similar to those reported in previous studies (Dahiya et al., 1985, Van Meirvenne and Hoffman, 1989, Goovaerts and Chiang , 1993, Cahn et al., 1994, Cambardella et al., 1994).

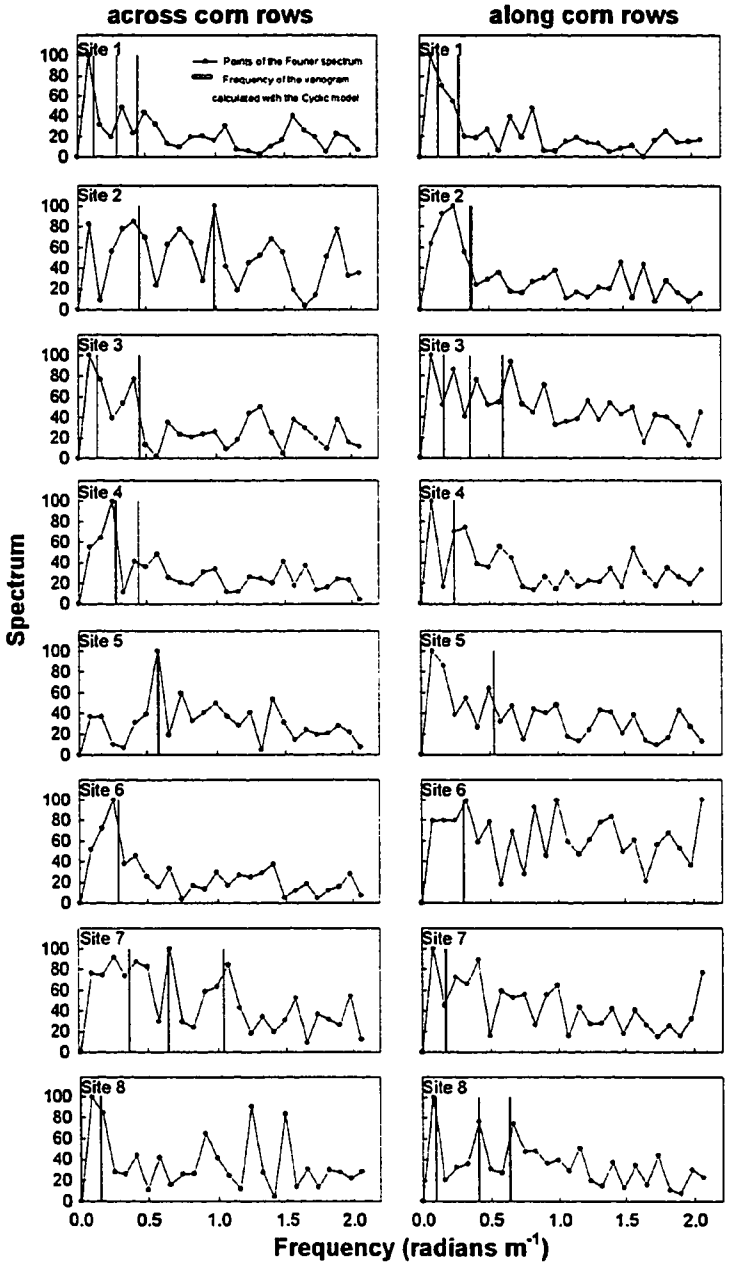

Figure 3. FFT analysis on raw data for soil NO_3^- concentrations at several sites.

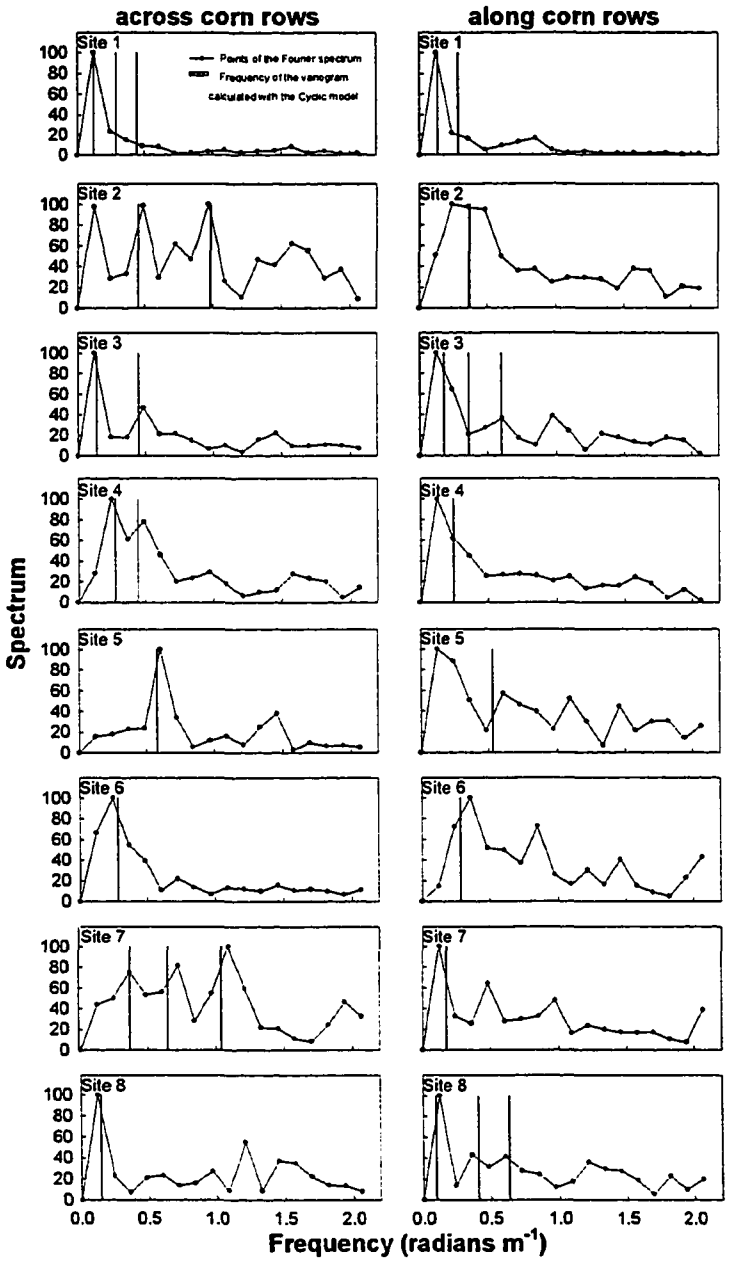

Figure 4. FFT analysis on semivariance data for soil NO_3^- at several sites.

Table 3. Coefficient of determination (R^2), and estimations of total variance, percentages of nugget and cyclic variances, and range of influence obtained from the fitting of cyclic models to soil NO_3^- variograms at several site-orientations.

Site	Or[1]	Spatial Component	R^2	Total variance	Nugget variance	Cyclic variance				Range
						Cyc-1	Cyc-2	Cyc-3	Total	
				----mg^2 NO_3^--N kg^{-2} soil----		---------- % ----------				- m -
1	H	None	0.97	24.8	31.1	53.0	11.5	4.4	68.9	0
1	V	None	0.95	59.6	36.7	47.7	15.6	None	63.3	0
2	H	Linear	0.63	89.2	57.6	8.7	10.3	None	19.0	53
2	V	Spherical	0.74	46.3	0.1	9.8	None	None	9.8	9
3	H	None	0.95	35.0	56.3	28.3	15.4	None	43.7	0
3	V	Spherical	0.89	13.6	-2.4	8.6	8.9	9.8	27.3	20
4	H	Linear	0.89	36.9	39.6	22.4	14.9	None	37.3	53
4	V	Spherical	0.91	11.5	22.7	19.9	None	None	19.9	28
5	H	None	0.74	6.0	70.1	29.9	None	None	29.9	0
5	V	Linear	0.81	9.1	38.7	9.0	None	None	9.0	53
6	H	None	0.84	337.5	56.0	44.0	None	None	44.0	0
6	V	None	0.59	456.9	83.3	16.7	None	None	16.7	0
7	H	Spherical	0.80	38.1	15.1	7.4	9.9	11.5	28.8	8
7	V	Spherical	0.60	29.8	52.3	9.0	None	None	9.0	11
8	H	None	0.53	33.3	78.5	21.5	None	None	21.5	0
8	V	None	0.87	55.2	56.6	19.6	11.9	11.9	43.4	0

[1] Or=Orientation: H=across corn rows, V=along corn rows

Table 4. Coefficient of determination (R^2), and estimations of total variance, percentage of nugget variance, and range of influence obtained from the fitting of Gs^+ models to soil NO_3^- variograms at several site-orientations.

Site	Or†	Model	R^2	Total variance	Nugget variance	Range
				----mg^2 NO_3^--N kg^{-2} soil----	-- % --	- m -
1	H	Spherical	0.33	28.1	29.1	27
1	V	Spherical	0.30	63.1	13.9	18
2	H	Linear	0.21	90.0	76.5	53
2	V	Spherical	0.61	46.7	24.4	12
3	H	Spherical	0.33	36.5	43.6	20
3	V	Spherical	0.56	13.6	53.4	28
4	H	Spherical	0.26	33.6	22.0	8
4	V	Exponential	0.39	11.2	49.3	9
5	H	Linear	0.02	6.5	88.3	53
5	V	Linear	0.68	9.2	47.8	53
6	H	Spherical	0.15	340.3	13.8	8
6	V	Spherical	0.10	464.3	71.1	10
7	H	Spherical	0.22	38.0	20.3	5
7	V	Spherical	0.39	30.7	63.9	34
8	H	Spherical	0.25	34.4	62.0	25
8	V	Spherical	0.33	61.3	68.5	30

† Or=Orientation: H=across corn rows, V=along corn rows

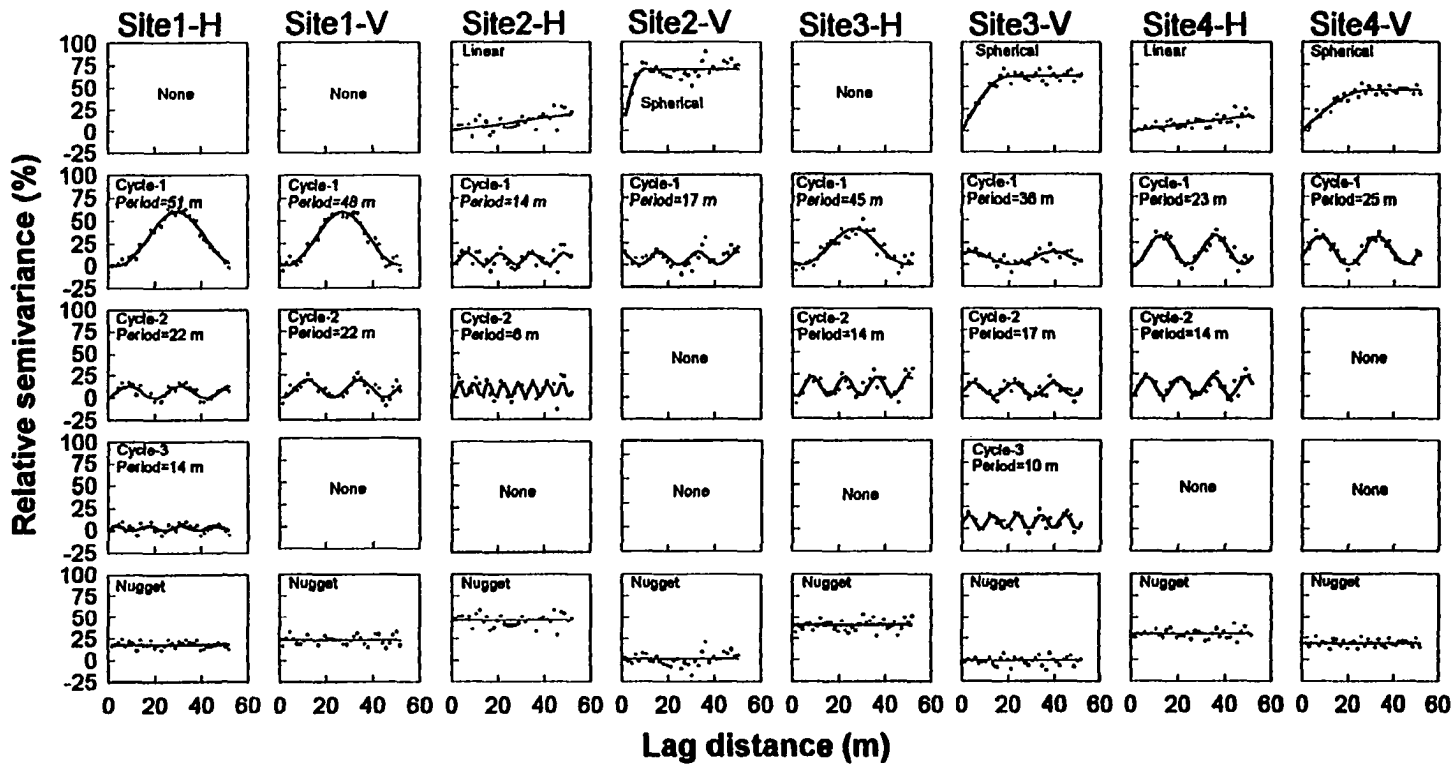

Figure 5. Components for cylic models and corrected residuals for soil NO_3^- semivariance data for sites 1 to 4.

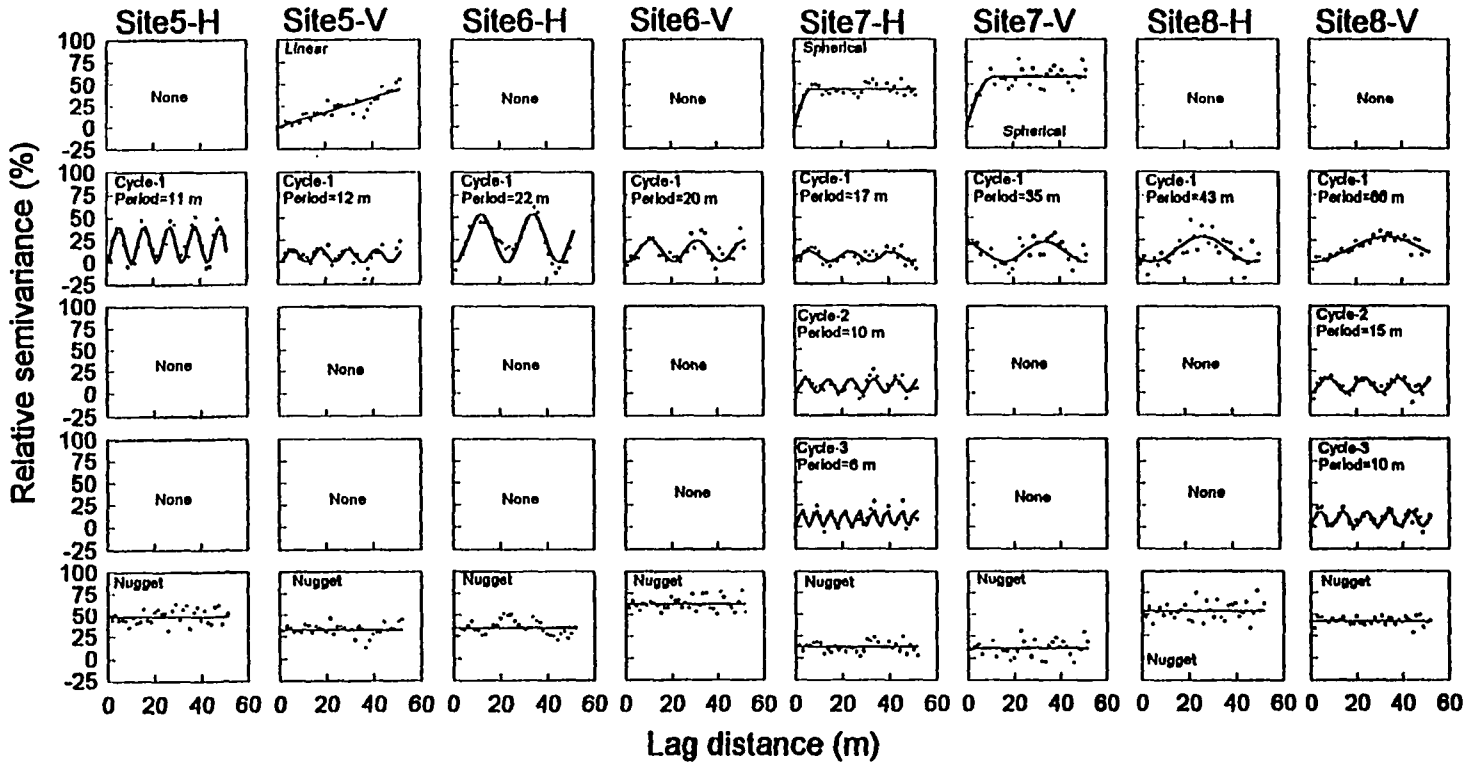

Figure 6. Components for cylic models and corrected residuals for soil NO_3^- semivariance data for sites 5 to 8.

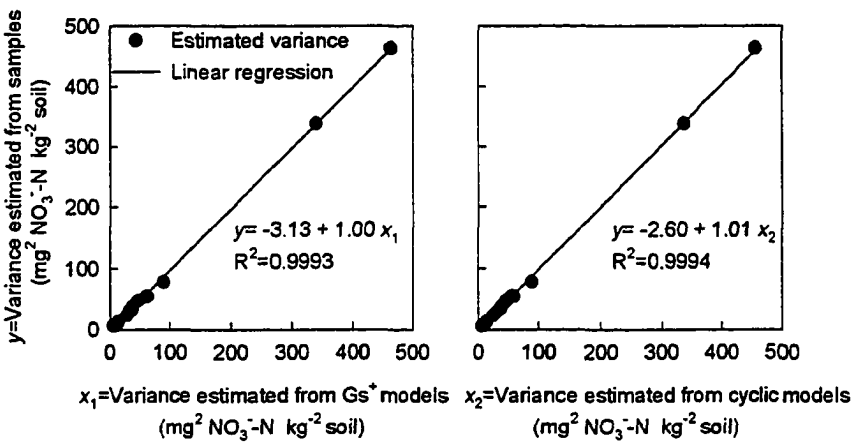

Figure 7. Observed relationships between the ordinary sample variance and the estimations of total variance from cyclic and non-cyclic models for soil NO_3^- concentrations at several sites.

It should be noted, however, that the ranges often changed substantially when cyclic components were considered (Table 3). As illustrated by the data from sites 1, 4, and 6 (Figures 5 and 6), the ranges given by the non-cyclic models other were determined by the position of the first cyclic peak. As a result, the nugget given by the model was artificially low (Table 4). It is, of course, difficult to distinguish between a regionalized component and a cyclic component when the distance sampled is less than the period of the cycle. These observations raise questions concerning the reliability of commonly used geostatistical techniques when cyclic trends are present. The observed cyclic trends clearly were important; estimates of the amounts of variance explained by each component revealed that the cyclic component explained more variability than did the regionalized component at 9 of the 16 datasets (Table 3).

The periods of the cyclic components ranged from 6 to 66 m. In some fields, cyclic patterns of similar period were observed along transects going parallel to the rows and going perpendicular to the rows. These can be explained by management operations oriented diagonally to the corn rows; farmers in Iowa often apply fertilizers and till soils by moving in straight lines that are 30 to 45 degrees diagonal to the direction in which corn rows will be planted. A management operation that moves diagonally to the rows would produce cyclic trends with periods greater than the width of the equipment. A management operation that moves parallel to rows would produce cyclic patterns only in the samples collected along the lines going perpendicular to the corn rows in this study, and such patterns were sometimes observed.

It seems likely that many of these cycles were caused by fertilizer applicators or tillage operations because the equipment used usually ranges from 8 to 14 m in width. Detailed information concerning management operations for each field was not collected. Fertilizer applicators would produce the large-scale cyclic patterns observed if fertilizer were not applied uniformly across the width of the applicator. If there were a gradient in rate of application across the applicator and fertilizer were applied in a serpentine pattern (a common practice), then cycles with periods at least twice the width of the applicator would be formed. Tillage operation could produce cyclic patterns if the tractor compacted the soil and thereby altered the transformation or movement of N in strips. Some of the cycles observed may have been caused by tile drainage system, which would alter the transformation and movement of N in strips.

The greatest variability was observed at site 6, and it seems likely that non-uniform application of anhydrous ammonia across the applicator was primarily responsible for the cyclic pattern. Anhydrous ammonia is injected into the soil as a mixture of gas and liquid, so it is often difficult to apply this fertilizer uniformly across the width of the applicator. Moreover, operators cannot detect non-uniform applications because the fertilizer is injected into the soil. In contrast, the UAN solution is sprayed through nozzles which permit visual detection of major problems related to uniformity of applications. Because each sample in this study consisted of 16 cores collected at about 9.5-cm intervals along a line perpendicular to the rows, cyclic patterns having periods less than 1.5 meter would have minimum impact on the variability observed in this study.

Relative frequency histograms of soil NO_3^- concentrations usually were symmetrical; statistical analysis showed significant skewness in only 3 of the 16 datasets (Fig 8). The site with the greatest skewness was site 6, which received anhydrous ammonia and had the highest concentration of NO_3^-. A relationship between NO_3^- concentration and degree of skewness should be expected because Babcock and Blackmer (1992) found that probability density functions for soil NO_3^- tended to become more skewed to the right as NO_3^- concentration increase. Cambardella et al. (1994) observed significant skewness in the distribution of soil NO_3^- after recent applications of anhydrous NH_3 and attributed this skewness to a few samples with high concentration coming from bands formed by the knives of the applicator. Although the effects of anhydrous fertilizer bands would have contributed to variability in our study, our sampling method should have minimized this problem. The presence of a cyclic component, however, could cause skewenss if only a portion of a cycle is sampled. Although Chan et al. (1994) reported that the shape of a variogram is often biased by values greater than four standard deviations from the mean, we observed no NO_3^- concentration exceeding three standard deviations from the mean.

Test for kurtosis showed that most of the histograms significantly differed from the normal distribution (Figure 8). Significant kurtosis indicates that samples tend to be grouped around the mean and far away from the mean, with less samples falling in between these two extremes (Snedecor and Cochran, 1980). Significant kurtosis is often found in datasets andit has not precluded use of variogram analysis in other studies (Cahn et al., 1994, Cambardella et al., 1994).

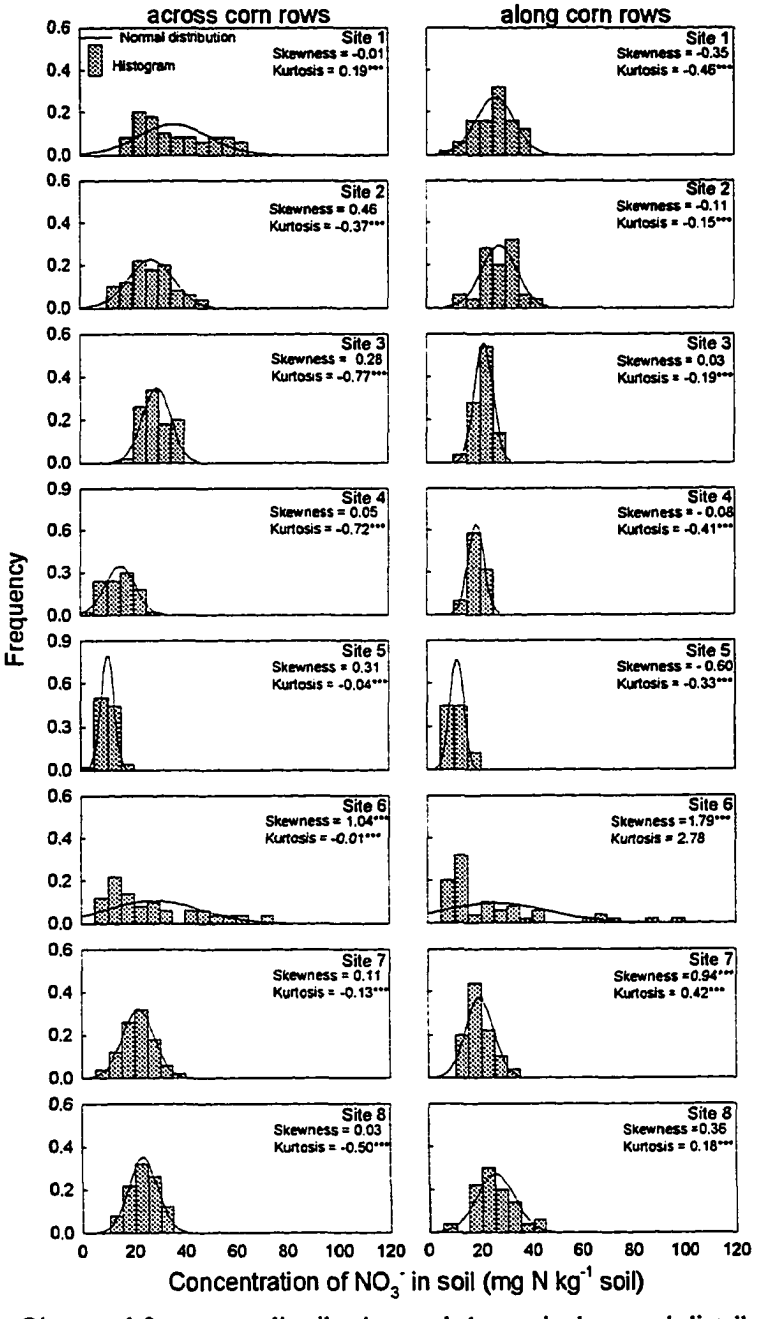

Figure 8. Observed frequency distribution and theoretical normal distribution for soil NO_3^- concentration at several sites.

If it were known that a field were managed by a practice that tended to produce cyclic patterns having a given range (i.e., 14 m), then sampling errors associated with the cycles could be minimized by collecting and compositing several cores at equal distances along a line segment having a length equal to the period. If it were known that rows introduce a smaller scale cycle, then sampling problems associated with both cycles would require a nested sampling pattern in which pairs of cores (one in the row, one between rows) were collected at equal distances along a line segment having a length equal to the period.

The results of this study illustrate that it would be extremely difficult to fully characterize the spatial structure of soil NO_3^- concentrations in situations were several small-scales and large scale cyclic patterns are superimposed. The only sure method would be to collect and analyze many single cores taken at close intervals over long distances. If this method is not followed and individual cores are separated by substantial distance, then small-scale cycles could not be detected and would be considered random error.

Overall, the results of this study indicate that cyclic patterns in soil NO_3^- concentrations on the scale of 5 to 30 m should be expected in many agricultural soils. The cycles could be caused for non-uniform applications of fertilizer, strips of compacted soil formed by heavy equipment used to till soils or harvest crops, strips of crop residue left by combines, tile drainage systems, or other "extrinsic" (Rao and Wagenet, 1985) sources of variability. Whatever the cause, identification of such cycles is essential to characterize the spatial structure of soil NO_3^- concentrations and to develop efficient sampling strategies to assess N availability. In many situations, identification of important cyclic patterns may

indicate need to revise fertilizer application techniques to reduce non-uniformity of application.

LITERATURE CITED

Babcock, B.A., and A.M. Blackmer, 1992. The value of reducing temporal input nonuniformities. Journal of agricultural and resource economics. 17 (2): 335-347.

Binford, G.D., A.M. Blackmer, and M.E. Cerrato. 1992. Relationships between corn yields and soil nitrate in late spring. Agron. J. 84:53-59.

Blackmer, A.M., D. Pottker, M.E. Cerrato, and J. Webb. 1989. Correlations between soil nitrate concentrations in late spring and corn yields in Iowa. J. Prod. Agric. 2:103-109.

Cahn, M. D., J. W. Hummel and B. H. Brouer. 1994. Spatial analysis of soil fertility for site-specific crop management. Soil Sci. Soc. Am. J. 58:1240-1248.

Cambardella, C. A., T. B. Moorman, J. M. Novak, T. B. Parkin, D. L. Karlen, Turco R.F. and A. E. Konopka. 1994. Field scale variability of soil properties in central Iowa soils. Soil Sci. Soc. Am. J. 588:1501-1511.

Clark, I. 1979. Practical Geostatistics. Applied Science Publishers, London.

Dahiya, I.S., K.C. Anluf, K.C. Kersebaum, and J. Richter. 1985. Spatial variability of some nutrient constituents of an Alfisol from loess. II. Geostatistical analysis. Z. Plfanzenernaehr. Bodenkd. 148:268-277.

Fox, R.H., G.W. Roth, K.V. Iverson, and W.P. Piekielek. 1989. Soil and tissue nitrate tests compared for predicting soil nitrogen availability to corn. Agron. J. 81:971-974.

Gamma Design Software. 1993. Gs^+ : Geostatistics for the environmental sciences 2.1 user's guide. Gamma Design Software, Plainwell, MI.

Goovaerts, P. Chiang ,. C.N. 1993. Temporal persistence of spatial patterns for mineralizable nitrogen and selected soil properties. Soil Sci. Soc. Am. J 57:372-381.

Ihnen, L.A., and J.P. Sall. 1985. The REG procedure. p. 655-709. *In* SAS user's guide: Statistics, 1985 ed. SAS Inst. Inc., Cary, N.C.

Ihnen, L.A., and J.H. Goodnight. 1985. The NLIN procedure. p. 575-606. *In* SAS user's guide: Statistics, 1985 ed. SAS Inst. Inc., Cary, N.C.

Kopp, J. E., and G. D. McKee. 1978. Methods for chemical analysis of water and wastes. Method 351.2, nitrogen, ammonia. EPA Report no. EPA-6000/4-79-020. EPA Environmental Monitoring and Support Laboratory, Cincinnati, OH.

Magdoff, F.R., D. Ross, and J. Amadon. 1984. A soil test for nitrogen availability to corn. Soil Sci. Soc. Am. J. 48:1301-1304.

Magdoff, F.R., W.E. Jokela, R.H. Fox, and G.F. Griffin. 1990. A soil test for nitrogen availability in the Northeastern United States. Commun. Soil Sci. Plant Anal. 21:1103-1115.

Meisinger, J.J., V.A. Bandel, J.S. Angle, B.E. O'Keefe, and C.M. Reynolds. 1992. Presidedress soil nitrate test evaluation in Maryland. Soil Sci. Soc. Am. J. 56:1527-1532.

Perdomo, C.H., and A.M. Blackmer. 1995a. Nitrogen availability in cornfields as affected by soybean residue. Agron. J. In preparation.

Perdomo, C.H., and A.M. Blackmer. 1995b. Identification of cyclic sources of variability in soils. Soil Sci. Soc. Am. J. In preparation.

Perdomo, C.H., and A.M. Blackmer. 1995c. Detecting superimposed cyclic patterns in soil properties. Soil Sci. Soc. Am. J. In preparation.

Perdomo, C.H., A.M. Blackmer, and. C.J. Green. 1995. Small-scale cycles in the spatial structure of soil nitrate concentrations of cornfields. Soil Sci. Soc. Am. J. In preparation.

Rao, P.S.C., and R.J. Wagenet. 1985. Spatial variability of pestices in field soils:Methods for data analysis and consequences. Weed Sci. 33(Suppl. 2):18-24.

Snedecor, G.W., and W.G. Cochran. 1980. Statistical methods. 7th ed. Iowa State Univ. Press, Ames.

Van Meirvenne, M., and G. Hofman. 1989. Spatial variability of soil nitrate nitrogen after potatoes and its change during winter. Plant Soil 120:103-110.

Wolfram, S. 1991. Mathematica, a system for doing mathematics by computer, 2d ed. Addison-Wesley, Redwood City, CA.

GENERAL SUMMARY

Studies were conducted from 1992-1994 to learn more about the spatial structure of soil NO_3^- concentrations in cornfields in late spring and to identify some major causes of variability in these concentrations. This information is specifically needed to aid in design of efficient sampling strategies for the late-spring test for N availability, which is a new management tool that enables site-specific evaluation and adjustment of fertilization practices. Overall objectives of this study included (i) evaluation of the possibility that windrows of soybean residue from a previous crop were a major source of variability in concentrations of soil NO_3^- and (ii) characterization of the amount and structure of variability of soil NO_3^- concentrations. An underlying assumption in these studies was that many common practices in row-crop agriculture should be expected to create cyclic variability in soil NO_3^- concentrations.

The objective of the first paper of this dissertation was to learn more about (i) the net effect of soybean residue on availability of N to corn in the following year and (ii) the importance of windrows of soybean residue as a source of spatial variability on concentrations of NO_3^- and exchangeable NH_4^+ in soils. Measurements were made in six fields selected for uniformity of windrows of residue formed during combining in production agriculture. Soil samples collected within and between windrows at various times during the spring revealed that soybean residues had only slight effects on N availability and that the direction of the effect was to decrease N availability. These findings were consistent with assessments of N status by chlorophyll meter readings on plant leaves in late spring and by

measurements of NO_3^- concentrations in cornstalks at the end of the season. Nonuniform applications of residue explained from insignificant to about half of the variability in concentrations of NO_3^- observed at the sites. The total amounts of variability were relatively small, however, at sites where the residue was responsible for a significant portion of the variability. Nonuniform application of N fertilizer seemed to be the most likely cause of spatial variability in soil NO_3^- concentrations at sites having the greatest variability.

The objective of the second paper included in this dissertation was to develop a method for characterization of cyclic components in variogram analysis and to compare this method to commonly used Fourier analysis methods. The study involved analysis of hypothetical datasets formed by imposing various levels of random noise on a cyclic function and analysis of a real dataset consisting of corn yield measurements made along a transect perpendicular to windrows of plant residue formed by harvesting the previous crop. Cyclic models were developed that identified cycles having appropriate periods in the hypothetical and real datasets. In the hypothetical dataset, a model consisting of a nugget and a cyclic component correctly identified the added periodicity even at the highest level of random noise. In the real dataset, a cyclic model consisting of a linear regionalized component and a cyclic component was superior to Fourier analysis for detecting the periodicity caused by windrows in a dataset with a strong regionalized component. This study led to the development of models that can partition spatial variability observed along transects into regionalized, cyclic, and random components.

The objective of the third paper was to extend the methodology developed in the second paper to partition variability when two or more cycles are superimposed in a dataset. The dataset used to test this approach was NO_3^- concentrations in 50 soil samples collected along a 76-m transect from a fertilized cornfield. Each sample was a composite of 16 3.2-cm-diam. cores collected at 9.37-cm intervals along the transect. A procedure was developed that involved fitting of a spherical model to a variogram, fitting a cyclic component to the residuals to make a spherical-one-cycle model, fitting another cyclic component to the residuals of the spherical-one-cycle model to make a spherical-two-cycle model, and repeating this process until the residuals show no statistically significant cyclic trends. Results showed that the amount of variability explained by the spherical component was small, and that an alternative model formed by a nugget and a three cyclic components was as least as good as the spherical-three-cycle model in describing the structure of the variogram. One of the cycles described by the models had a period resembling the width of fertilizer applicators commonly used in Iowa. Comparisons of the results from this model with FFT analysis showed that the cycles identified by the model agreed well with results from FFT. Overall, this result indicates that this technique can be used to identify superimposed cyclic trends in datasets collected along a transect.

The fourth paper presents studies of small-scale variability in soil NO_3^- concentrations and soil water content at 10 different cornfields in 1994. At each site, 120 samples were collected from the surface 30-cm layer of soil along a 9.1-m transect. Results showed that variability in concentrations of soil NO_3^- tended to be higher in sites that received N

fertilization and that young plants in rows were an important source of variability in concentrations of soil NO_3^- and soil water content. Geostatistical models developed in the second and third papers were used to characterize this variability, that at many sites appeared in variograms analysis as a cycle with a period determined by the distance between rows.

The last paper presents studies of large-scale variability in concentrations of soil NO_3^- at 8 different cornfields in 1993. At each site, 50 samples were collected from the surface 30-cm layer of soil along 75-m transects along and across corn rows. To minimize small-scale variability, each soil sample was a composite sample of 16 cores collected along a 1.5-m line perpendicular to the corn rows. Results showed that the amounts of variability in soil NO_3^- concentrations varied among sites and that cyclic patterns were detected in variogram analyses at most sites. Some of these cyclic patterns seem to be caused by fertilizer applicators or other farming operations.

Overall, results of studies reported in this dissertation show that cyclic patterns are an important component of the spatial structure of soil NO_3^- concentrations in cornfields. Consideration of these cyclic patterns should enable more complete characterization of the spatial structure of soil NO_3^- concentrations in fields and, therefore, enable design of more efficient sampling strategies to assess NO_3^- concentrations within these fields. In addition, the ability to detect previously unrecognized cyclic patterns in soil NO_3^- concentrations gives the ability to demonstrate the benefits of using practices that minimize formation of troublesome cyclic patterns in fields.

ACKNOWLEDGMENTS

I would like to acknowledge here people who have helped me to attain the PhD degree at Iowa State. First, I would like to thank Dr. A.M. Blackmer. I have been very fortunate to have had Dr. Blackmer as my advisor throughout my graduate career; he combines the research skills of a senior scientist with the enthusiasm of a youngster. His commitment to the science of agriculture is remarkable. I gratefully recognize the contribution of Diane, Julie, and Darcy Blackmer for supporting Dr. Blackmer through his long hours of work.

I want to extent a special note of appreciation to Dr. Cary Green for his help and friendship during my graduate studies in Iowa State. He always was ready to give an advice and to make easy the completion of any task. Dr. Green was responsible for collecting the data used in the 1994 studies and the inclusion of the fourth paper in this dissertation would have not been possible without his cooperation.

I would like to thank Drs. J.L. Baker, N.E. Christians, and R.M. Cruse for serving on my Ph.D. committee. A special thank you is extended to Dr. R. Horton for serving on my Ph.D. committee, for excellent teaching in the classroom, and for helping me in locating additional bibliographic material. I have been exposed to several excellent professors during my studies at Iowa State, and Dr. Horton is one of the best.

I would like to thank Dr. Antonio Mallarino for allowing me to use his computer for running the Gs^+ programs and for his help with statistical analyses. I would like to recognize also some fellow graduate students who have enhanced my graduate school experience both

during my master and my Ph.D. studies: Greg Binford , Kiam Chung Chin, Glenn Davis, Brian Meese, Tom Morris, Tom Thompson, Nanchang Yang have been very special colleagues, and their friendship has helped make graduate school a very enjoyable experience. I thank Susan White for assistance with statistical analyses. I also acknowledge the contribution of the several hourly workers who helped with sample analyses.

A special thank you is given to my parents and my sister Lilian for their love, support, and encouragement across the distance.